Bendix Aerospace Systems Division

NO.	ATM 1118
REV. NO.	
PAGE	i OF ii
DATE	10/30/72

LEAM
Thermal Design, Analysis and Tests
Final Report

This ATM summarizes the LEAM thermal control design, analysis and test program including the DVT T/V test and the qual/flight T/V acceptance tests. The data presented herein show the test program was successful and the LEAM will perform within its temperature specifications at the Apollo 17 ALSEP deployment site of Taurus-Littrow.

Prepared by G. Psaros

Approved by E. Granholm

TABLE OF CONTENTS

LIST OF FIGURES

LIST OF FIGURES (CONT.)

LIST OF TABLES

3.0 SUMMARY

A brief description of the LEAM, the thermal control concept, design and materials is presented. The parametric thermal analyses used in arriving at the final configuration are discussed along with the results and analytical correlation of the DVT T/V test and the qual/ flight T/V acceptance tests. The results presented herein show that the test program was successful.

The thermal performance predictions at the Apollo 17 ALSEP deployment site of Taurus-Littrow are compared to planar lunar surface predictions and are shown to be within the temperature specifications of -22 to 149°F.

4.0 INTRODUCTION

The experiment consists of central electronics and three sensors the up, east and west sensors. The up sensor is the Primary Cosmic Dust (PCD) experiment. The east/west sensors are the Sensor Ejecta experiment (i.e secondary spray particles enamating from sites of meteorite impacts on the lunar surface. Each sensor listens passively and records dust/meteorite impingements.

The Up and East sensors are dual film grid arrays and acoustical impact plate to provide particle speed, direction and angular resolution. The West sensor is a single film/grid array and acoustical impact plate which does not measure particle velocity or incident angle.

The thermal design of the LEAM is the result of the film material specified by the principal investigator and film developmental tests by Union Carbide. Modification of the optical properties of these films were required to provide the necessary thermal properties as determined by thermal analyses and thermal breadboard model testing. Verification of the overall thermal design and the first attempt at correlation was provided by the DVT model in the thermal vacuum chamber. Thermal modifications were made to the qual and flight models as a result of the DVT T/V test. These models were then subjected to the qual and flight T/V acceptance tests.

The LEAM experiment is self contained with the exception of the +29 Volt line supplied by the ALSEP Central Station. The operational modes consist of the heater in the automatic mode and in the manual mode. A survival mode is provided if necessary.

Figure 4.1 illustrates the general overall dimensions of the experiment. The external components are pointed out in Figures 4.2 and 4.3 which show the LEAM in the deployed and stowed conditions respectively.

FIGURE 4.1

LEAM PHYSICAL DIMENSIONS

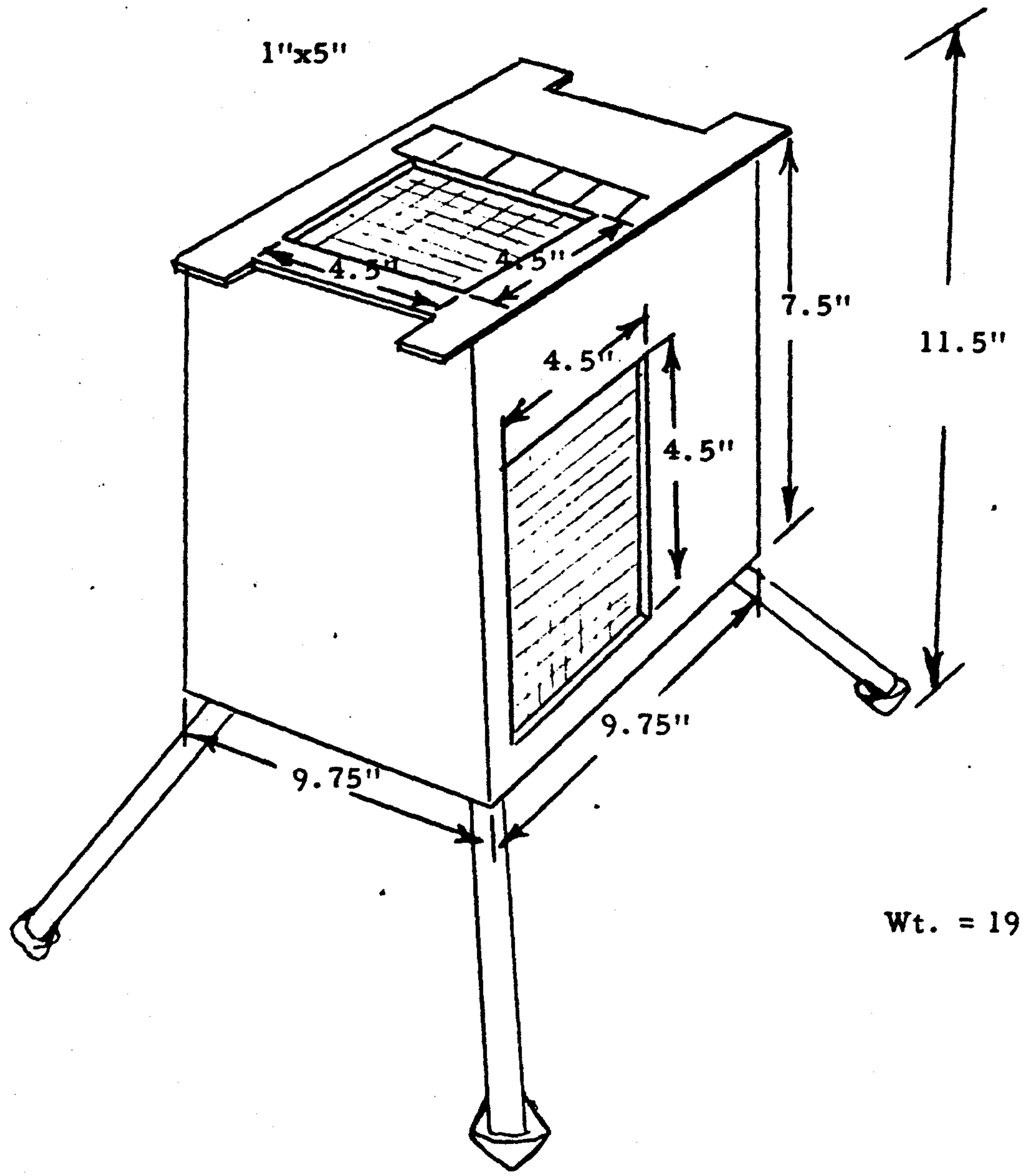

Wt. = 19.5 lb.

FIGURE 4.2

LEAM DEPLOYED VIEW

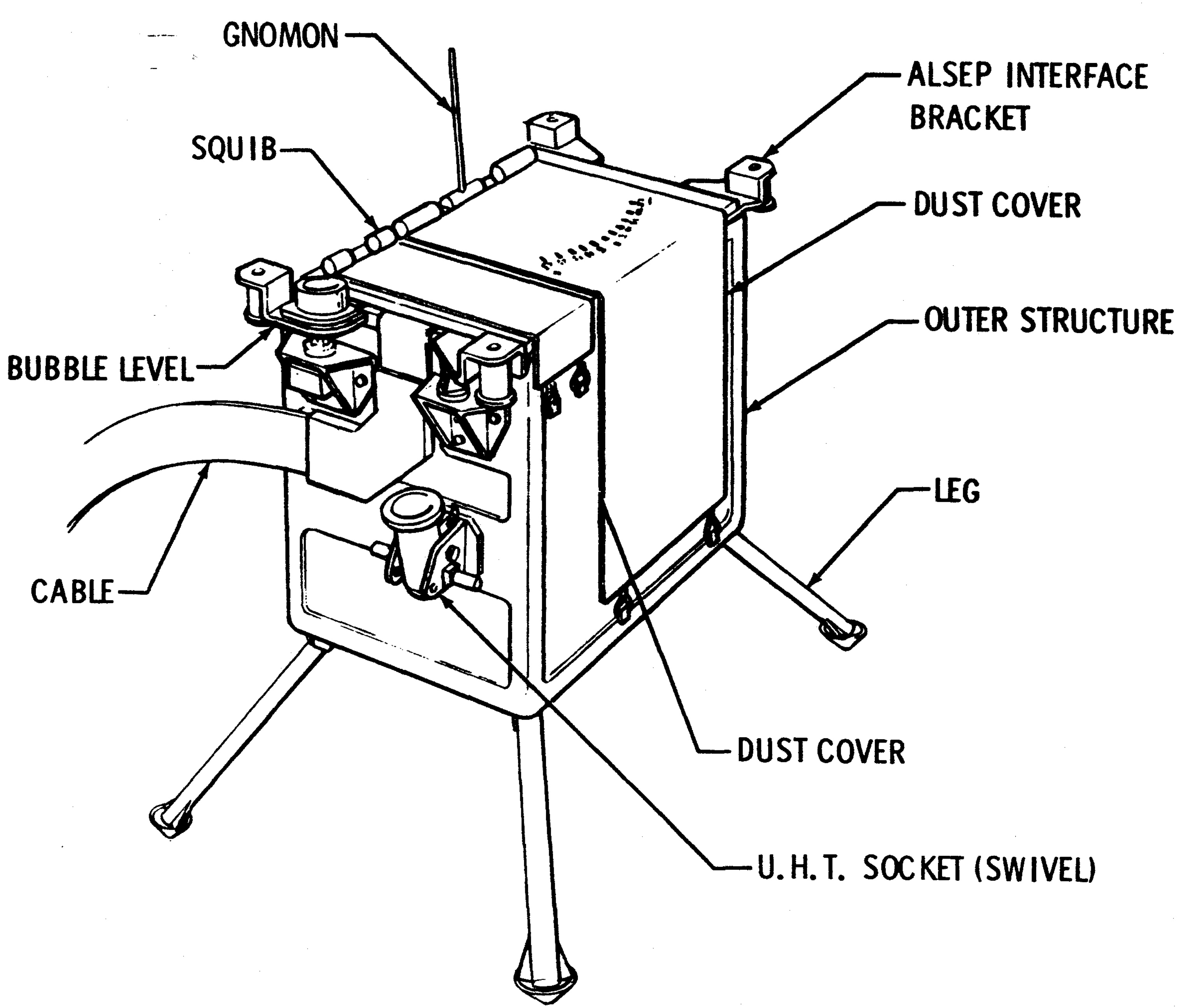

FIGURE 4.3

LEAM STOWED VIEW

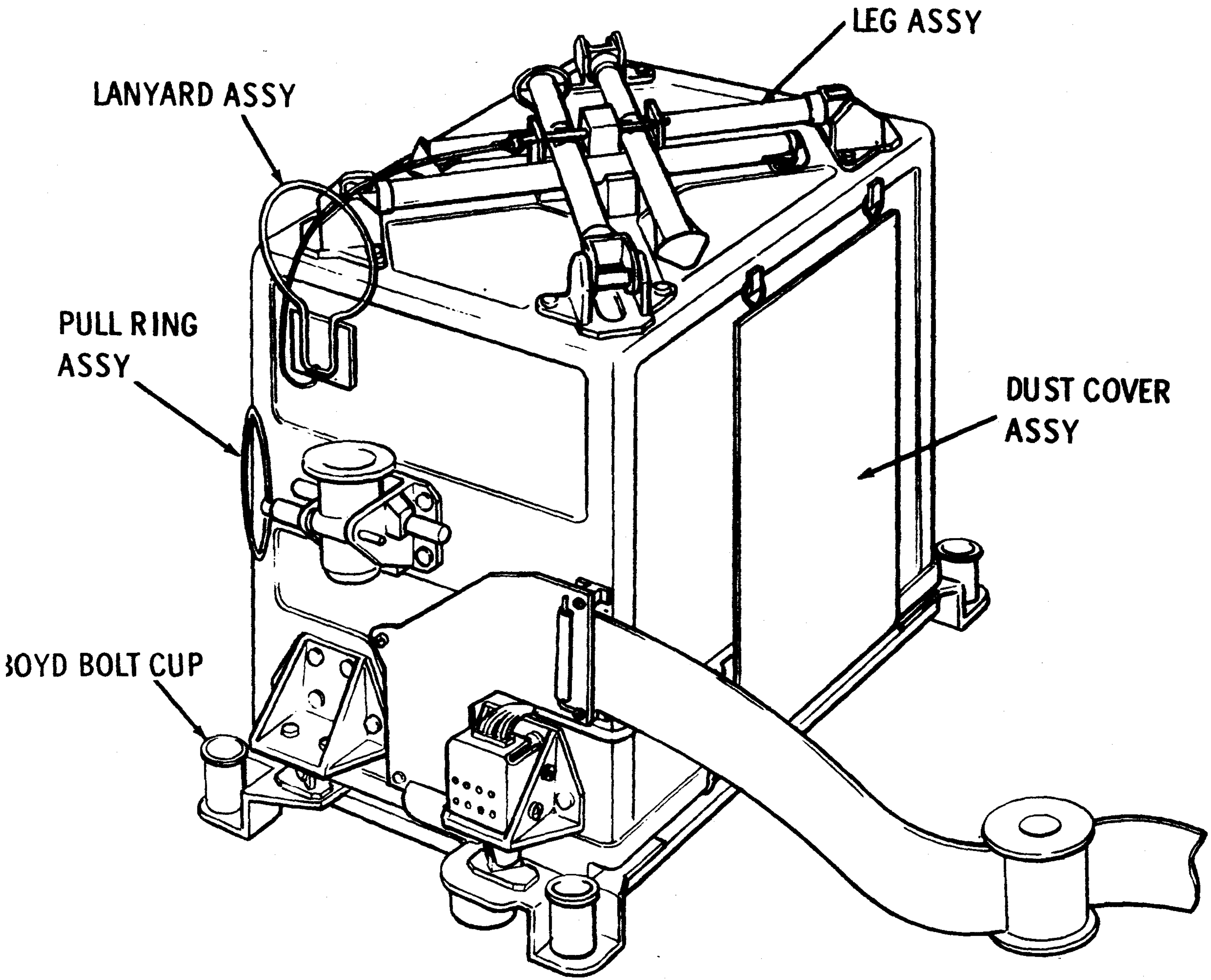

5.0 THERMAL DESIGN CONSIDERATIONS

5.1 ENVIRONMENT

Per the Grumman specification LED-520-IF, the direct solar flux at the lunar surface is 130 watts/ft. The annual declination of ± 3.5% which has previously been computed for the ALSEP experiments is superimposed on the mean value. The temperature excursion of the lunar surface is 250 at lunar noon to -300°F at lunar night. The lunar surface profile per LED-520-IF is shown in figure 5.1. The temperature of space is taken as -459°F.

5.2 TEMPERATURE REQUIREMENTS

The electronic and sensor temperature limits for the LEAM experiment are:

TABLE 5.1

	Electronics	Sensors
Operational (°F)	-22 to 149	-400 to 400
Non-operational (°F)	-65 to 180	-400 to 400
Lunar night survival (°F)	-67	-400

5.3 SCIENCE REQUIREMENTS

The LEAM science requirements consists of the following items:

1. All sensors must have an unobstructed view of the environment.
2. Experiment elevation must be equal to or above the average lunar surface elevation up to a radius of 1 kilometer
3. Deployment distance from the ALSEP radioisotope thermal electric generator equal to or greater than 30 feet.
4. East-west alignment must be within ±5°.
5. Low attenuation of particle velocity (Parylene was specified by the P.I. to support the 1750 Å aluminum ionization film layer since it is the thinnest, strongest film developed to date and has been used on similar cosmic particle sensors on PIONEER).

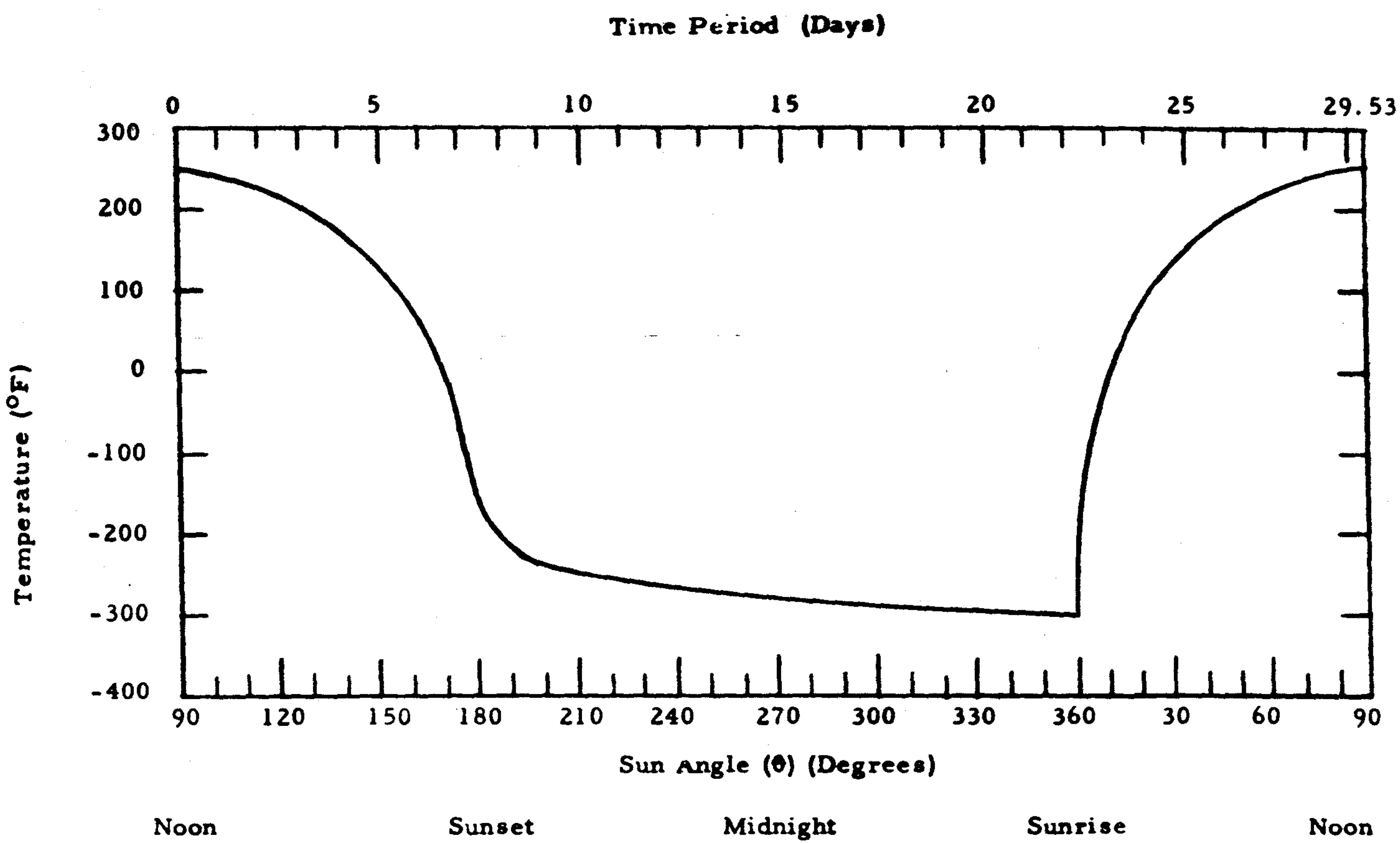

Variation of Lunar Surface Temperature (Subsolar Point) During a Complete Lunation

Figure 5.1

5.4 OTHER CONSIDERATIONS AND REQUIREMENTS

1. Total power allotted to the experiment is 7.0 watts.

2. Removal of the experiment from the ALSEP subpack and deployment on the lunar surface must be accomplished by one astronaut.

3. Thermal control coatings will be susceptible to degradation by:

   a. thermal-vacuum radiation effects. (i.e., ultraviolet, electron-protons and etc.)

   b. dust accumulation by LM ascent, deployment process and natural events and settling. (Note: to minimize dust coverage on the radiator and sensors, dust covers are provided and removed by ground command after the LM ascent to minimize dust accumulation by the first two processes.)

4. The experiment must be designed for latitudes of ±25 degrees and longitudes of ±60 degrees (Note: ALSEP array E will be deployed at 20.2° north latitude and 30.80 east longitude).

5. The Lunar panorama about the Apollo 17 ALSEP deployment site Taurus-Littrow which includes the North, East and South Massifs and the sculptured hills.

6.0 THERMAL CONTROL CONCEPT

The thermal control concept is passive and consists of isolating the electronics from the lunar environment by insulating with multilayer radiation shield insulation and by using low conductive materials and mechanical standoffs to minimize thermal conduction to the lunar surface. A thermal radiator is provided to reject the excess electronic power dissipation during the lunar day. A heater is provided to maintain the electronics above their lower operating temperature limit during lunar night. Thermal control coatings with low solar absorptances are used on all external surface to minimize the solar loads during the lunar day.

7.0 THERMAL PROPERTIES OF MATERIALS

The optical properties of the sensor materials are presented in table 7.1. This table shows the material of each component, its coating, solar absorptance (α_s) and infrared emittance (ϵ_{IR}). Table 7.2 presents the structural/thermal subsystem materials and their respective coatings. The conductivities of the materials are used in the thermal analysis and tabulated in table 7.3.

The goniometric solar absorptance and infrared emittance properties of the parylene film vacuum deposited with aluminum used as the forward film on the up and east sensors were measured and tabulated in tables 7.4 and 7.5 respectively. The solar absorptance was determined by measuring the reflectance at 20°, 45°, 60°, and 75° from the normal in an Edwards integrating sphere reflectometer. Measurements were performed in the wavelength region 0.28 to 2.5 microns. This spectral data was integrated over the solar spectral distribution as defined by Johnson.

The directional reflectance in the wavelength region 2 to 26 microns was measured using a Gier Dunkle heated cavity reflectometer. Measurements were performed at 20°, 45°, 60°, and 68° from the normal. The directional emittance was computed for each incidence angle by integrating the spectral data over a 300°K Planckian distribution function. This directional emittance data was plotted versus $\sin^2\theta$ and integrated to obtain the hemispherical value of 0.133.

TABLE 7.1

SENSOR MATERIALS

Sensor	Material	Coating	α_s	ϵ_{ir}
Up-Forward Film	1750 Å Parylene	700 Å Al 3250 Å SiO	0.25	0.1
East-Forward Film	1750 Å Parylene	700 Å Al 3250 Å SiO	0.25	0.1
West-Film	3 mil Molybdenum	Vacuum Deposit-Al	0.10	0.03
Up-Rear Film	3 mil Molybdenum	Sand Blasted	-	0.06
East-Rear Film	3 mil Molybdenum	Sand blasted	-	0.06
Up-Suppressor Grid	Lexan Frame Be-Cu Grid	S-13G	0.2	0.9
East-Suppressor Grid	Lexan Frame Be-Cu Grid	S-13G	0.2	0.9
West-Suppressor Grid	Lexan Frame Be-Cu Grid	24% S-13G 76% Al Tape	0.124*	0.254*
Up-Sensor Frame	Lexan	S-13G	0.2	0.9
East-Sensor Frame	Lexan	S-13G	0.2	0.9
West-Sensor Frame	Lexan	24% S-13G 76% Al Tape	0.124*	0.254*

*Average Properties

α_s - solar absorptance

ϵ_{IR} - infrared emittance

TABLE 7.2

STRUCTURAL/THERMAL MATERIALS AND COATINGS

1. EXTERNAL STRUCTURE:

Painted on outside with S13G paint ($\alpha_s{}^{*}/E_H = 0.2/0.9$), except for surface facing moon, which is faced with aluminized tape ($E_H = 0.05$). Inside surfaces covered with aluminized tape.

2. INTERNAL STRUCTURE

Sensor cavities painted with 3M Velvet Coat ($E_H = 0.9$). Surfaces facing superinsulation bag covered with aluminized tape.

3. RADIATOR:

Fifteen square inches of second surface mirrors exposed to space ($\alpha_s{}^{**}/E_H = .08/.80$) and mounted to 60 mil aluminum plate.

4. RADIATOR MASKING:

21 layers of 1/4 mil Mylar separated by 20 layers of silk separators. Outer layer is 2 mil aluminized teflon, teflon side out ($\alpha_s/E_H = .20/.69$).

5. CORNER SUPPORT MASKING

Same construction as above.

6. THERMAL BAG

41 layers of 1/4 mil aluminized Mylar separated by 40 layers of silk separators. Outside layer is 5 mil aluminized Kapton with aluminized side out. Inside layer is 1 mil aluminized Kapton with aluminized surface facing internal structure. ($E_H = .05$)

* Solar Absorptance/Hemispherical Infrared Emittance

** Average Properties for Entire Radiator

TABLE 7.3 CONDUCTIVITY VALUES USED IN THE ANALYSES

MATERIAL	K ($BTU/FT^2 \cdot HR. {}^\circ F/FT$)
Aluminum 2024	109
Aluminum 6061	99
Aluminum-Pure	135
Beryllium Copper	68
Copper-Pure	226
Epoxy Fiberglass	0.25
Lexan	0.11
Molybdenum	84.5
Quartz (Fused Silica)	0.68
Polyurathane Foam	0.038
Stainless Steel Screws	9.4

Parylene Film Vacuum Deposited with Aluminum

TABLE 7.4
SOLAR ABSORPTANCE

Angle of Incidence (degrees)	Solar Absorptance (α_S)
20	$.27_8$
45	$.29_3$
60	$.30_6$
75	$.33_4$

TABLE 7.5
EMITTANCE

Directional Emittance				Hemispherical Emittance (ϵ_H)
$\theta = 20°$	$\theta = 45°$	$\theta = 60°$	$\theta = 68°$	
0.08_8	0.11_0	0.15_6	0.19_4	0.13_3

8.0 THERMAL DESIGN

8.1 GENERAL

The sensor assemblies and central electronics are mounted to a common internal structure conductively coupled to a horizontal thermal plate of aluminum as shown in Figure 8.1. Figure 8.2 illustrates the primary thermal control components and their relation with respect to each other. The exploded views of the single sensor and the dual sensor are illustrated in Figures 8.3 and 8.4. These figures show the various component locations such as the sensor electronics. The short electrical leads required for some of the electronics have necessitated mounting these components within the sensor assembly.

Conductively coupling the power dissipating electronics to the sensors via the internal structure reduces the heater power required. Further, the edges of the thermal radiator plate are attached to the external structure and leg assembly by low conductive phenolic mounts to provide mechanical support and isolation.

The radiator consists of 5 square inches of spectrally selective second surface mirrors (i.e. a low solar absorptance (0.08) and a high infrared emittance (0.80)). The mirrors are 8 mils quartz (fused silica) vacuum deposited with silver. This surface is highly stable to long term ultraviolet and charged particle bombardment.

The sensor surfaces facing and radiatively coupled to the multilayer insulation bag are taped with aluminized tape having an emittance of 0.05. The sensor cavities are coated with 3M-401-C10 black velvet coat having an emittance of 0.9 to reduce the internal temperature gradients. The internal surface of the fiberglass outer structure is taped with aluminized tape with an emittance of 0.05.

The multilayer insulation bag consists of 41 layers of 1/4 mil double aluminized mylar spaced with 40 layers of silk netting. The outer and inner surfaces of the insulation bag are 5 mil and 1 mil Kapton respectively aluminized on the external surfaces to reduce radiative coupling to the structure. To prevent air entrapment during ascent, the insulation is vented.

FIGURE 8.1

LEAM INTERNAL STRUCTURE

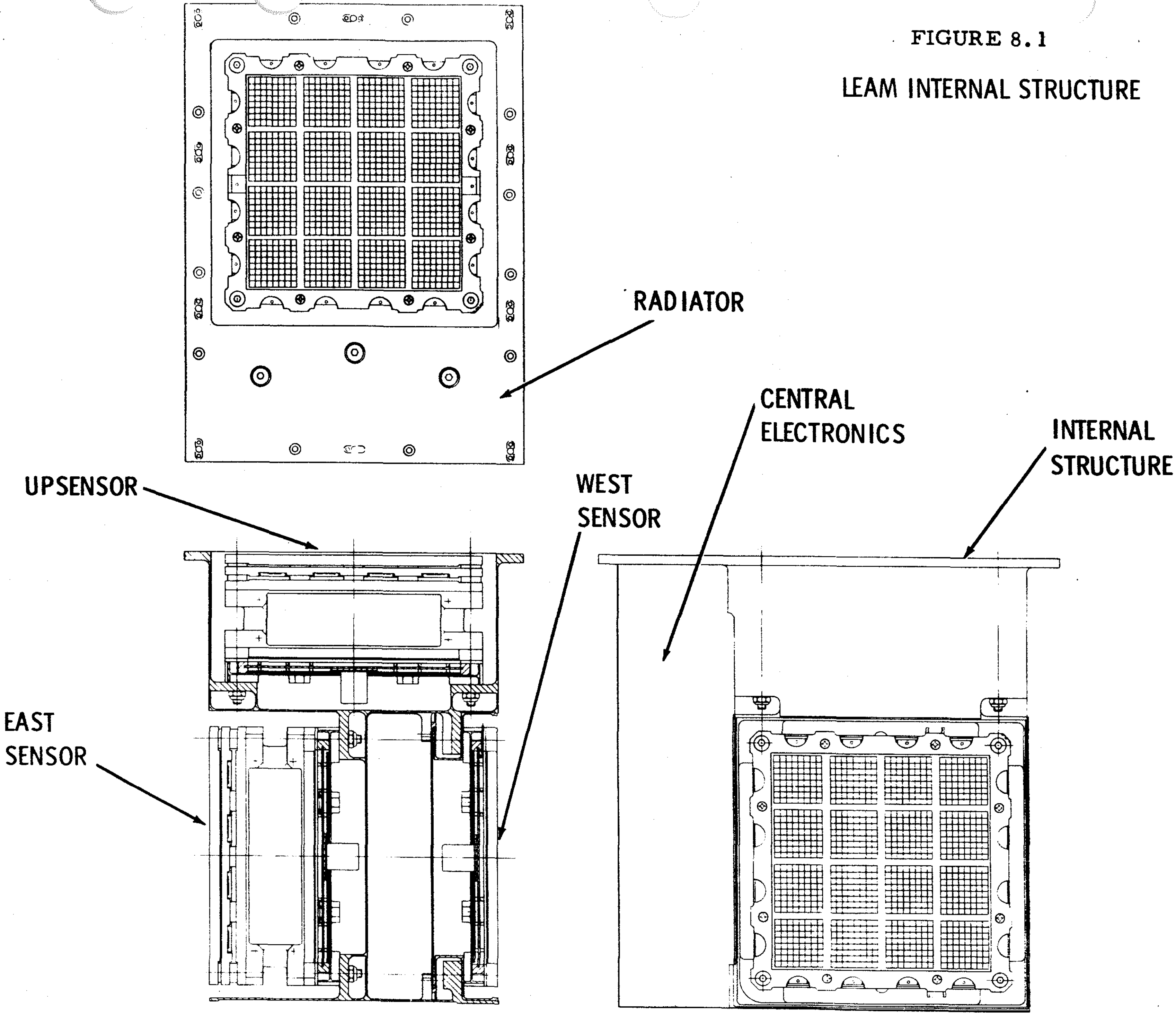

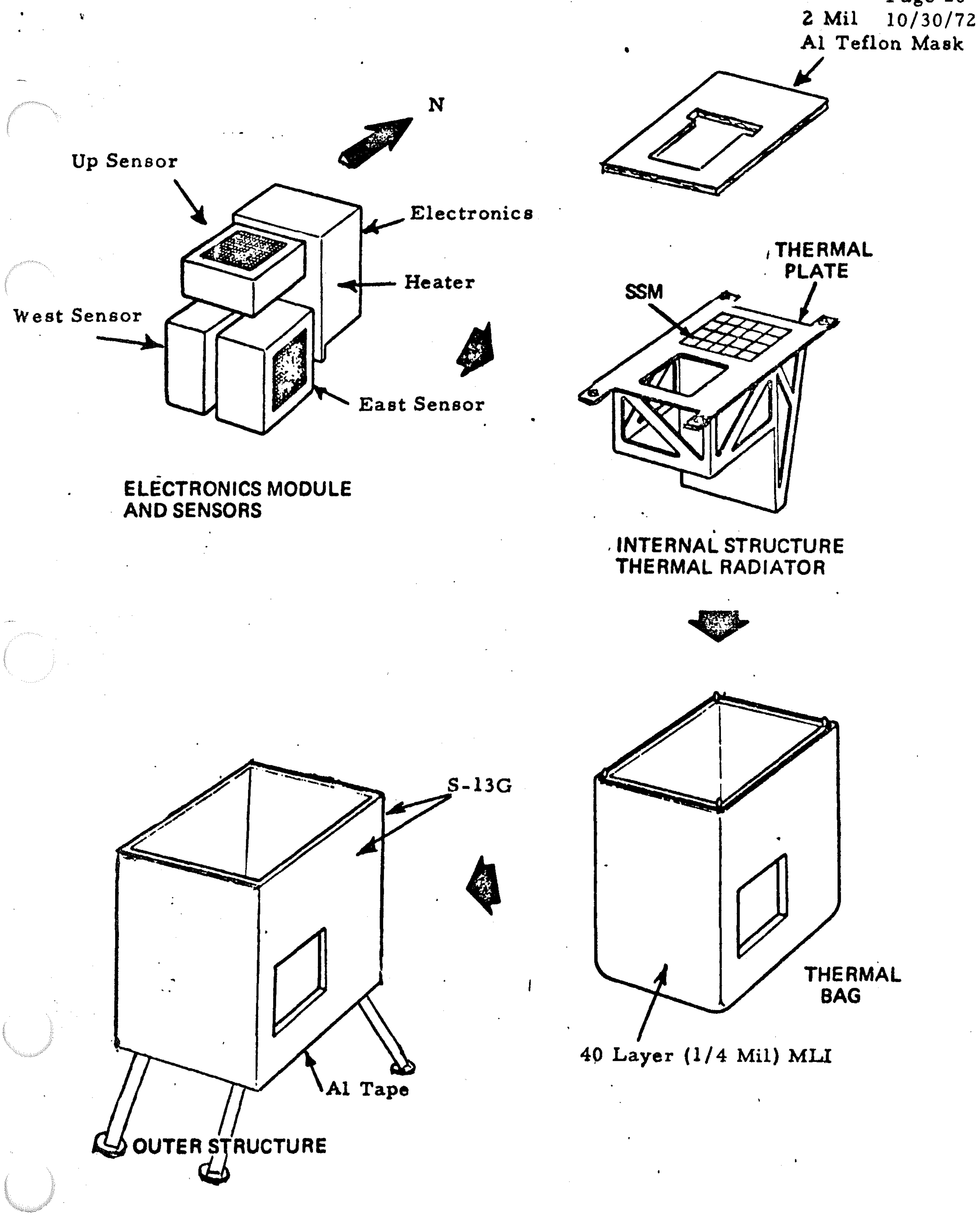

FIGURE 8.2

LEAM THERMAL CONTROL FEATURES

GURE 8.3

EXPLODED VIEW OF SINGLE SENSOR

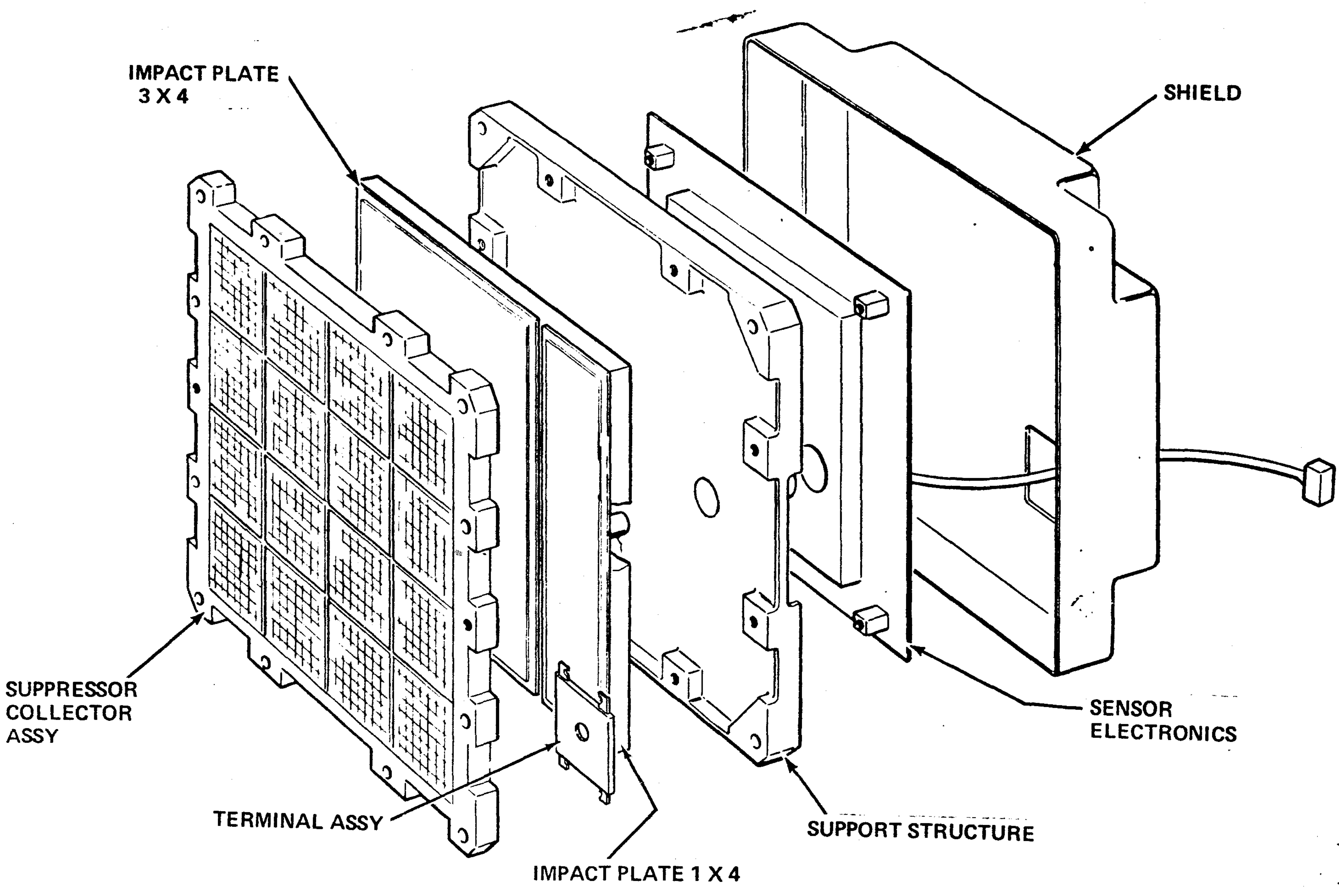

FIGURE 8.4

EXPLODED V[illegible] OF DUAL SENSOR

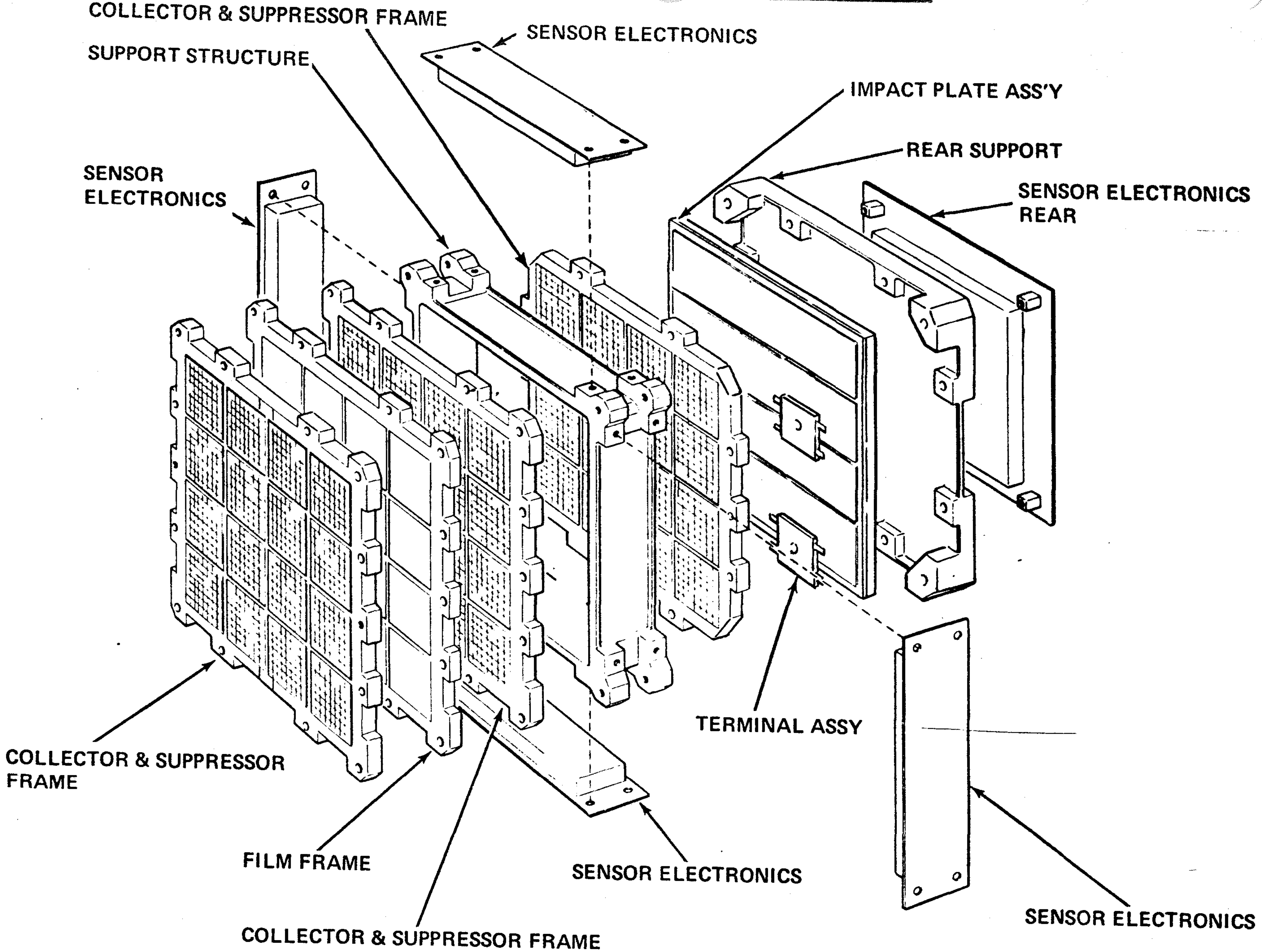

The masking used to regulate the radiation temperature consists of 21 layers of 1/4 mil double aluminized mylar spaced with 20 layers of silk netting. An outer surface of 2 mil teflon aluminized on the internal surface which possesses second surface mirror characteristics is provided to reduce the solar load on the mask,

Two sets of dust covers are provided. The first constructed of bright white dacron cloth style N-2468/1 type 55 protects the sensor and the critical thermal surfaces during traverse and deployment and removed by the astronaut. The second covers the sensor and radiator and are attached to spring retraction devices. The cover set consists of two separately actuated sections. The one covering the radiator is constructed of two layers of 2 mil teflon aluminized on one side with the two aluminum sides facing each other. The second covering the up and west sensors consists of a 1 mil Kapton outerlayer and a 2 mil teflon inner layer with both layers aluminized on the side facing each other. The east sensor covering is identical to the radiator cover. The optical properties of aluminized teflon are $\alpha_s/\epsilon_{IR} = 0.2/0.69$ and aluminized Kapton are $\alpha_s/\epsilon_{IR} = 0.4/0.57$. Removal of the latter covers are by ALSEP command subsequent to LM ascent and LSPE activation.

8.2 THERMAL MATH MODEL

The thermal math model which conceptually describes the LEAM experiment is composed of 97 nodes and has 428 conductive and radiative resistances. The nodal breakdown is listed in Table 8-1.

Computation of radiation resistances was assisted by the Confac II program, which computed view factors, and the Absorp program, which calculated script F values. Surface coatings and finishes for principal components with associated thermal surface properties are listed in Section 7.0.

Conductive resistances for the math model were computed by scaling drawings describing various components of the experiment and by applying the appropriate conductivities. The conductivity values used in the analysis appear in Section 7.0, Table 7.3.

Solar inputs for the various cases were computed by multiplying selected projected areas times the local $_s$ and then by the solar constant, 442 BTU/hr ft^2. Heat dissipation inputs were taken from current power dissipation figures and are listed in Table 8.2.

TABLE 8-1 NODAL DESCRIPTION FOR THE ANALYSIS

DEFINITION	NODE #	DEFINITION	NODE #
UP SENSOR		EAST SENSOR	
OUTER FRONT GRID FRAME	1	OUTER FRONT GRID FRAME	101
FRONT FILM	2	FRONT FILM	102
FRONT FILM FRAME	3	FRONT FILM FRAME	135
FRONT FILM GRID	35	FRONT FILM GRID	135
INNER FRONT GRID FRAME	4	INNER FRONT GRID FRAME	104
FORWARD ELECTRONICS		FORWARD ELECTRONICS	
SOUTH	5	SOUTH	105
WEST	6	TOP	106
NORTH	7	NORTH	107
EAST	8	BOTTOM	108
REAR GRID FRAME	9	REAR GRID FRAME	109
REAR FILM - CENTER	30	REAR FILM - CENTER	130
REAR FILM - EDGE	31	REAR FILM - EDGE	131
REAR FILM FRAME	11	REAR FILM FRAME	111
REAR ELECTRONICS	13	REAR ELECTRONICS	113
HEAT TRANSFER PLATE	25	HEAT TRANSFER PLATE	125
SUPPORT STRUCTURE		SUPPORT STRUCTURE	
SOUTH	14	SOUTH	114
WEST	15	TOP	115
NORTH	16	NORTH	116
EAST	17	BOTTOM	117
SENSOR ENCLOSURE		SENSOR ENCLOSURE	
SOUTH	18	SOUTH	118
WEST	19	TOP	22
NORTH	20	NORTH	120
EAST	21	BOTTOM	121
BOTTOM	22	REAR	122

TABLE 8.1 (Cont.)

DEFINITION	NODE #
WEST SENSOR	
GRID FRAME	209
FILM 1 x 4	230
FILM 3 x 4	231
FILM FRAME	211
REAR ELECTRONICS	213
HEAT TRANSFER PLATE	225
SENSOR ENCLOSURE	
TOP	22
BOTTOM	221
REAR	222
RADIATOR - SECONDARY	23
RADIATOR - PRIMARY	24
CENTRAL ELECTRONICS	32
INTERFACE BRACKET CORNERS	
SOUTHWEST	41
NORTHWEST	42
NORTHEAST	43
SOUTHEAST	44
FIBERGLASS ENCLOSURE	
SOUTH	61
WEST	62
NORTH	63
EAST	64
BOTTOM	65
FIBERGLASS ENCLOSURE CORNERS	
SOUTHWEST	51
NORTHWEST	52
NORTHEAST	53
SOUTHEAST	54
TOP FLANGE UNDER SECONDARY RADIATOR	33
TOP FLANGE UNDER PRIMARY RADIATOR	34

DEFINITION	NODE #
SUPERINSULATION INSIDE	
SOUTH	71
WEST	72
NORTH	73
EAST	74
BOTTOM	75
SUPERINSULATION OUTSIDE	
SOUTH	81
WEST	82
NORTH	83
EAST	84
BOTTOM	85
SECONDARY RADIATOR MASKING	93
PRIMARY RADIATOR MASKING	94
SUPERINSULATION OVER CORNER MOUNTS	
SOUTHWEST	141
NORTHWEST	142
NORTHEAST	143
SOUTHEAST	144
OUTER SECTION OF CORNER MOUNTS	
SOUTHWEST	241
NORTHWEST	242
NORTHEAST	243
SOUTHEAST	244
SQUIB FIBERGLASS FLANGES	56, 57
SQUIBS	58, 59

TABLE 8-2 POWER DISSIPATION VALUES USED IN THE ANALYSIS

Definition	Dissipation-Watts Noon	Night	Survival
Up Sensor			
Forward Electronics	0.32	.34	0
Rear Electronics	0.28	.30	0
East Sensor			
Forward Electronics	0.32	.34	0
Rear Electronics	0.28	.30	0
Microphone Heater	0	0.60	0.60
West Sensor			
Electronics	0.27	0.29	0
Microphone Heater	0	1.90	1.90
Survival Heater	0	0	0.95
Central Electronics	1.70	1.82	0
Radiator			
Nominal Heater	0	0.60	0.60
Survival Heater	0	0	0.95
Total	3.17	6.49	5.00

8.3 POWER DISSIPATION

The LEAM power dissipation is presented in Table 8.3 for the functional, contingency and standby modes of operation. The thermal control heaters are thermostatically controlled over a temperature range of (0-9°F). The total power at lunar night is 6.6 watts of which 3.2 watts are obtained from a heater. For contingency operation on additional 0.21 watts of power are commandable into the experiment.

TABLE 8-3

LEAM Power Dissipation

	Power (Watts)	Notes
Functional	2.99 3.18 3.40	@ +149°F @ +68°F @ -22°F
Heater	3.20	(0-9°F) Control Range
Total	6.6	(3.4 + 3.2) Watts
Contingency	0.21	Commandable
Standby	4.96	1.8 Fixed + 3.2 Controlled

8.4 ANALYTICAL THERMAL DESIGN STUDIES

Analytical thermal design studies were conducted to determine the following:

(a) Optimum sizing of thermal plate
(b) Heater power requirements
(c) Multilayer insulation conductivity effects
(d) Thermal plate mask width effects
(e) Thermal performance due to thermal control coating degradation by dust and ultraviolet radiation
(f) Steady state performance at all solar angles
(g) Effects of deployment latitude and Taurus Littrow effects
(h) Effects of levling and mislaignment errors
(i) Central Station and probe cable heat leaks
(j) Lunar surface temperature effects
(k) Nominal lunar surface thermal performance during both lunar day & night
(l) Lunar night survival power requirements
(m) Proposed modifications for improved performance.

The thermal math model was then used for prediction and correlation of the engineering model thermal DVT T/V test, and the qual and flight T/V acceptance tests and modified as required for accuracy. Figure 8.5 illustrates the model network of the dual film sensor used in the math model.

Figure 8.5

LEAM DUAL FILM SENSOR THERMAL-MATH MODEL

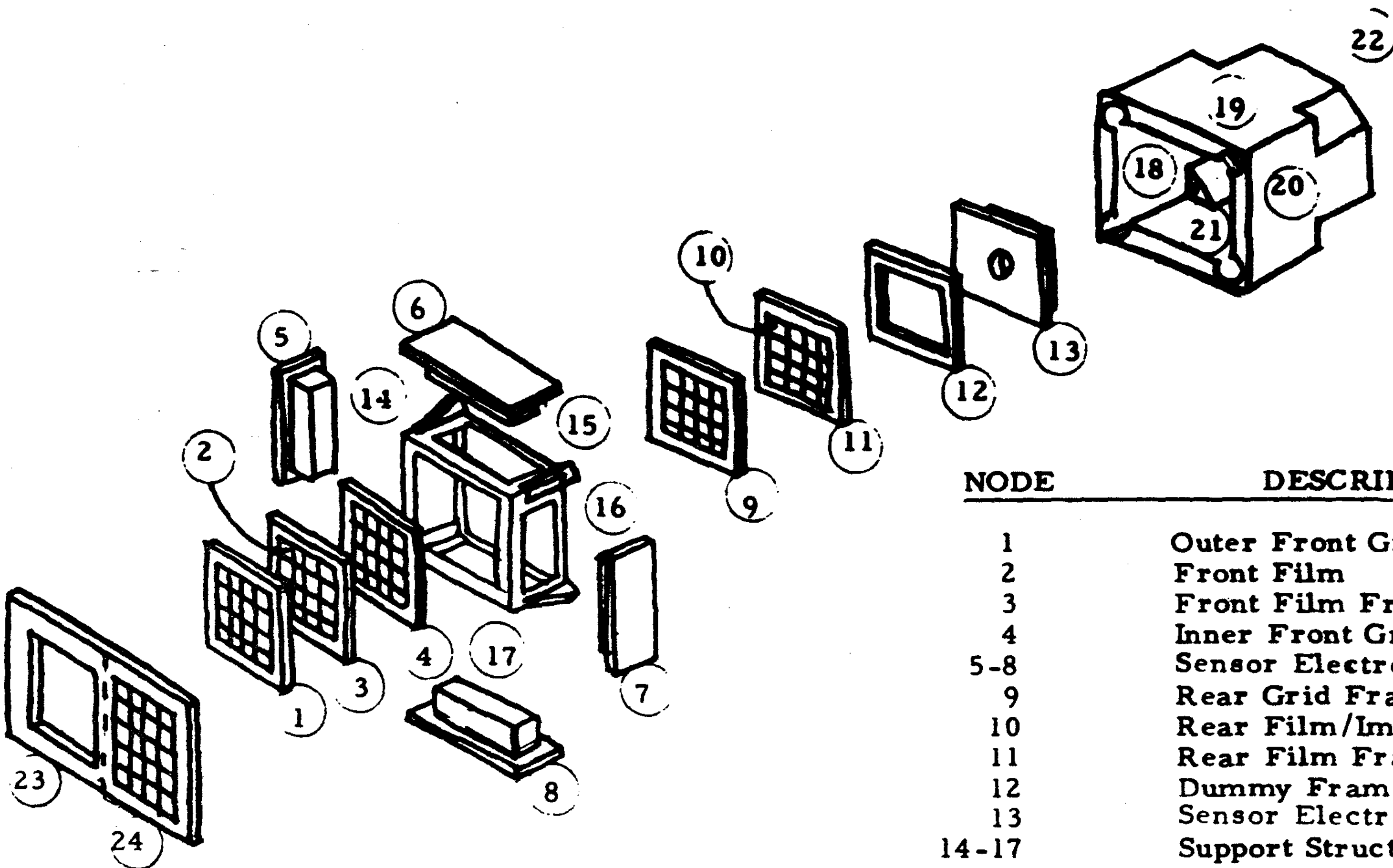

NODE	DESCRIPTION
1	Outer Front Grid Frame
2	Front Film
3	Front Film Frame
4	Inner Front Grid Frame
5-8	Sensor Electronics
9	Rear Grid Frame
10	Rear Film/Impact Plate
11	Rear Film Frame
12	Dummy Frame
13	Sensor Electronics
14-17	Support Structure
18-22	Sensor Enclosure
23-24	LEAM Radiator Plate

100
SPACE

Table 8.4 presents the analytical results from the thermal model for the noon, night and survival cases. Additional case temperatures are shown for a solar angle 10° past sunrise and 10° before sunset.

The noon case predictions show the Up sensor front film temperature at 246°F, the electronics and microphone temperatures remain below the upper specification limit for this case.

Night and survival case listings illustrate the temperature distribution for the two cold conditions and show all electronic temperatures above the appropriate lower specification limit. Comparisons between the two cases give an indication of temperature decrease in going from 6.5 watts power dissipation (night) to 5 watts (survival), and yield a temperature/power relationship of more than 20°F per watt for cold cases.

Sunrise and sunset cases are presented for reference data only. The LEAM experiment as deployed will not have its axis aligned with east-west while the data generated in the analysis assumed parallel alignment. The moon deployment case will cause lower temperatures for these conditions since the solar vector will be off-normal to the sensor openings.

Analytical data presented in Table 8.5 summarizes the night and day energy balances for the experiment. The small differences (.03 & .01 watts) between heat transfer data and power dissipation figures are due to computer round-off. Principal changes from the DVT model are smaller night losses through the interface bracket and radiator, and larger night losses through the Up and East Sensors. The Qualification model interface bracket is made of fiberglass while the DVT brackets were made of titanium. The current radiator size is 5 square inches while the DVT had 10 square inches. The addition of polyurethane separators between the grid and film frames cause an increased night loss through the sensors for the qual-model.

Table 8-4 LEAM TEMPERATURES

DEFINITION	NODE #	Temperature ~°F NOON	NIGHT	SURVIVAL	SUNRISE +*	SUNSET -**
Up Sensor						
Outer Front Grid Frame	1	107	- 44	-76	-12	-32
Front Film	2	246	- 41	-74	- 8	-29
Front Film Frame	3	123	- 38	-71	- 4	-25
Forward Electronics	5	138	- 10	-48	27	4
Support Structure	14	138	- 10	-48	27	3
Rear Film	30	141	- 5	-47	32	8
Rear Electronics	13	141	- 4	-46	33	9
East Sensor						
Outer Front Grid Frame	101	133	- 42	-72	53	-13
Front Film	102	134	- 38	-70	203	-10
Front Film Frame	103	135	- 35	-67	62	- 9
Forward Electronics	105	139	- 7	-44	46	7
Support Structure	114	139	- 7	-44	46	7
Rear Film	130	142	- 2	-43	49	11
Rear Electronics	113	142	- 1	-42	49	12
West Sensor						
Grid Frame	209	128	- 82	-103	-23	7
Film	230	139	- 9	-42	27	37
Film Frame	211	139	- 9	-41	27	26
Electronics	213	140	- 7	-40	28	27
Central Electronics	32	144	2	-44	37	14
Internal Structure	22	139	- 5	-40	34	7
Radiator	24	129	- 13	-46	21	- 2
Lunar Surface	200	250	-300	-300	5	5
Spec Limit (Electronics)		149 (65°C)	- 22 (-30°C)	-67 (-55°C)		

* Solar Angle at 10°

** Solar Angle at 170° Approximate Values Since Heaters Will Be Cycling

Table 8-5 LEAM ENERGY BALANCES

COMPONENT	Heat Transfer - Watts Night	Noon
Radiator	-0.56	-1.23
Up Sensor	-1.36	-1.16
East Sensor	-1.35	-0.44
West Sensor	-0.85	-0.26
Interface Bracket	-0.99	.06
Masking	-0.67	- .24
Superinsulation	-0.42	.09
Cable	-0.31	0
	-6.51	-3.18
Power Dissipation	6.48	3.17

The lunar day thermal performance at 25 degrees latitude is presented in Figures 8.6 to 8.15 for power dissipation of 3.18 watts. Figures 8.6, 8.7 and 8.8 show lunar day performance for undegraded thermal properties. Figures 8.9, 8.10 and 8.11 show the effect on performance where all the external surfaces are totally degraded and the sensors and radiator are clean. Figure 8.12 shows the effect of degrading the sensor and radiator to an effective solar absorptance of 0.2 when all other external surfaces are totally degraded. Figures 8.13, 8.14, and 8.15 show the effect of totally degrading all external surfaces. Table 8.6 presents a summary of the effect of these optical properties changes on the peak radiator temperature. Note that when the radiator and sensors are undegraded the experiment will be within the temperature specifications.

The performance during lunar day when the dust cover is on and all the external surfaces are degraded to an $\alpha_S/\epsilon_{IR} = 1.0$ is presented in figure 8.16 for no power dissipation. Peak radiator temperature for this contingency condition is 140°F. Since there is no power dissipation, the electronics will be well within the upper operating temperature limit of 149°F.

Figure 8.6

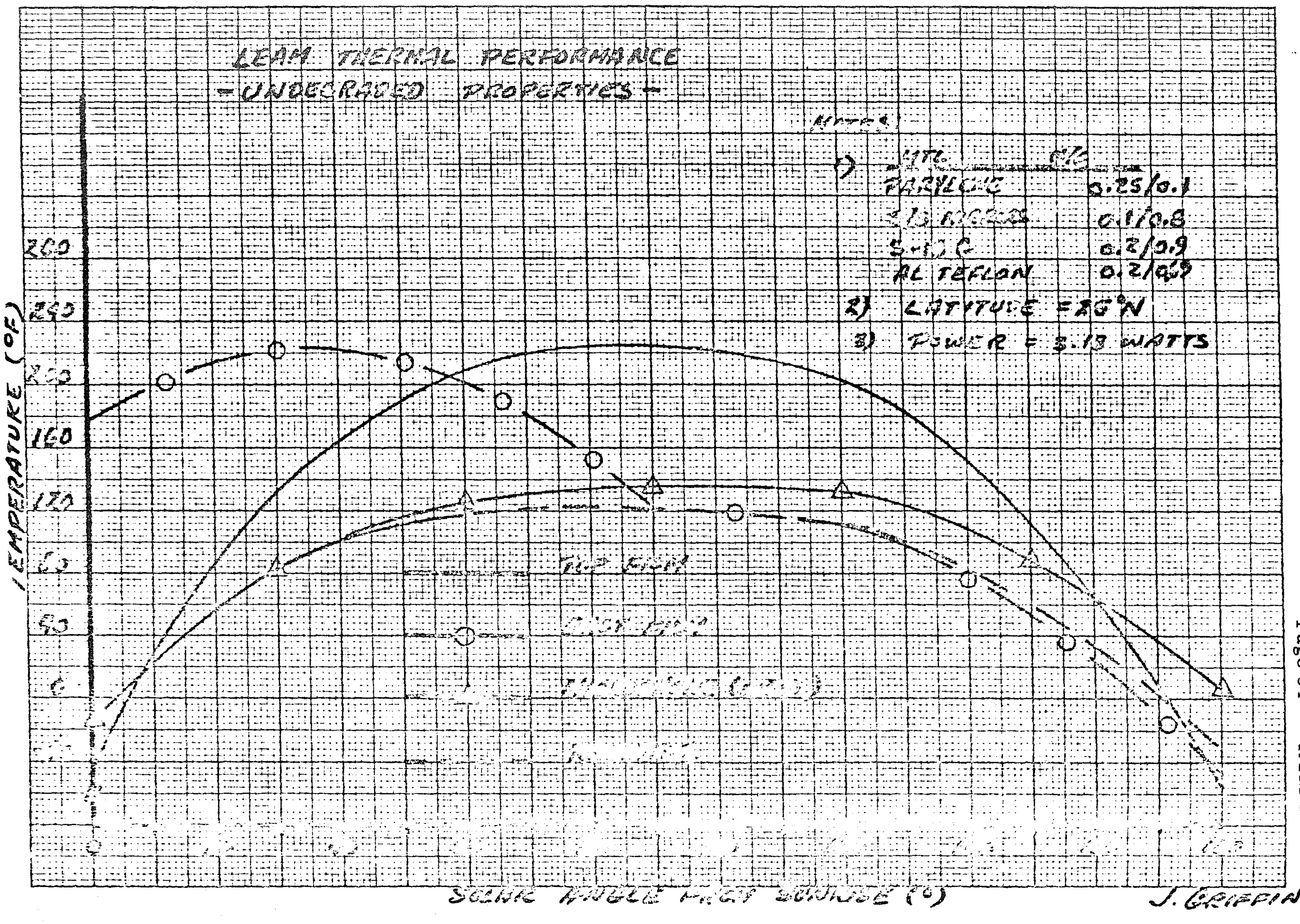
LEAM THERMAL PERFORMANCE
-UNDEGRADED PROPERTIES-
NOTES:
PARYLENE 0.25/0.1
0.1/0.8
0.2/0.9
AL TEFLON
2) LATITUDE = 26°N
3) POWER = 3.13 WATTS
TEMPERATURE (°F)
200
160
J. GRIFFIN

Figure 8.7

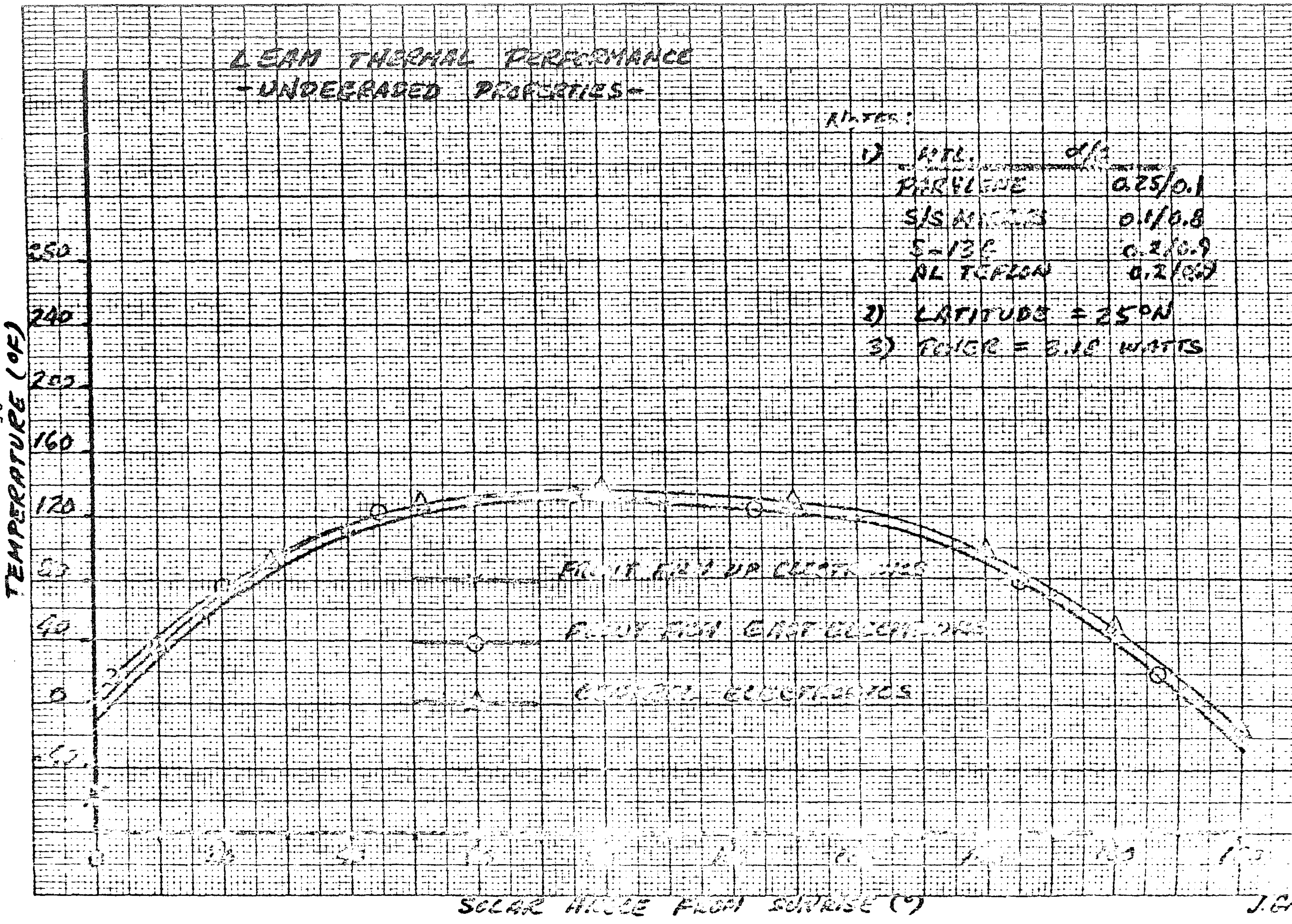
LEAM THERMAL PERFORMANCE
-UNDEGRADED PROPERTIES-
NOTES:
1) MTL. α/ε
PARYLENE 0.25/0.1
S-13G 0.2/0.9
AL TEFLON
2) LATITUDE = 25°N
TEMPERATURE (°F)
280
240
200
160
120
80
40
0
-40
SOLAR ANGLE FROM SUNRISE (°)

K&E 10 X 10 TO ½ INCH 46 1323
7 X 10 INCHES MADE IN U.S.A.
KEUFFEL & ESSER CO.

Figure 8.8

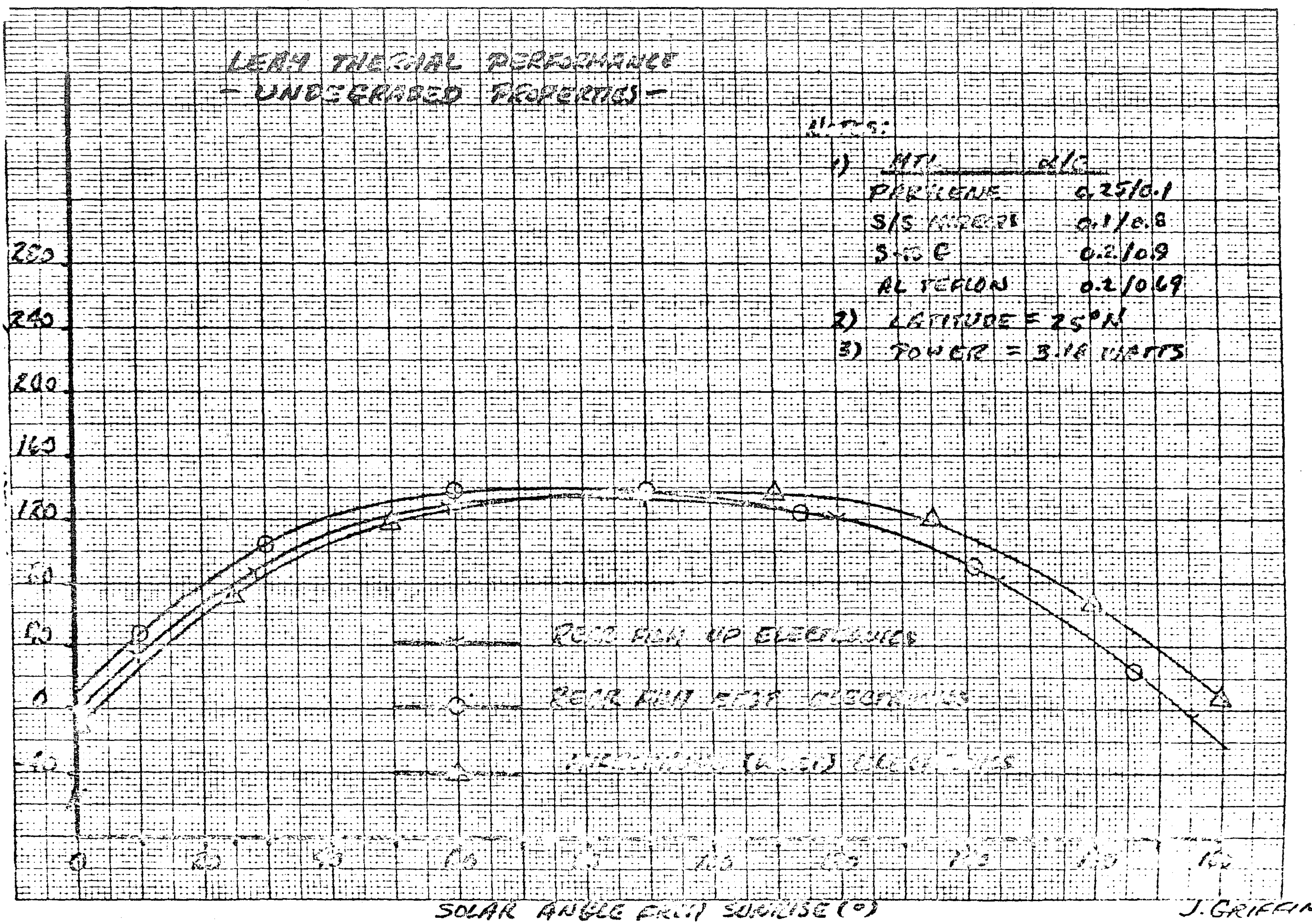

Figure 8.9

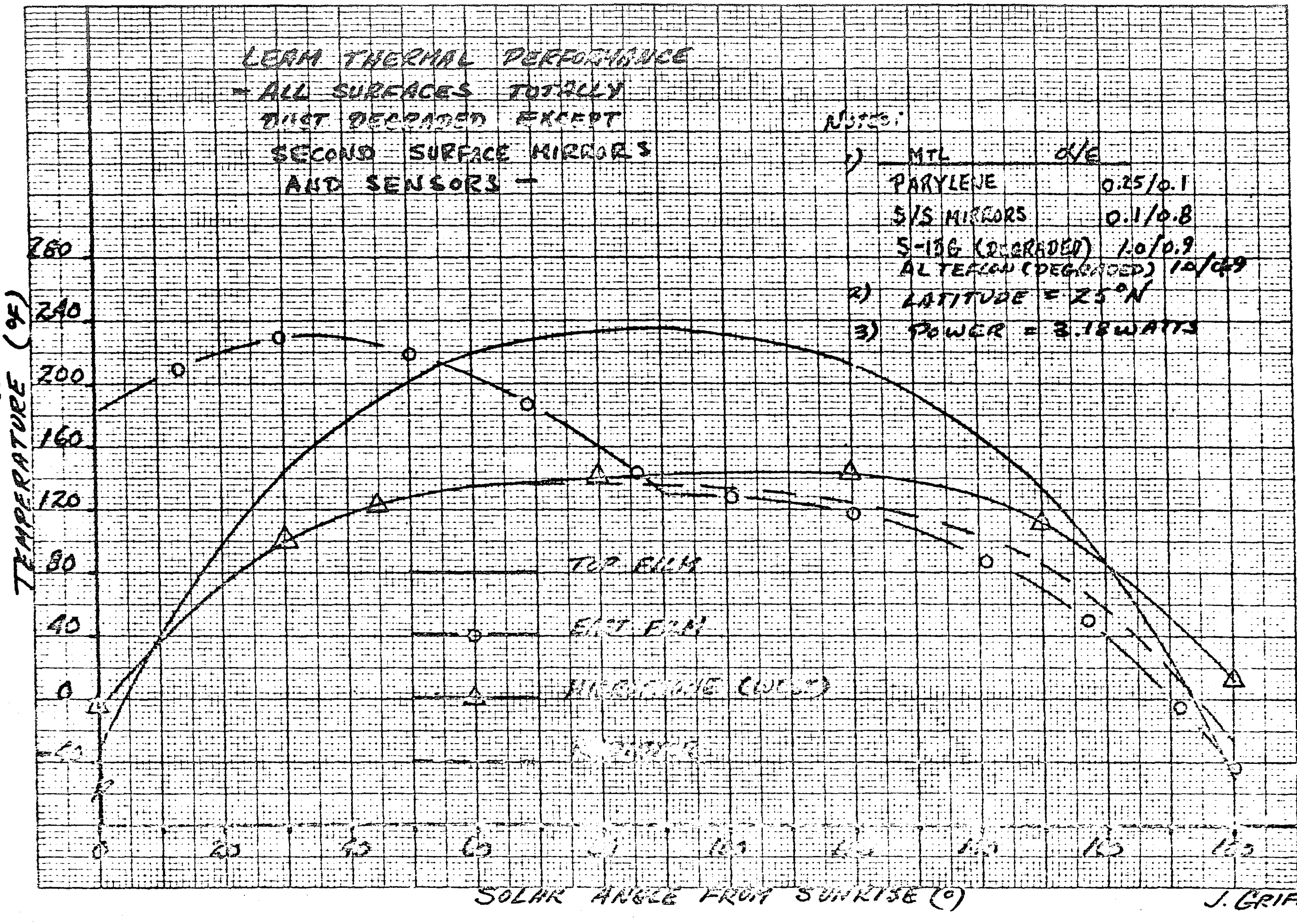
LEAM THERMAL PERFORMANCE
- ALL SURFACES TOTALLY
DUST DEGRADED EXCEPT
SECOND SURFACE MIRRORS
AND SENSORS -
NOTES:
1) MTL α/ε
PARYLENE 0.25/0.1
S/S MIRRORS 0.1/0.8
S-13G (DEGRADED) 1.0/0.9
2) LATITUDE = 25°N
3) POWER = 3.18 WATTS
TOP FILM
TEMPERATURE (°F)
SOLAR ANGLE FROM SUNRISE (°)
J. GRIF
280
240
200
160
120
80
40
0

Figure 8.10

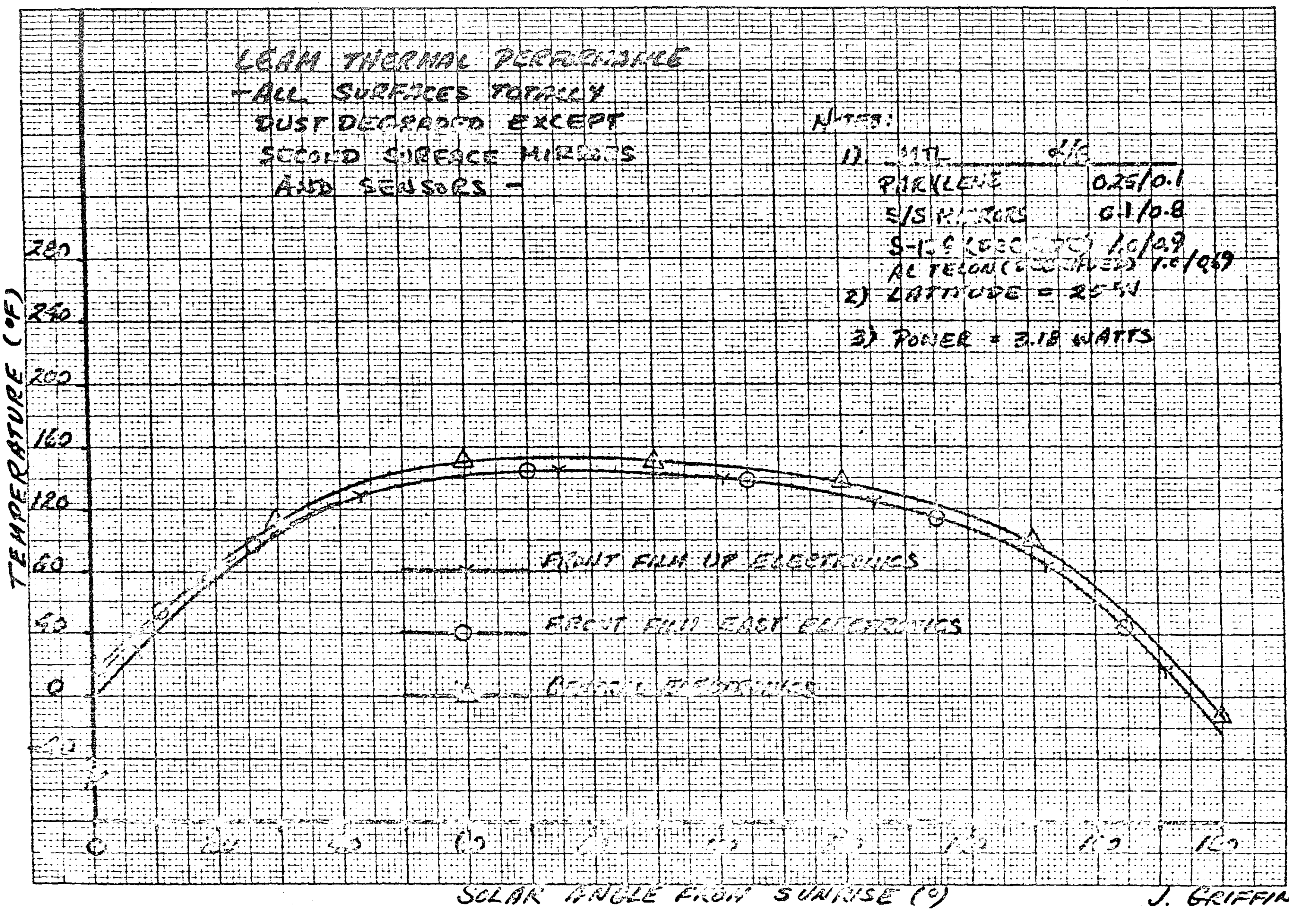
LEAM THERMAL PERFORMANCE
-ALL SURFACES TOTALLY
DUST DEGRADED EXCEPT
SECOND SURFACE MIRRORS
AND SENSORS -
NOTES:
1) MTL α/ε
PARYLENE 0.25/0.1
S/S MIRRORS 0.1/0.8
2) LATITUDE = 25°N
3) POWER = 3.18 WATTS
FRONT FILM UP ELECTRONICS
FRONT FILM EAST ELECTRONICS
TEMPERATURE (°F)
280
240
200
160
120
80
40
0
SOLAR ANGLE FROM SUNRISE (°)
J. GRIFFIN

Figure 8.11

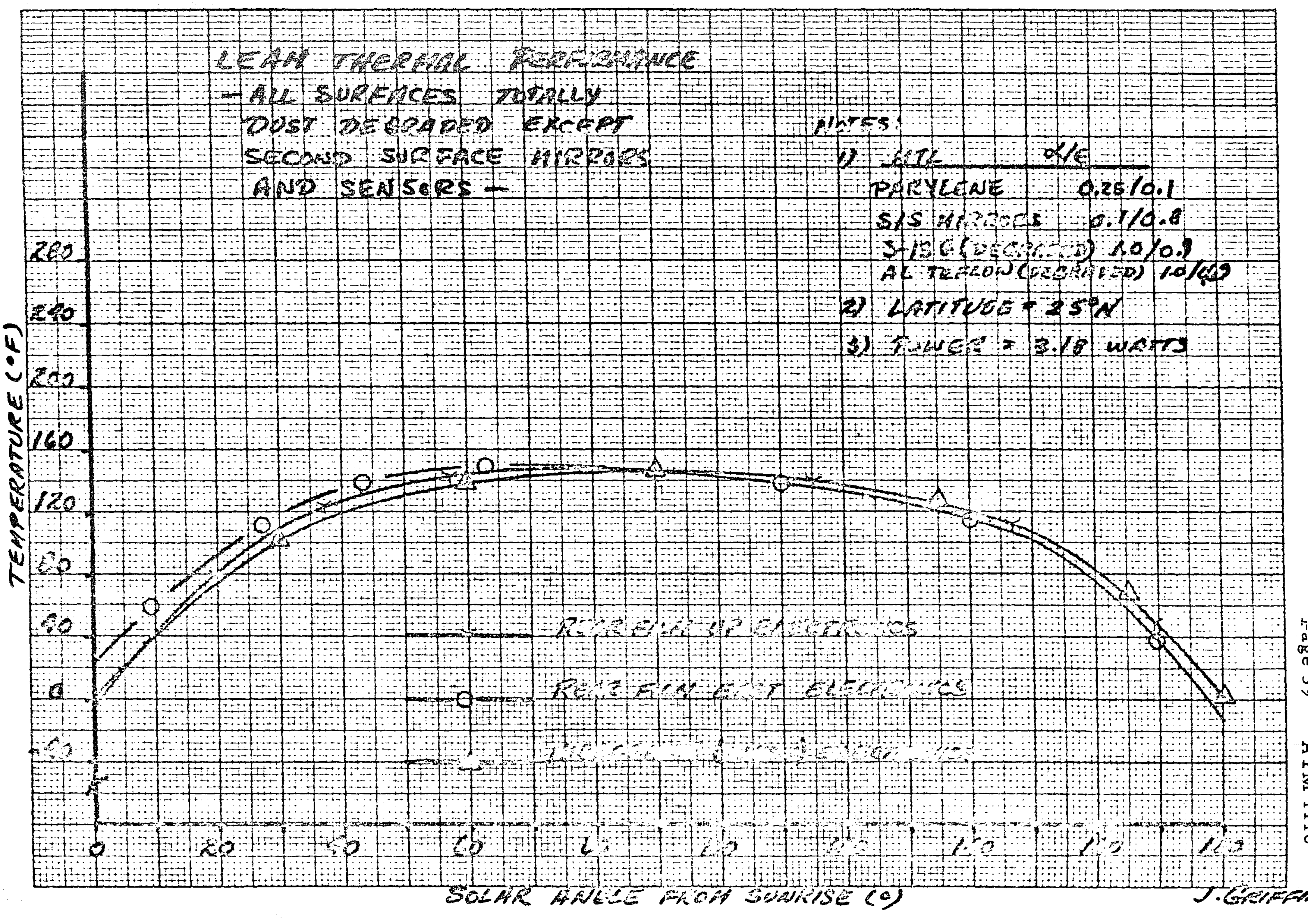
LEAM THERMAL PERFORMANCE
— ALL SURFACES TOTALLY
DUST DEGRADED EXCEPT
SECOND SURFACE MIRRORS
AND SENSORS —
NOTES:
1) MTL α/ε
PARYLENE 0.25/0.1
S/S MIRRORS 0.1/0.8
S-13G (DEGRADED) 1.0/0.9
AL TEFLON (DEGRADED) 1.0/0.9
2) LATITUDE = 25°N
3) POWER = 3.18 WATTS
TEMPERATURE (°F)
280
240
200
160
120
80
40
0
-40
0
20
40
60
SOLAR ANGLE FROM SUNRISE (°)
J. GRIFF

Figure 8.12

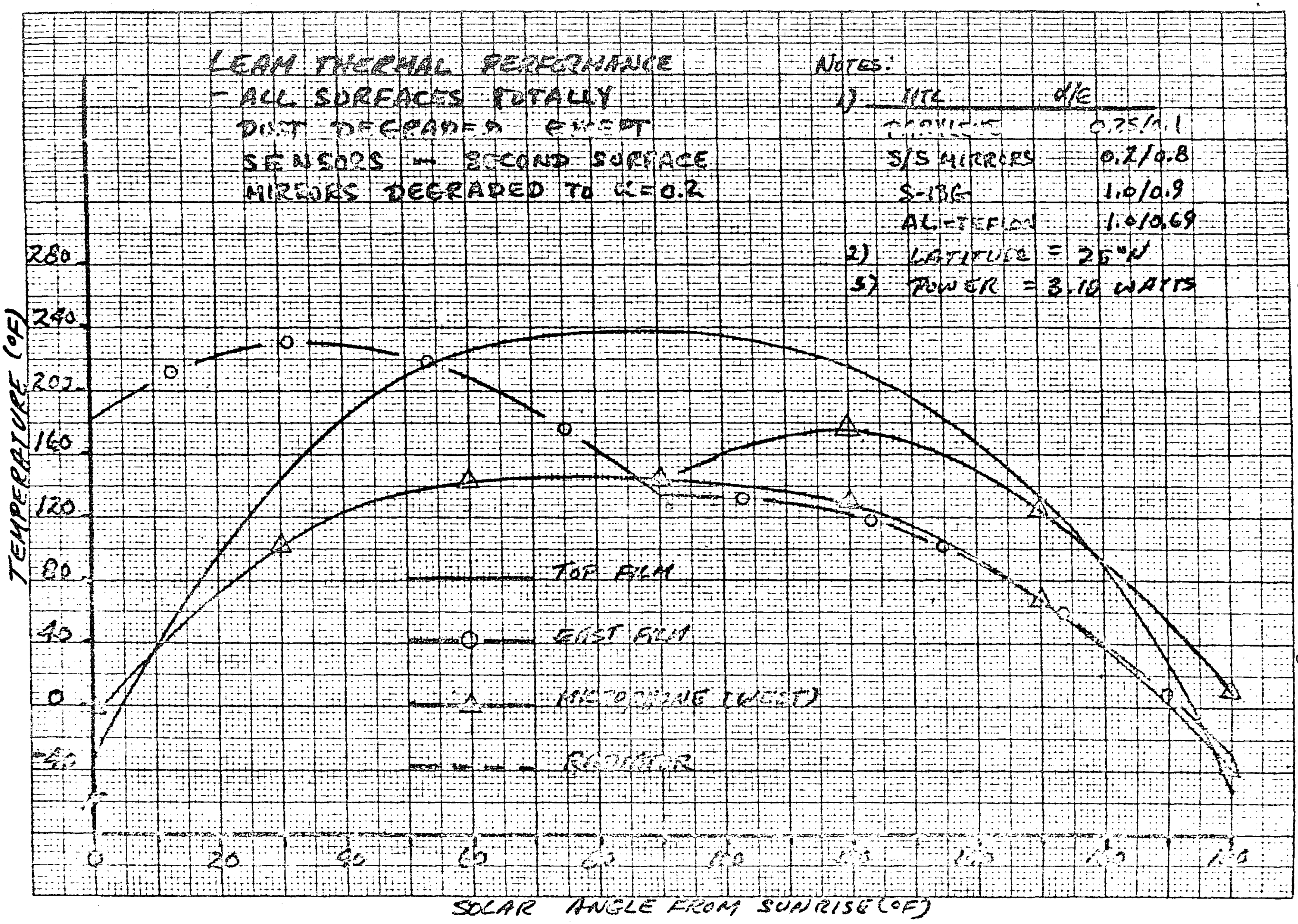
LEAM THERMAL PERFORMANCE
– ALL SURFACES TOTALLY DUST DEGRADED EXCEPT SENSORS – SECOND SURFACE MIRRORS DEGRADED TO α = 0.2
NOTES:
1) MTL α/ε
S/S MIRRORS 0.2/0.8
S-13G 1.0/0.9
AL-TEFLON 1.0/0.69
2) LATITUDE = 25°N
3) POWER = 3.18 WATTS
TEMPERATURE (°F)
280
240
200
160
120
80
40
0
-40
0
20
40
60
TOP FILM
EAST FILM
SOLAR ANGLE FROM SUNRISE (°F)

Figure 8.13

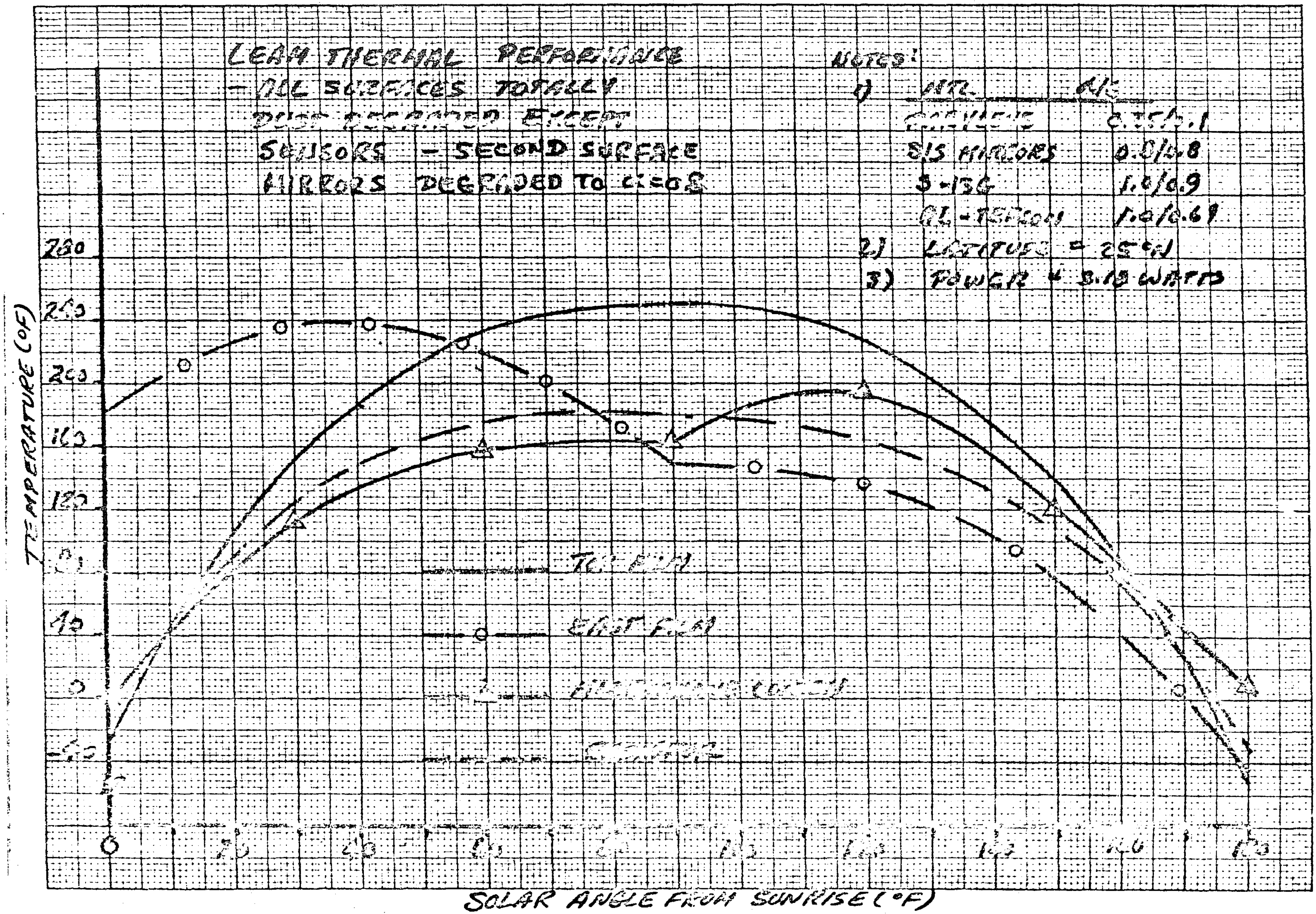
LEAM THERMAL PERFORMANCE
SENSORS - SECOND SURFACE
NOTES:
S/S MIRRORS
S-13G
1.0/0.9
TOP FILM
EAST FILM
280
200
TEMPERATURE (°F)
SOLAR ANGLE FROM SUNRISE (°F)

Figure 8.14

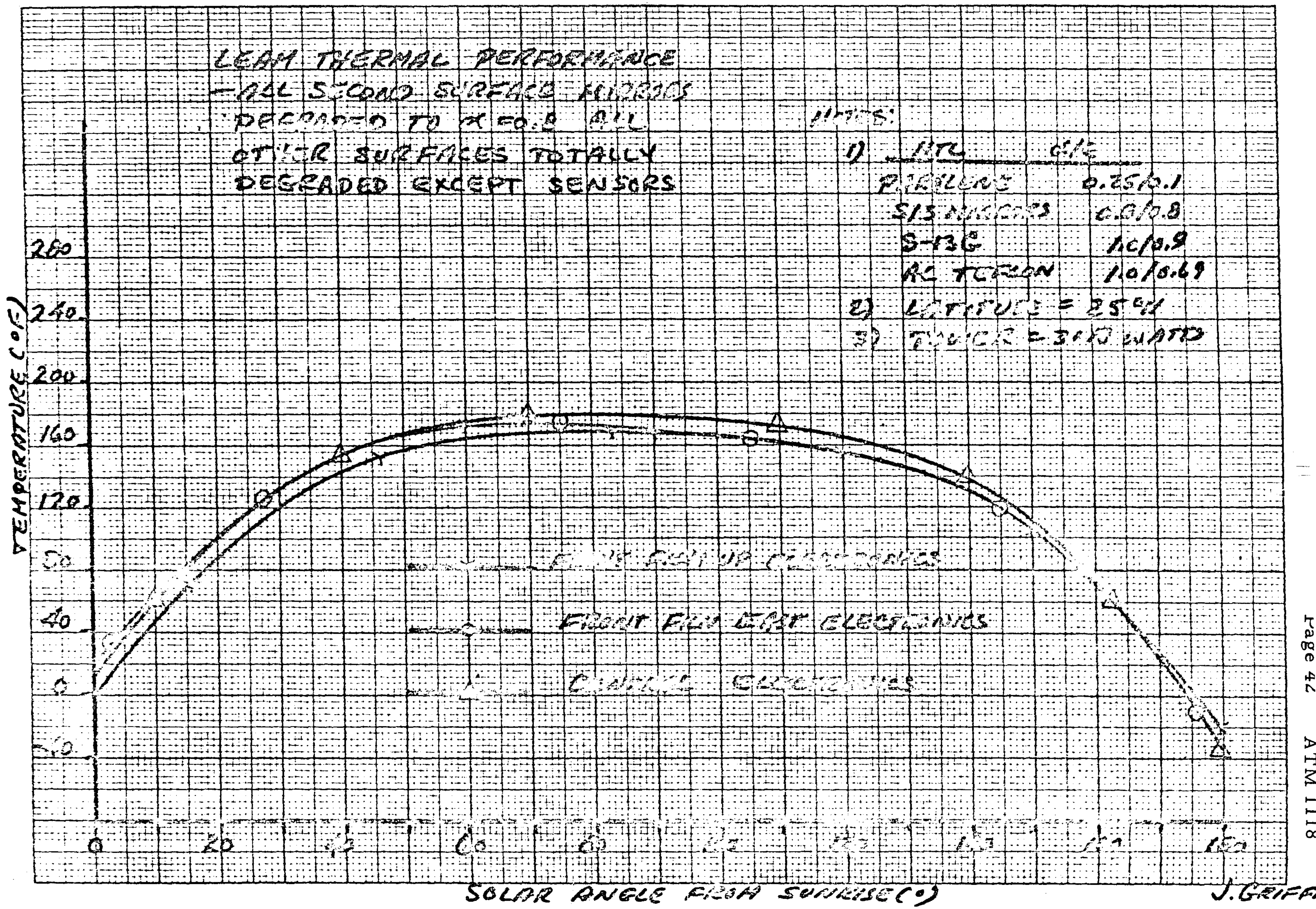
LEAM THERMAL PERFORMANCE
OTHER SURFACES TOTALLY
DEGRADED EXCEPT SENSORS
S-13G
TEMPERATURE (°F)
280
240
200
160
120
40
0
20
160
SOLAR ANGLE FROM SUNRISE (°)
J.GRIFF

Figure 8.15

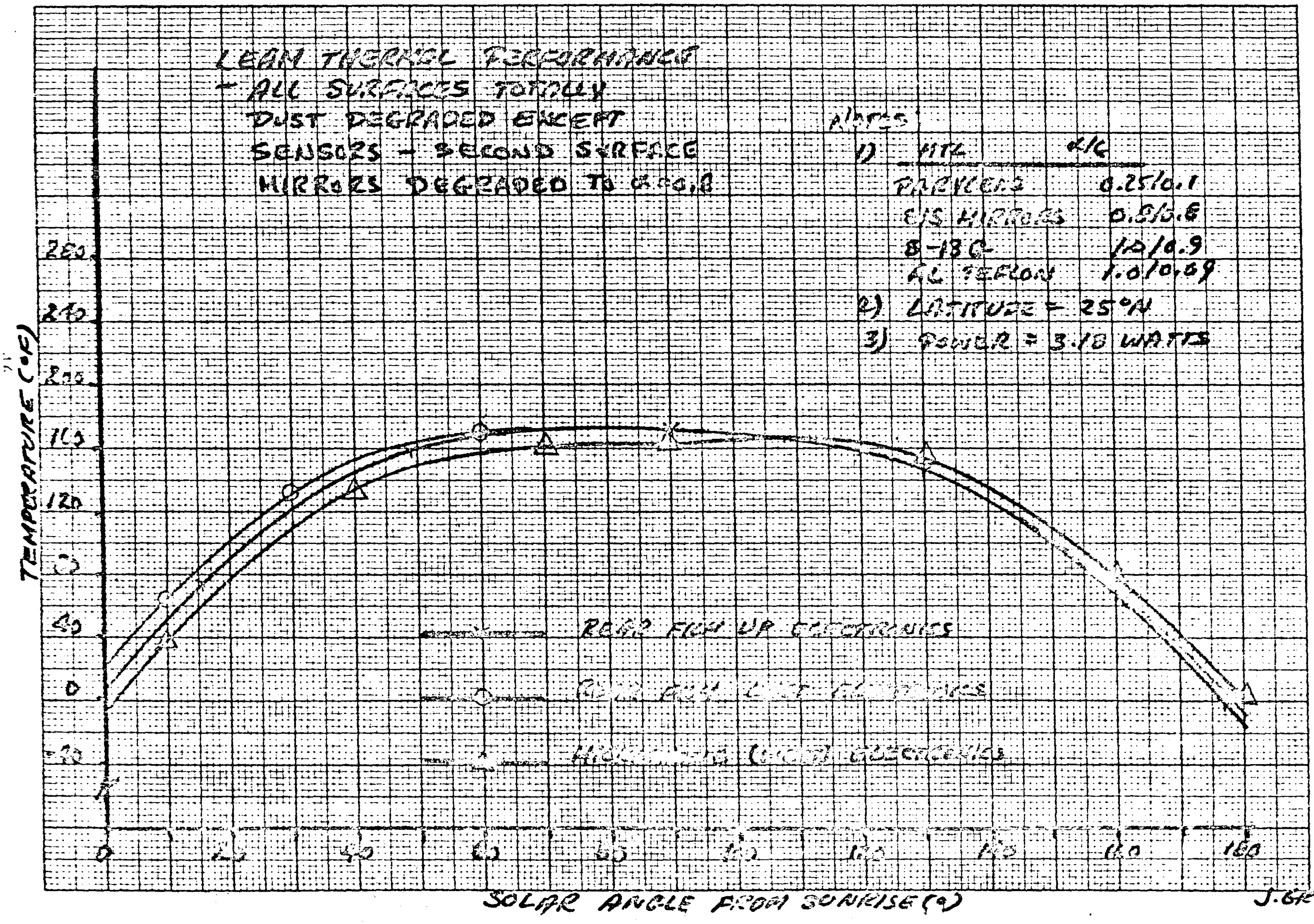
DUST DEGRADED EXCEPT
NOTES
2) LATITUDE = 25°N
3) POWER = 3.18 WATTS
TEMPERATURE (°F)
SOLAR ANGLE FROM SUNRISE (°)

TABLE 8.6

EFFECT OF EXTERNAL SURFACE PROPERTIES ON RADIATOR TEMPERATURE

Solar Absorptance		Radiator Temperature
Radiator & Sensor	All other External Surfaces	(°F)
1. Nominal	Nominal	124
2. Nominal	1.0	136
3. 0.2	1.0	146
4. 0.8	1.0	182

Figure 8.16

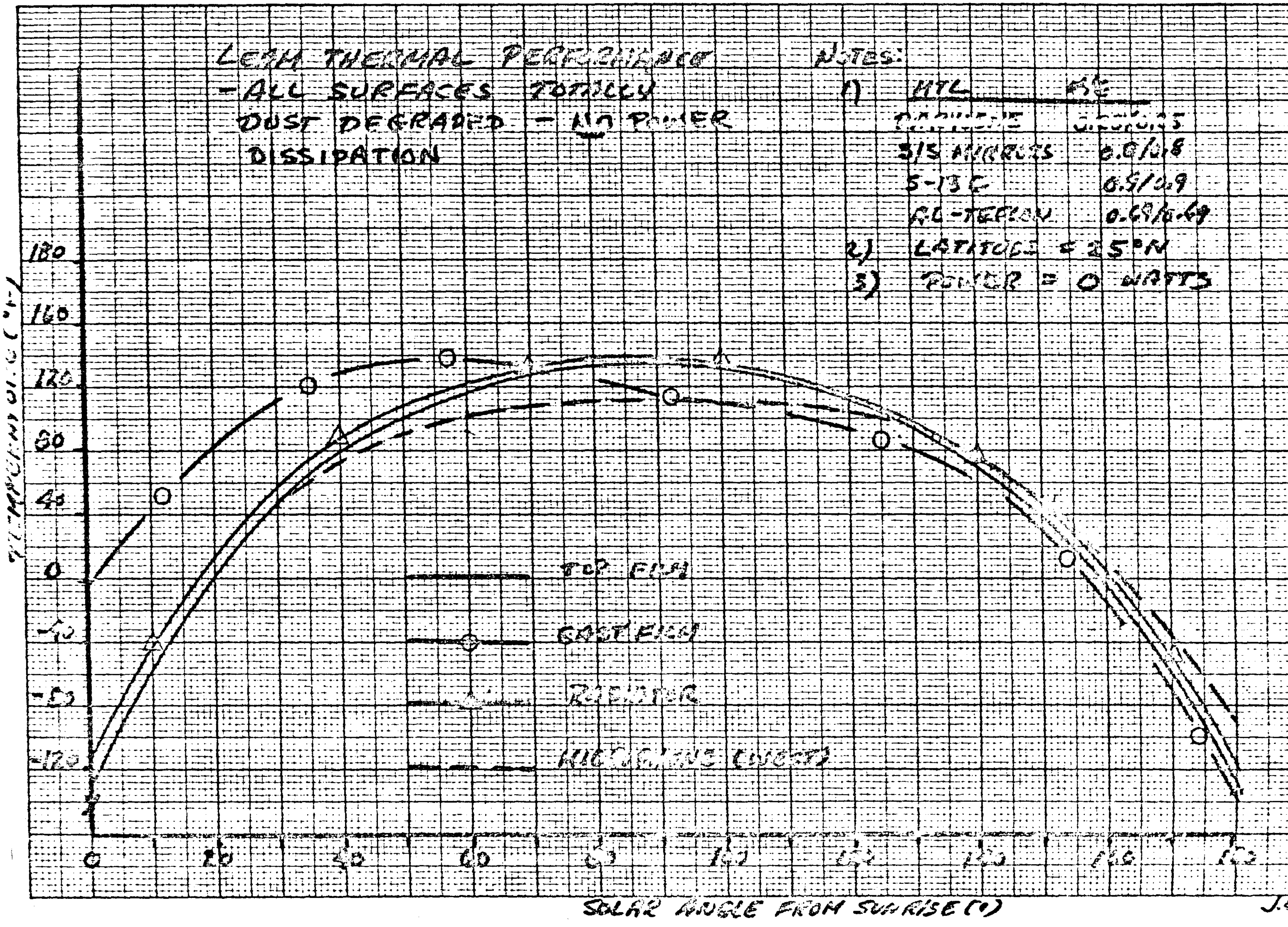

J. GRIFF

8.5 APOLLO 17 MISSION PERFORMANCE

The terrain about the Apollo 17 ALSEP deployment site at Taurus-Littrow is considerably more mountainous than the terrain of all previous deployment sites as can be seen from the panoramic view of Figure 8.17 and the 100 meter contour map shown in Figure 8.19. As a consequence, a study was made to assess the effect upon the LEAM thermal performance at lunar noon.

In general, the effect of mountainous terrain is to: (1) decrease the radiator's view of space, (2) increase the albedo incident on the experiment and (3) increase the direct lunar terrain radiation to the vertical surfaces and add a small thermal load to horizontal surfaces.

The multimode thermal math model was updated to reflect the change in view factors. Two terrain conditions were considered. The first assumed that the terrain had the same slope as the peak of the north massif (i.e. 15°). The second condition utilized an average slope of 7 degrees which was obtained by integrating over the 360° panorama. Table 8.7 presents the results of the study and compares the effect of the two slope conditions to a planar terrain. Note that for the 7° slope all temperatures are within the upper operating temperature limit of 149°F, whereas for the 15° slope condition the central electronics exceeds the upper operating temperature limit by 3.9°F.

Since the 7° slope is the most realistic condition, it is concluded that no modifications are required for this experiment.

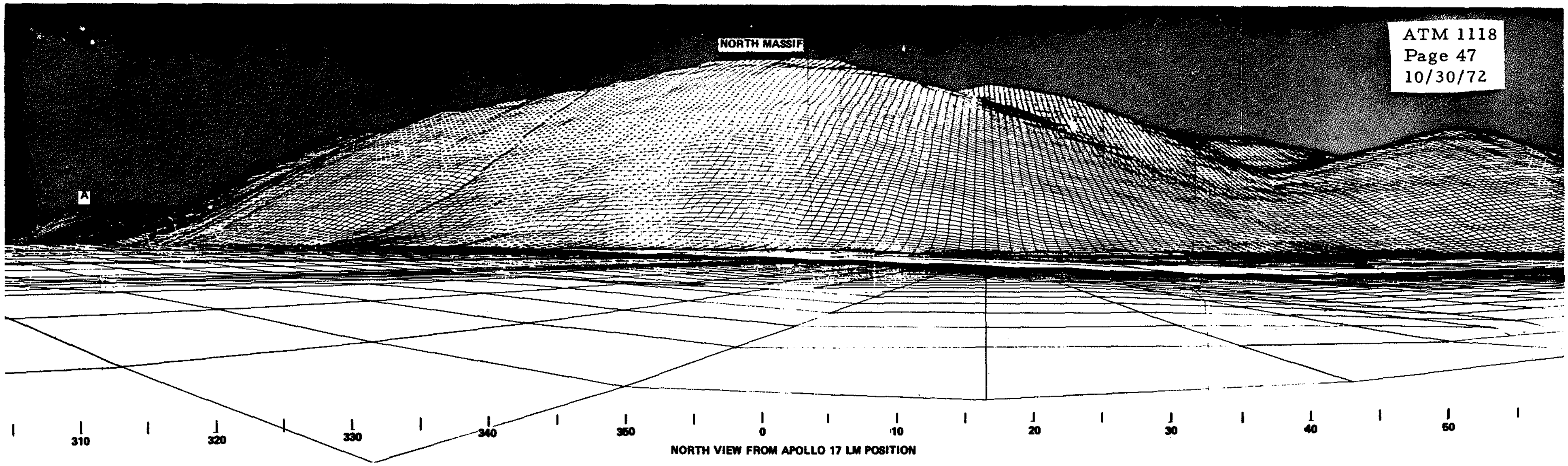

NORTH VIEW FROM APOLLO 17 LM POSITION

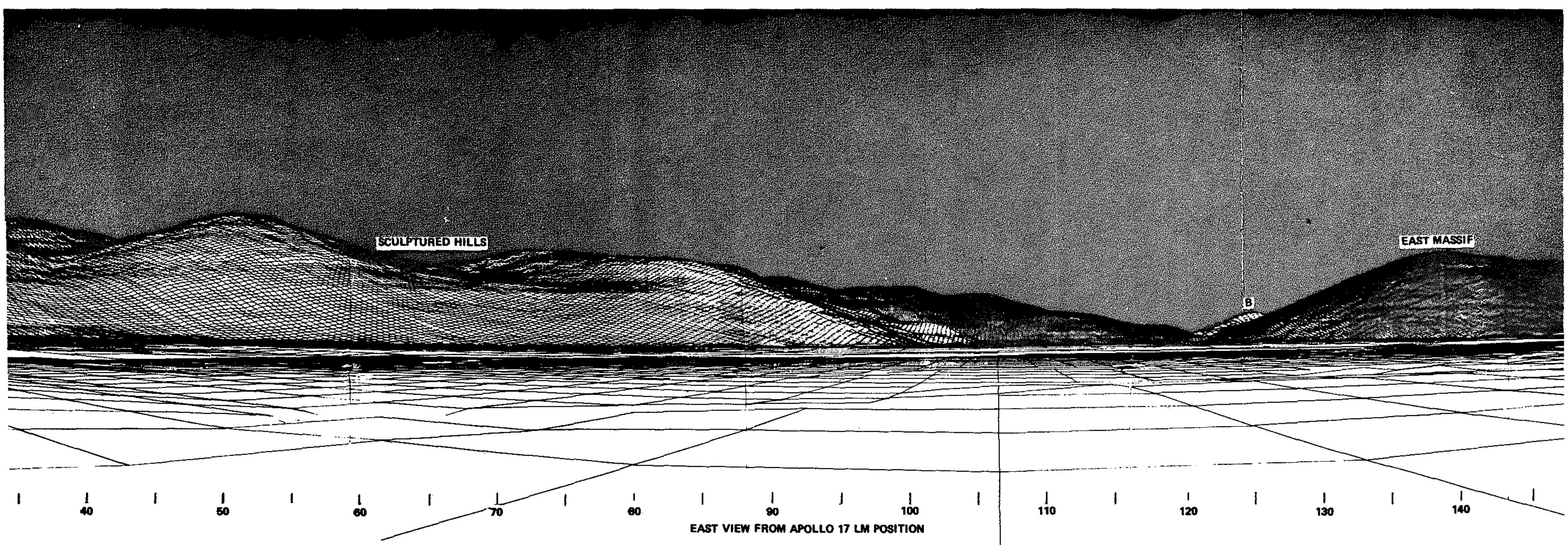

EAST VIEW FROM APOLLO 17 LM POSITION

FIGURE 8. 17 Computer Generated Panorama

ATM 1118
Page 48
10/30/72

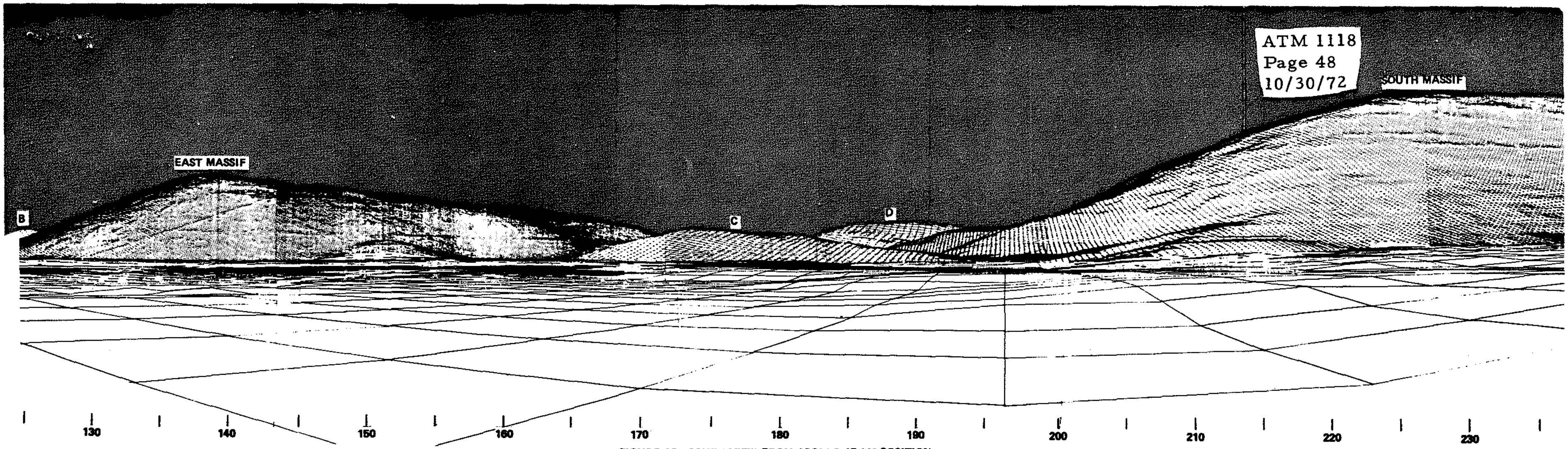

FIGURE 1C - SOUTH VIEW FROM APOLLO 17 LM POSITION

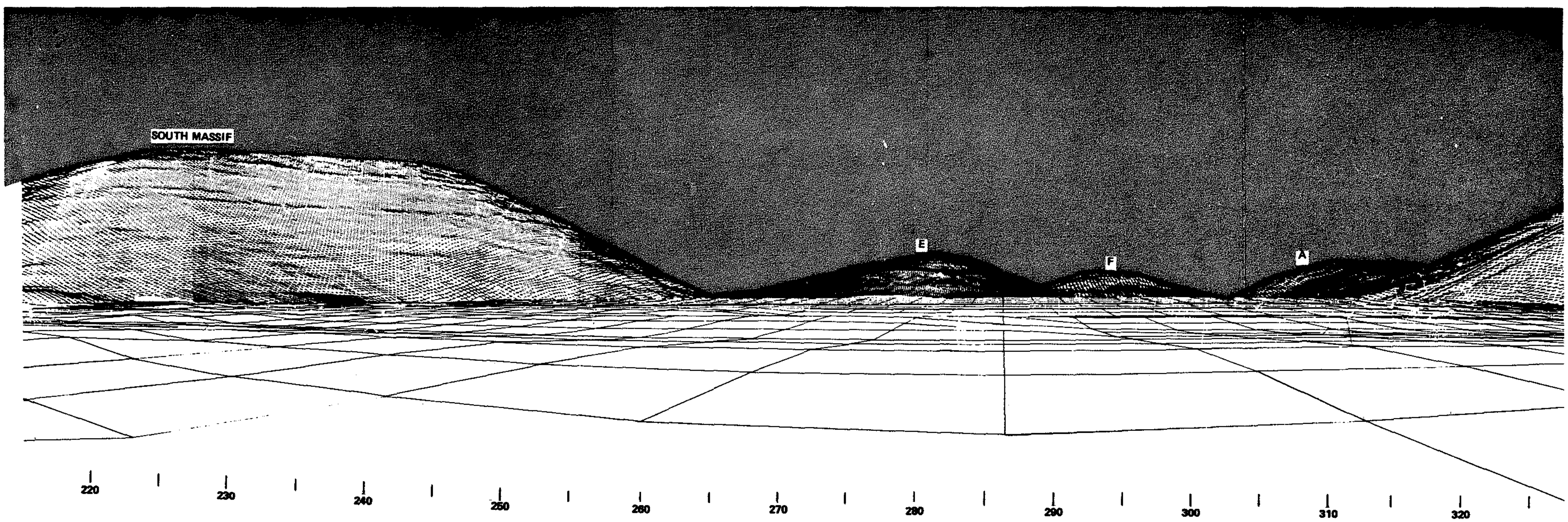

WEST VIEW FROM APOLLO 17 LM POSITION

FIGURE 8. 17 Computer Generated Panorama (Cont.)

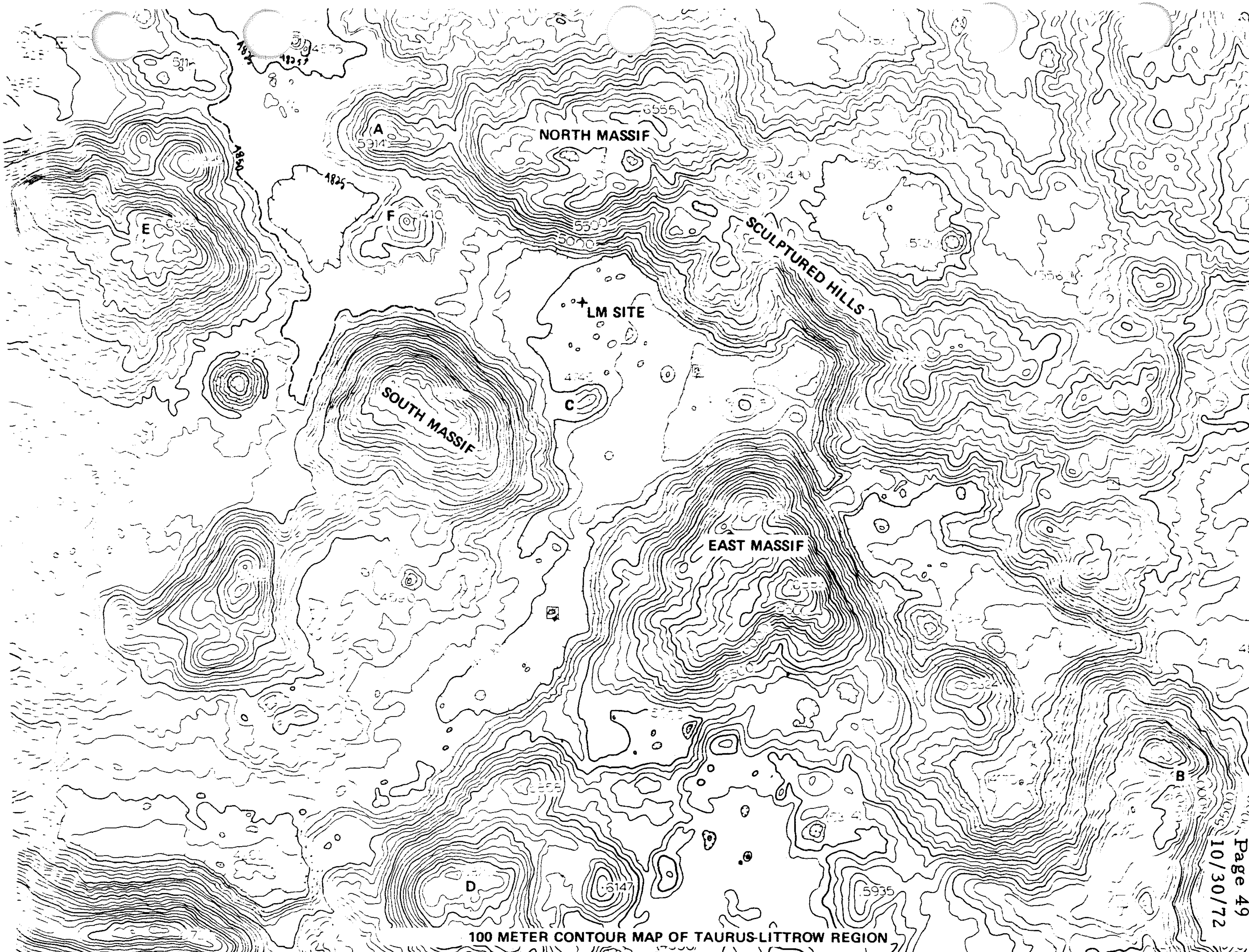

FIGURE 8.18 ALSEP DEPLOYMENT SITE

TABLE 8.7

Lunar Terrain Effects on LEAM Component Temperatures

	Node	Planar Terrain T(°F)	15° slope T °F	7° slope T °F
UP Sensor				
Outer Front Grid Frame	1	96.4	110.0	102.8
Front Film	2	226.8	237.4	231.6
Front Film Frame	3	112.5	127.0	119.6
Forward Electronics	5	127.2	145.0	136.0
Support Structure	14	127.1	144.9	135.9
Rear Grid Frame	9	127.4	144.7	135.8
Rear Film/Impact Plate	30	130.0	147.4	138.7
Rear Electronics	13	130.8	148.2	139.5
East Sensor				
Outer Front Grid Frame	101	121.8	133.0	127.4
Front Film	102	122.7	134.6	128.0
Front Film Frame	103	123.7	136.4	130.1
Forward Electronics	105	129.2	145.5	137.0
Support Structure	114	129.1	145.4	137.0
Rear Film/Impact Plate	130	131.2	147.3	139.2
Rear Electronics	113	131.9	148.1	139.1
Rear Grid Frame	109	129.0	144.9	137
West Sensor				
Grid Frame	209	115.0	120.5	118.0
Small Film/Impact Plate	230	127.9	142.7	134.9
Large Film/Impact Plate	231	127.8	142.5	134.9
Electronics	213	128.9	144.0	136.9
Central Electronics	32	133.5	152.9	142.2
Internal Structure	33	126.6	146.2	136.5
Radiator	23, 24	123.9	144.9	133.9

9.0 DVT T/V TEST

The purpose of the DVT T/V test was to verify the thermal performance during lunar noon conditions and to determine the total power required for lunar night operation. The environmental conditions simulated during the test were lunar night, sunrise, and noon. Lunar surface simulator temperatures were -300°F, -150°F and +250°F for the three primary test conditions. Carbon arc solar simulation was utilized for the noon and sunrise conditions. An additional lunar noon condition was performed using infrared lamps for comparison with the carbon arc results.

The DVT model is shown in Figure 9.1 with thermocouples mounted just prior to T/V chamber deployments. The electronic package power dissipations for the central electronics and sensor microphone electronics were simulated by appropriately sized heaters bonded to an aluminum plate for the central electronics and to epoxy fiberglass plates for the microphone electronics as shown in Figure 9.2. The lunar surface simulator consisted of a 34 inch diameter plate with a 7 inch lip perpendicular to the plate. The simulator was vertical, as a consequence, the legs were attached to the surface as shown in Figure 9.3.

Thermocouple locations on the single and dual sensors are illustrated in Figures 9.4 (west sensor), 9.5 (up sensor) and 9.6 (east sensor). Thermocouples mounted on the internal and external structures are shown in Figures 9.7 and 9.8 respectively.

Temperature profiles of the central electronics, the radiator and the west sensor quartz plate are presented in Figure 9.9. The termination of each test condition is noted.

The lunar night test results for 5, 6, and 7 watt conditions are presented in Table 9.1 along with the analytic correlation for each respective condition. A comparison between the 5 watt survival condition and the 5 watt night condition is made in Table 9.2. The power dissipation of each component is presented in addition to the components temperature. Correlation of the survival condition is shown in Table 9.3.

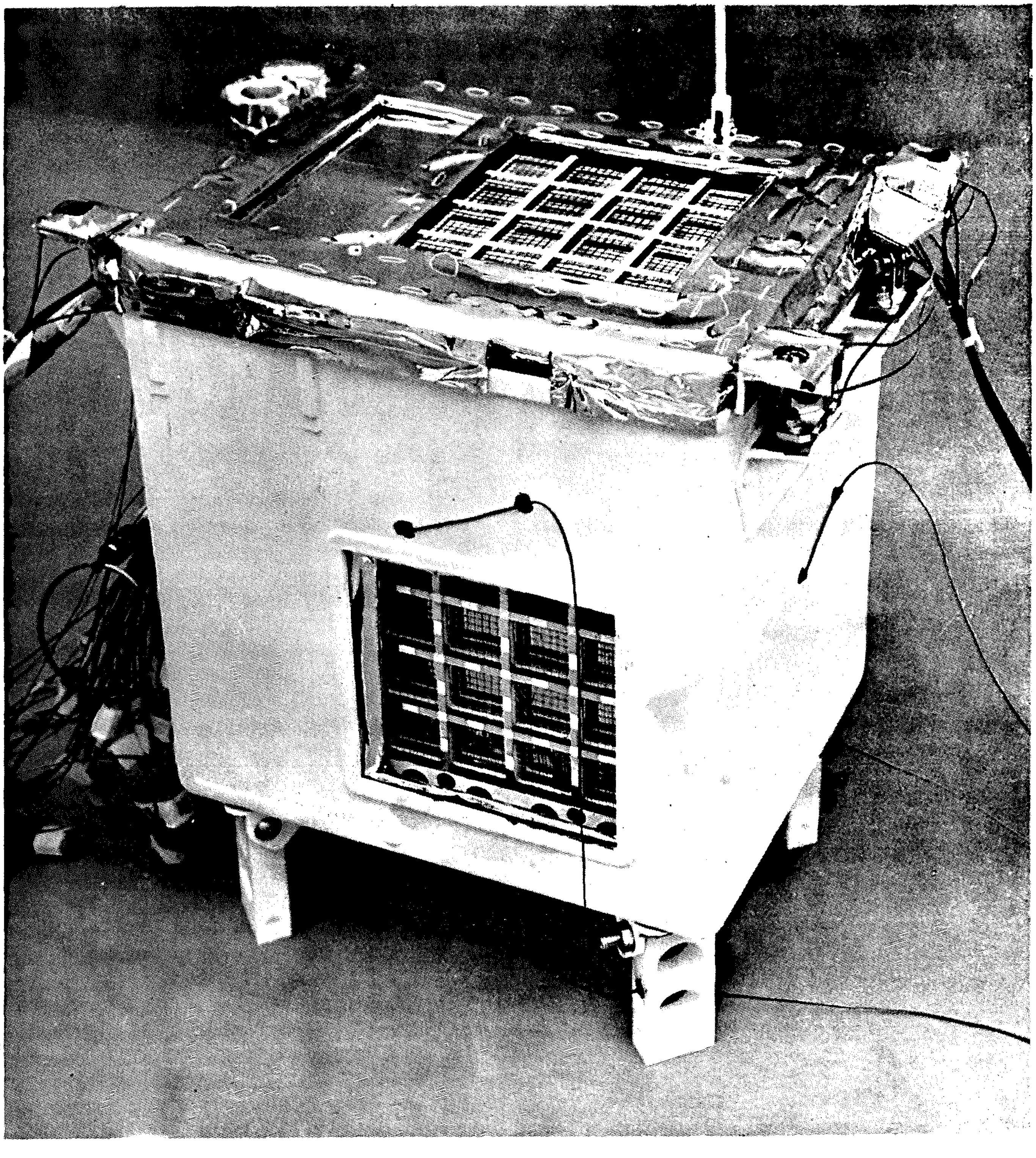

9270-500

LEAM DVT Model

Figure 9.1

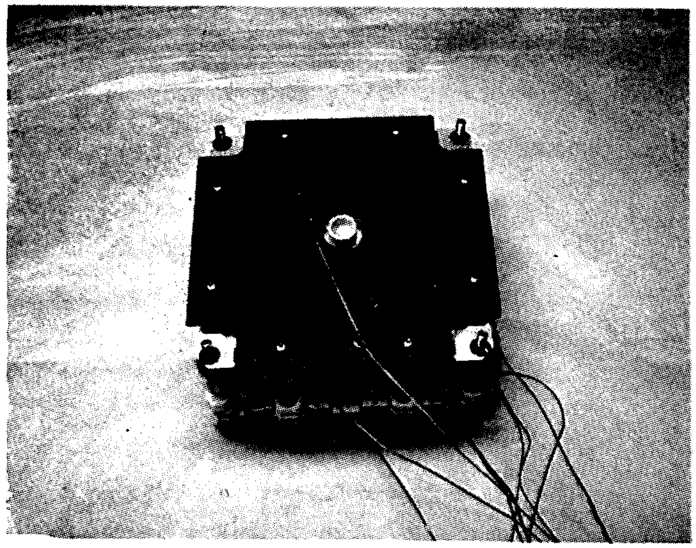

EAST SENSOR MICROPHONE "BOARD"

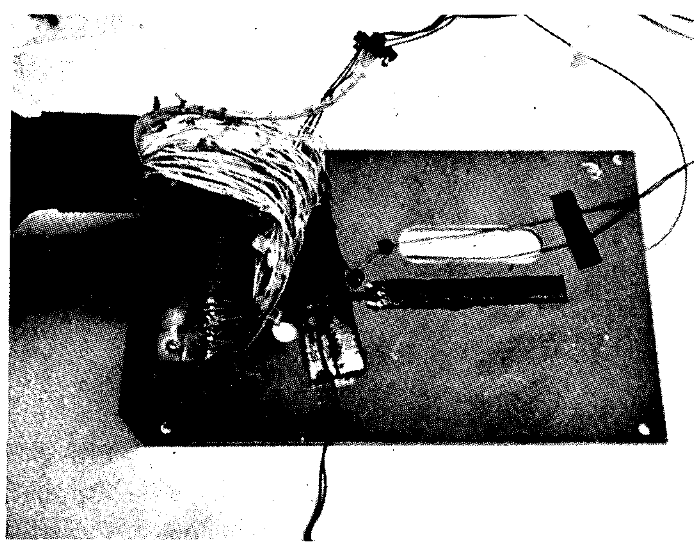

9270-501

CENTRAL ELECTRONICS "BOARD"

Simulated Electronics

Figure 9.2

9270-505

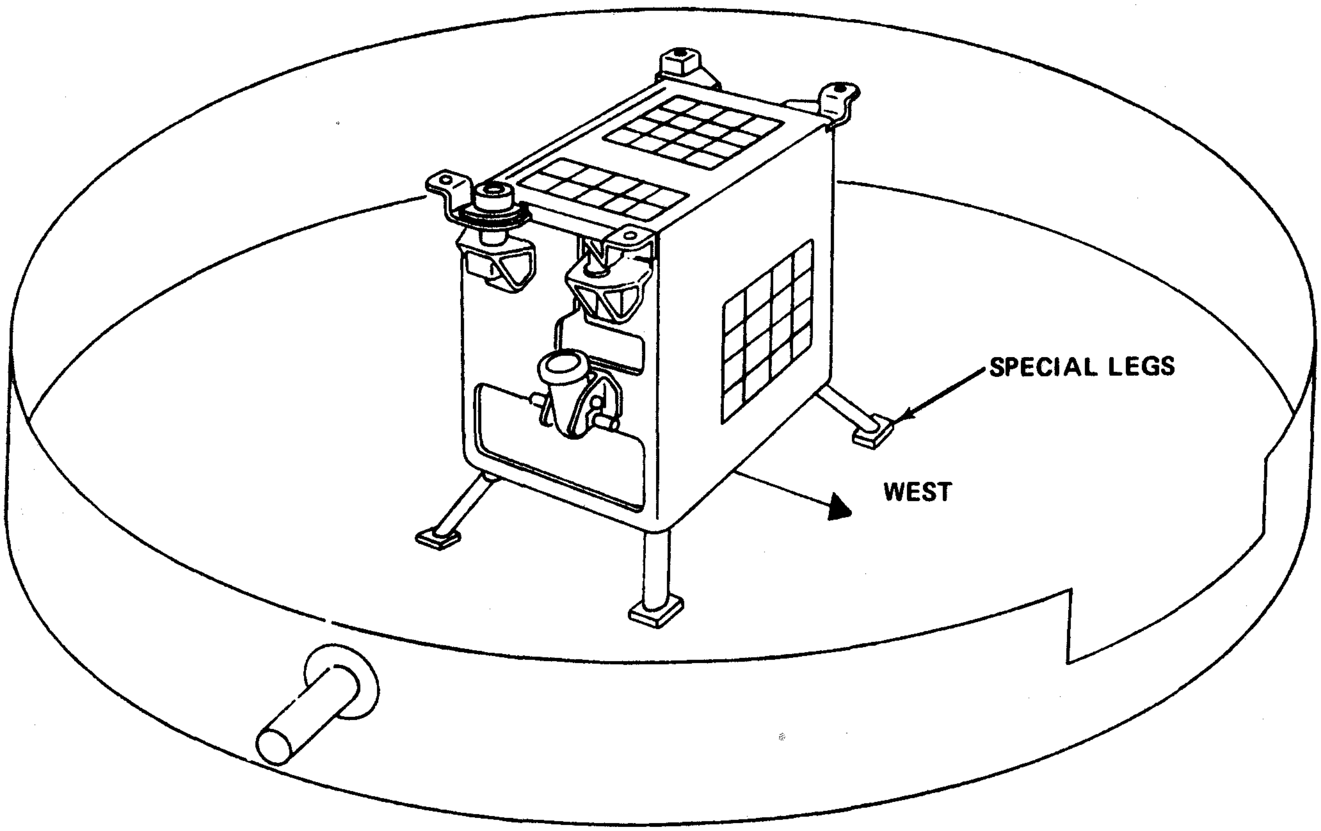

Figure 9.3 DVT Model on Lunar Surface Simulator

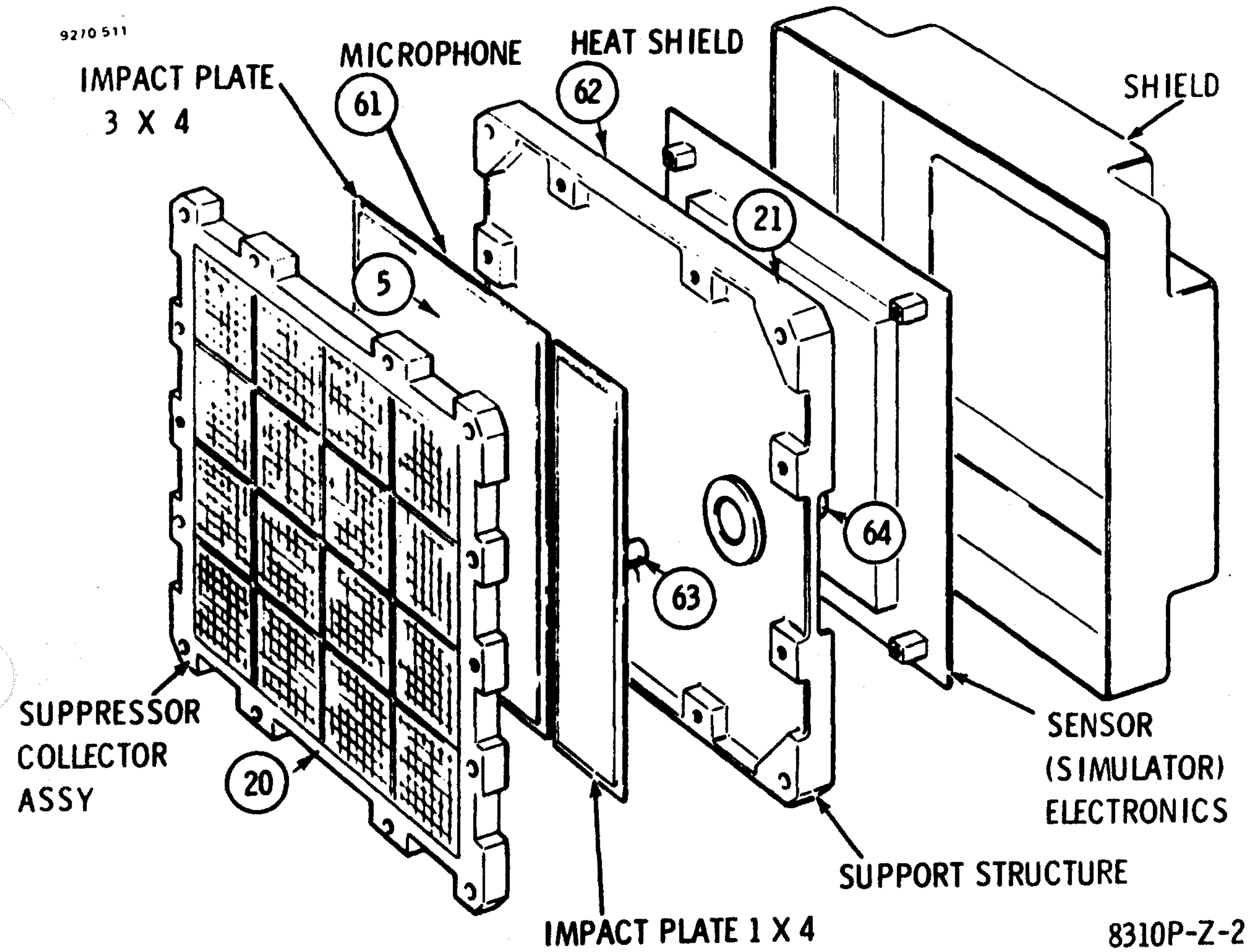

Figure 9.4 Exploded View of Single Sensor (T/C Locations West Sensor)

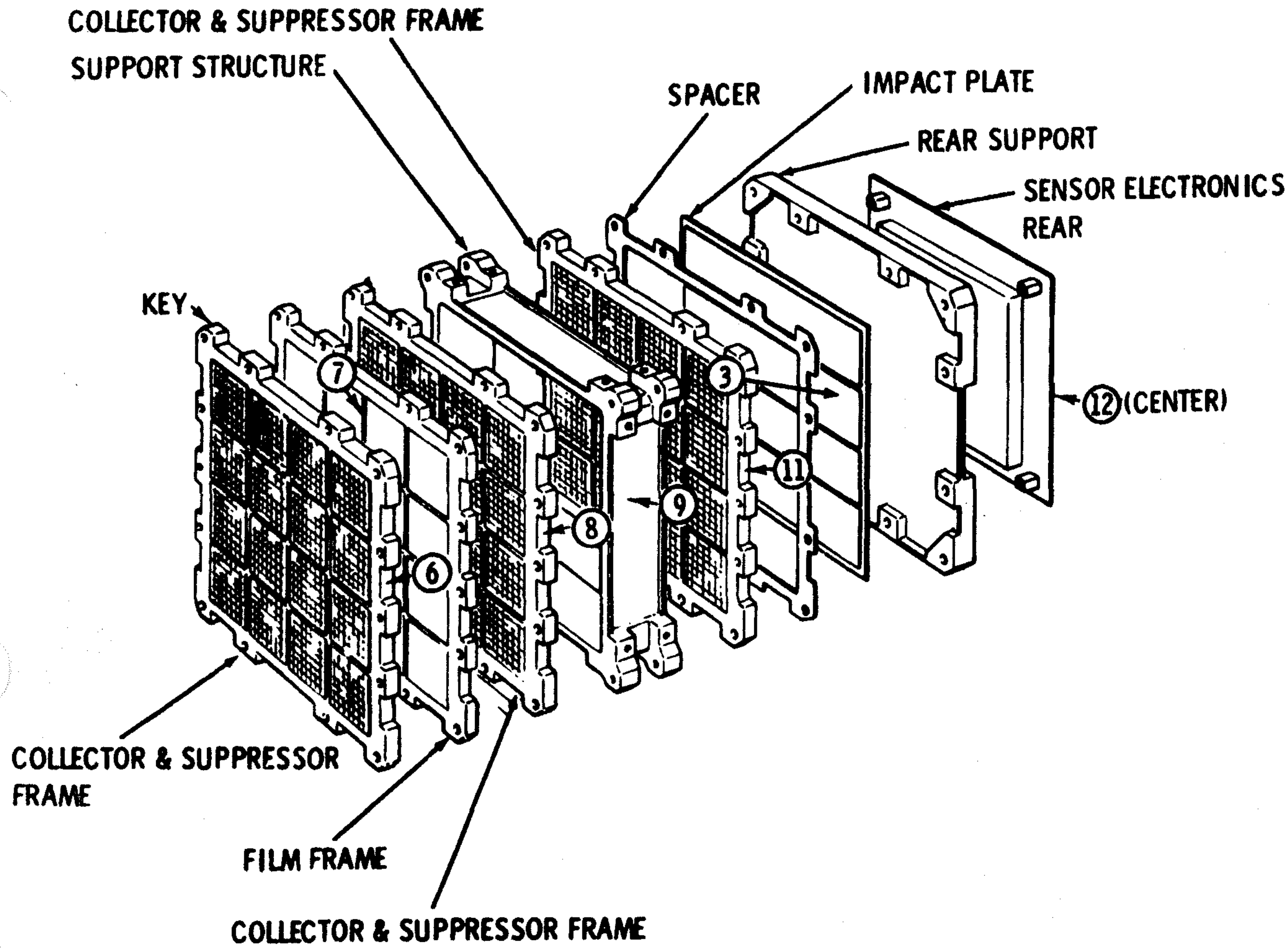

Figure 9.5 Exploded View of Dual Sensor
(T/C Locations Up Sensor)

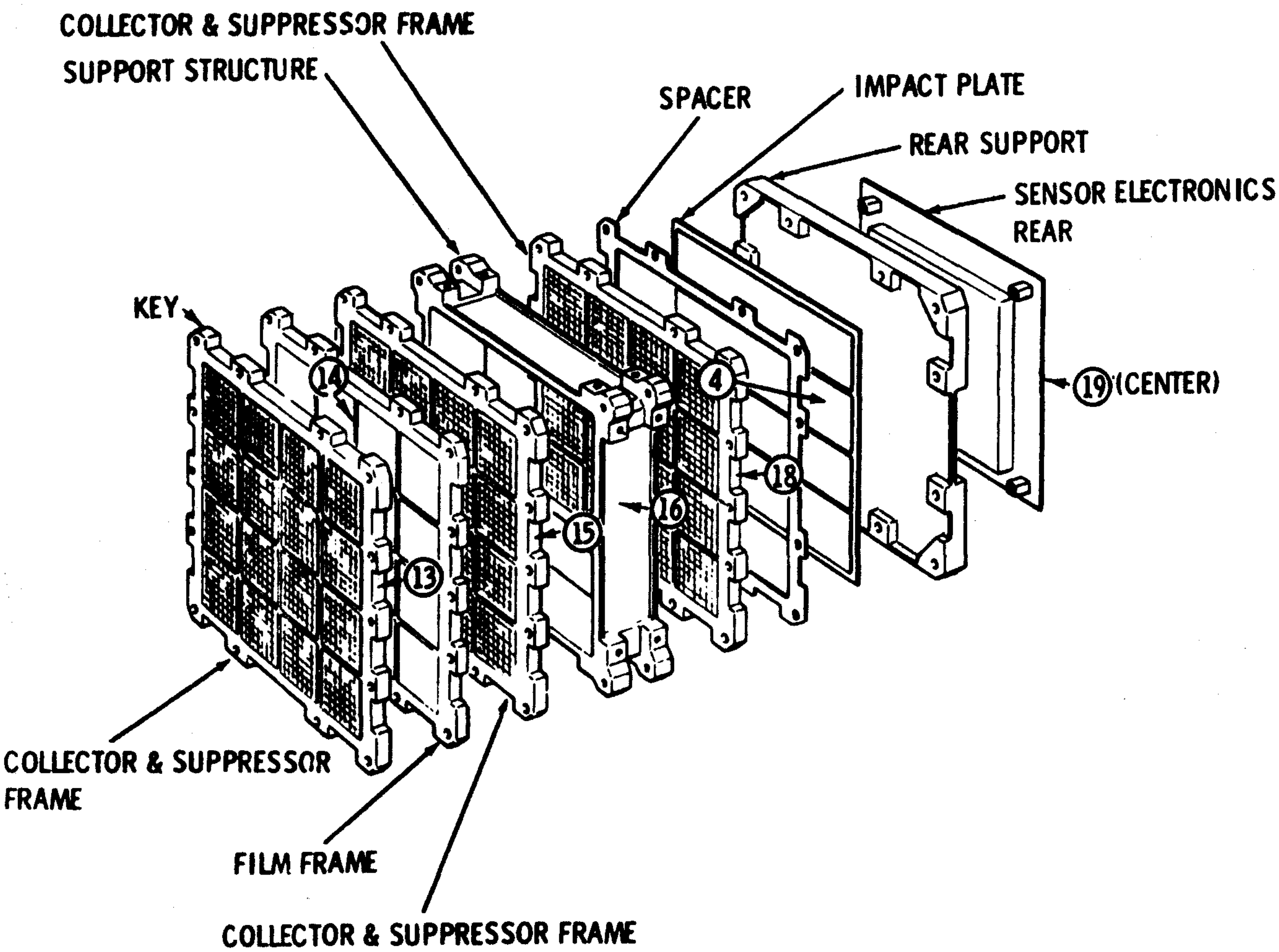

Figure 9.6 Exploded View of Dual Sensor (T/C Locations East Sensor)

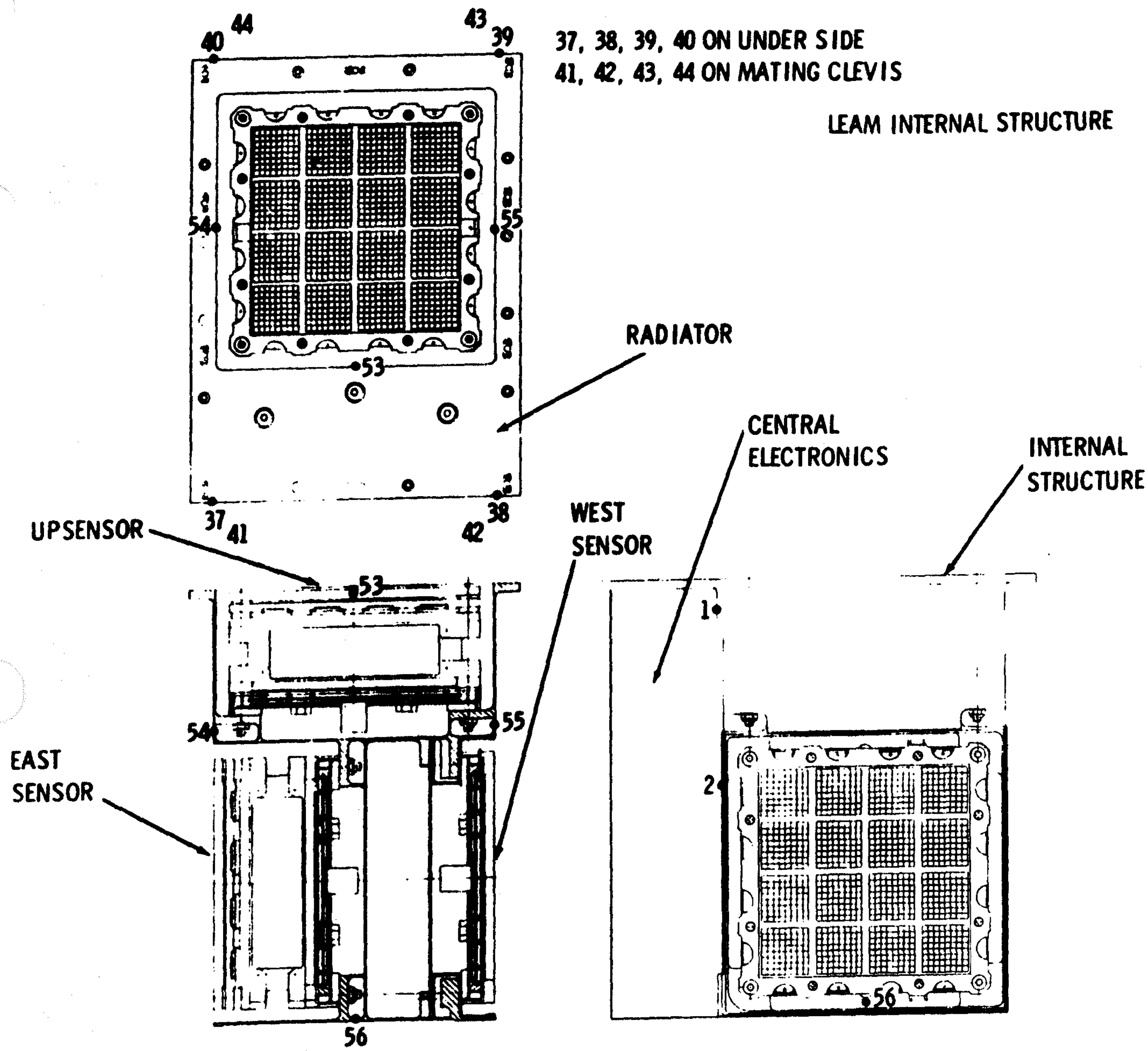

Figure 9.7 LEAM Internal Structure
(T/C Locations)

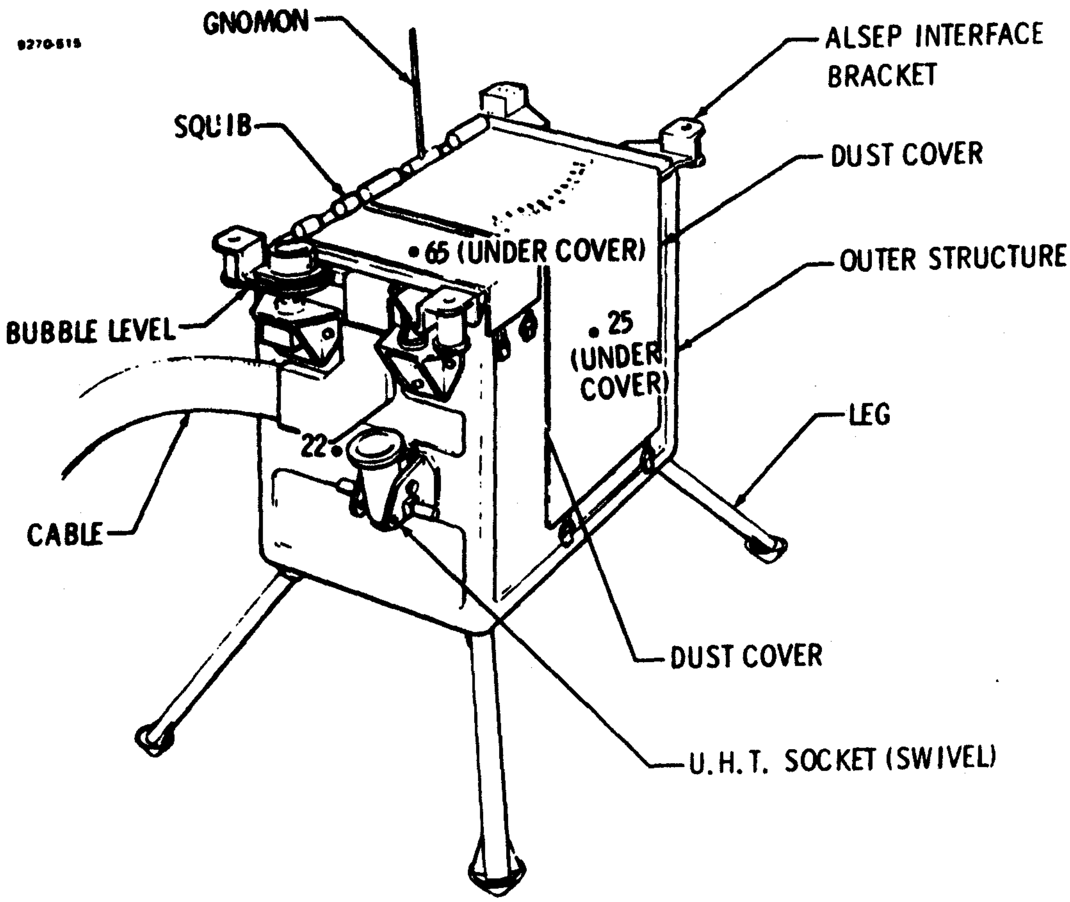

Figure 9.8 LEAM External Structure N-W
(T/C Locations)

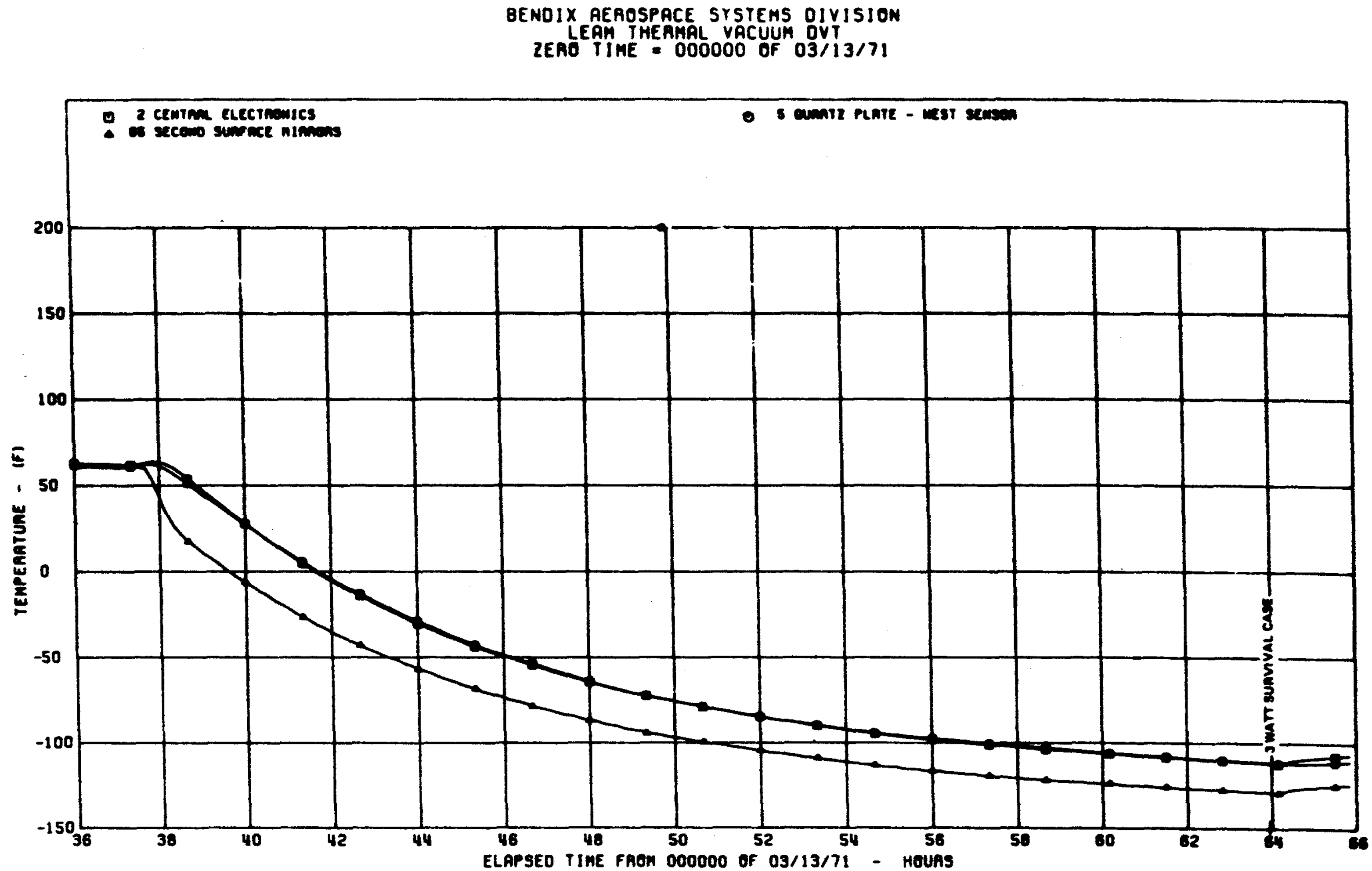

Figure 9.9 Graphical History of Test

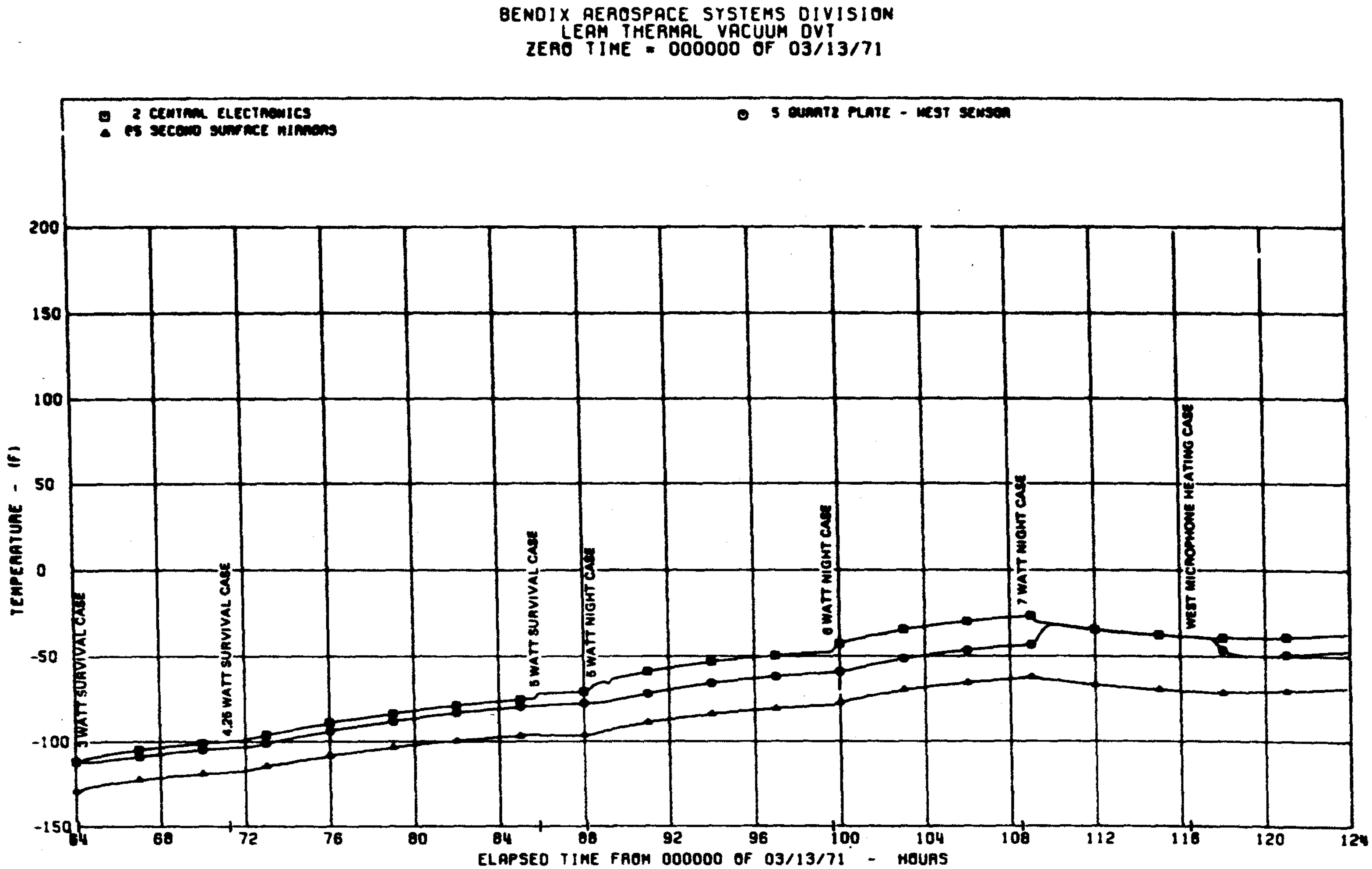

Figure 9.9 **Graphical History of Test (Cont.)**

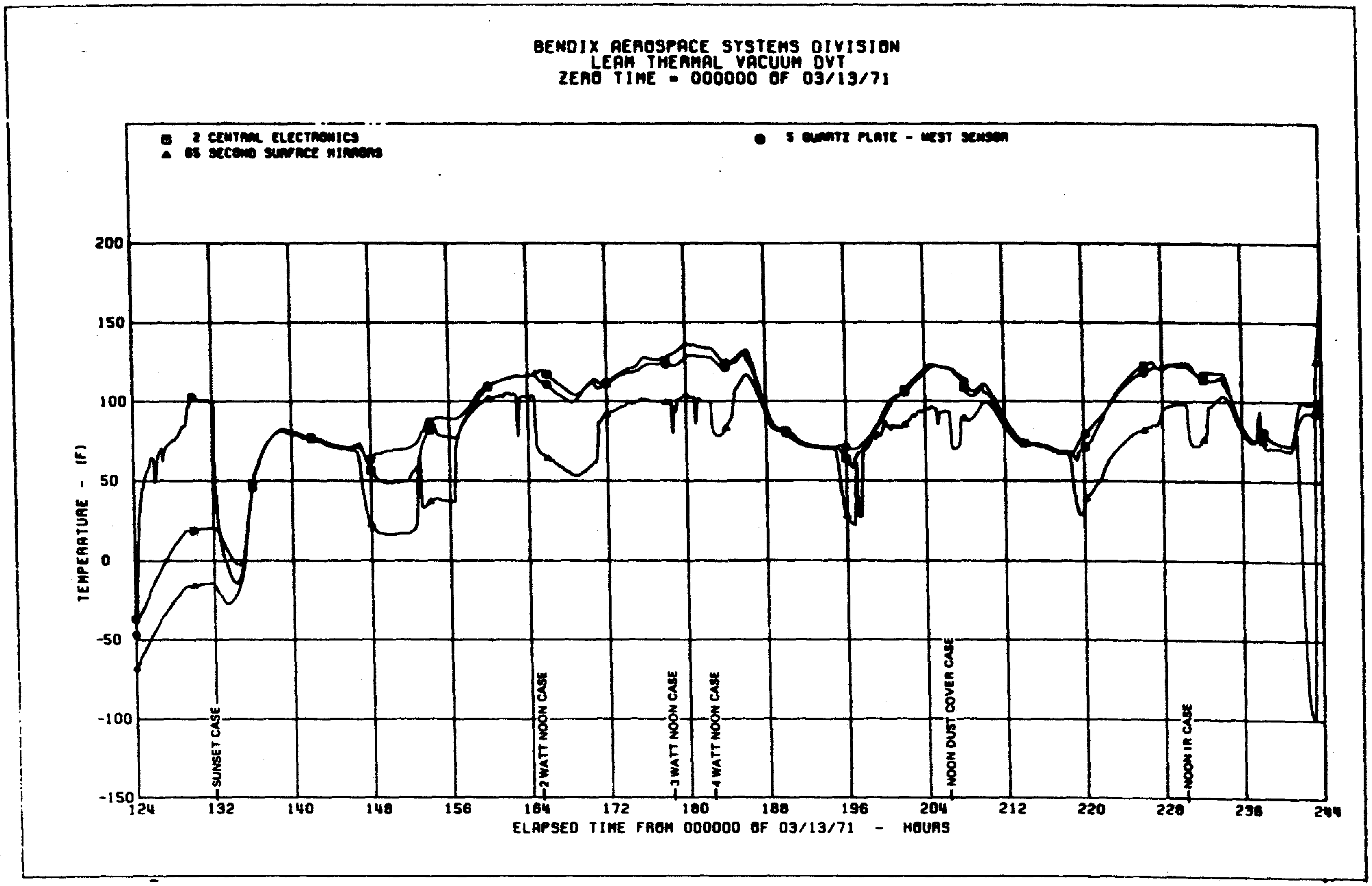

Figure 9.9 Graphical History of Test (Cont.)

TABLE 9.1

NIGHT CASE COMPARISONS TEMPERATURE °F

IDENTIFICATION	5 WATTS Test	5 WATTS Anal	6 WATTS Test	6 WATTS Anal	7 WATTS Test	7 WATTS Anal
CENTRAL ELECTRONICS	- 71	- 77	- 48	- 46	- 27	- 19
UP SENSOR						
FWD GRID FRAME	-113	-137	- 98	-117	- 84	-100
FWD FILM FRAME	-111	-111	- 97	- 89	- 83	- 70
SUPPORT STRUCT	- 78	- 81	- 59	- 57	- 43	- 35
REAR GRID FRAME	- 78	- 77	- 59	- 54	- 42	- 34
IMPACT PLATE	- 76	- 70	- 57	- 48	- 40	- 29
REAR ELECTRONICS	- 71	- 69	- 52	- 47	- 36	- 28
EAST SENSOR						
FWD GRID FRAME	-113	-133	- 97	-115	- 83	- 99
FWD FILM FRAME	-104	-107	- 88	- 86	- 74	- 69
SUPPORT STRUCT	- 75	- 77	- 56	- 54	- 39	- 35
REAR GRID FRAME	- 75	- 73	- 55	- 52	- 38	- 33
IMPACT PLATE	- 73	- 67	- 54	- 46	- 37	- 27
REAR ELECTRONICS	- 67	- 66	- 49	- 45	- 32	- 27
WEST SENSOR						
GRID FRAME	- 98	-102	- 82	- 86	- 67	- 73
IMPACT PLATE	- 78	- 82	- 60	- 63	- 44	- 47
ELECTRONICS	- 54	- 81	- 37	- 62	- 21	- 46
STRUCTURE	- 76	- 83	- 56	- 60	- 38	- 39
STRUCTURE	- 77	- 82	- 58	- 58	- 41	- 38
STRUCTURE	- 75	- 82	- 56	- 58	- 39	- 38
STRUCTURE	- 72	- 77	- 53	- 54	- 35	- 34
RADIATOR	- 96	- 88	- 79	- 65	- 63	- 44

TABLE 9.2

COMPARISON BETWEEN 5 WATT SURVIVAL AND 5 WATT NIGHT CASES

	5 WATT SURVIVAL	5 WATT NIGHT
HEATING COMPONENT	DISSIPATION WATTS	
UP ELECTRONICS	0	0.33
EAST ELECTRONICS	0	0.33
WEST ELECTRONICS	0	0.25
CENTRAL ELECTRONICS	0	1.13
UP ELECTRONICS HEATER	0.26	0.27
EAST ELECTRONICS HEATER	0.26	0.26
WEST ELECTRONICS HEATER	2.65	1.73
RADIATOR HEATER	2.06	0.76
COMPONENT	TEMPERATURE ^0F	
UP ELECTRONICS	-76	-71
EAST ELECTRONICS	-73	-67
WEST ELECTRONICS	-64	-54
CENTRAL ELECTRONICS	-75	-71
UP MICROPHONE	-77	-76
EAST MICROPHONE	-75	-73
WEST MICROPHONE	-79	-78

In general, none of the component temperatures changed a great deal, indicating the existence of satisfactory thermal coupling between the electronic components and the heater locations.

TABLE 9.3

SURVIVAL CASE COMPARISON TEMPERATURE °F

IDENTIFICATION	TEST	ANALYSIS
CENTRAL ELECTRONICS	-112	-127
UP SENSOR		
FWD GRID FRAME	-142	-173
FWD FILM FRAME	-140	-151
SUPPORT STRUCTURE	-114	-125
REAR GRID FRAME	-114	-124
IMPACT PLATE	-112	-122
REAR ELECTRONICS	-112	-121
EAST SENSOR		
FWD GRID FRAME	-143	-169
FWD FILM FRAME	-136	-146
SUPPORT STRUCTURE	-112	-119
REAR GRID FRAME	-113	-119
IMPACT PLATE	-110	-117
REAR ELECTRONICS	-109	-117
WEST SENSOR		
GRID FRAME	-128	-140
IMPACT PLATE	-111	-128
ELECTRONICS	-102	-129
STRUCTURE	-114	-126
STRUCTURE	-114	-125
STRUCTURE	-112	-123
STRUCTURE	-111	-120

A dust cover on condition was performed to examine the temperature distribution when the sensor openings were covered. Table 9.4 provides a comparison of selected temperatures with and without dust covers for 3 watt power dissipation at lunar noon conditions.

Table 9.5 compares the carbon arc and the IR lamp test results for 3 watt power dissipation at lunar noon. The IR lamp condition was performed to obtain necessary data for incorporation into the qual and flight T/V acceptance tests which are performed with IR lamps only.

The lunar noon test results for 2, 3 and 4 watts power conditions and their respective analytical correlation are presented in Table 9.6.

NOON DUST COVER COMPARISON

IDENTIFICATION	TEMPERATURE °F 3 WATTS COVERS OFF	3 WATTS COVERS ON
CENTRAL ELECTRONICS	126	121
UP ELECTRONICS	123	117
EAST ELECTRONICS	125	120
WEST ELECTRONICS	127	124
UP MICROPHONE*	124	116
EAST MICROPHONE	125	120
WEST MICROPHONE	123	121

*Microphone temperatures are approximately the same as impact plate temperatures.

TABLE 9.4

IR NOON CASE COMPARISONS

IDENTIFICATION	TEMPERATURE °F 3 WATTS Carbon Arc	3 WATTS IR Lamps
CENTRAL ELECTRONICS	126	124
UP SENSOR		
FWD GRID FRAME	104	100
FWD FLM FRAME	111	90
SUPPORT STRUCTURE	122	118
REAR GRID FRAME	122	117
IMPACT PLATE	124	119
REAR ELECTRONICS	123	120
EAST IMPACT PLATE	125	123
EAST ELECTRONICS	125	123
WEST IMPACT PLATE	123	122
WEST ELECTRONICS	127	126
RADIATOR	99	98

TABLE 9.5

TABLE 9.6

NOON CASE COMPARISONS

IDENTIFICATION	2 WATTS Test	2 WATTS Anal	3 WATTS Test	3 WATTS Anal	4 WATTS Test	4 WATTS Anal
	TEMPERATURE °F					
CENTRAL ELECTRONICS	116	108	126	125	134	144
UP SENSOR						
FWD GRID FRAME	105	58	104	66	103	75
FWD FILM FRAME	115	98	111	106	107	116
SUPPORT STRUCTURE	117	105	122	117	126	131
REAR GRID FRAME	116	107	122	118	125	131
IMPACT PLATE	118	109	124	120	128	133
REAR ELECTRONICS	116	110	123	121	127	134
EAST SENSOR						
FWD GRID FRAME	104	115	111	120	115	127
FWD FILM FRAME	119	113	127	120	131	128
SUPPORT STRUCTURE	116	109	124	119	129	131
REAR GRID FRAME	117	111	124	120	130	132
IMPACT PLATE	117	113	125	123	130	135
REAR ELECTRONICS	118	113	125	123	130	135
WEST SENSOR						
GRID FRAME	113	118	119	122	124	128
IMPACT PLATE	117	116	123	124	128	134
ELECTRONICS	121	117	127	125	132	134
STRUCTURE	112	103	118	115	123	128
STRUCTURE	115	104	121	115	126	129
STRUCTURE	114	104	121	115	125	129
STRUCTURE	115	107	123	118	129	130
RADIATOR	104	90	99	100	99	112

10.0 QUAL T/V ACCEPTANCE AND DESIGN LIMIT TESTS

The qual T/V acceptance and design limit tests are performed to determine the functional and thermal performance of the experiment when integrated into the ALSEP system. Figure 10.1 illustrates the qual model in a deployed condition prior to deployment of the dust covers. The qual model as deployed in the thermal/vacuum chamber at the termination of the qual T/V test is illustrated in Figure 10.2 with the dust covers deployed. Of interest in this photograph are the two radiometers utilized in the IR lamp solar simulation and the thermocouples as mounted to the external surfaces. Figure 10.3 reveals precisely the thermocouple locations.

The Qual test conditions for lunar noon acceptance, lunar noon design limit and lunar night are tabulated in Table 10.1.

These chamber conditions, experiment powers and solar flux levels were input to the thermal math model. The resulting correlation is presented in Table 10.2, and reveals that good correlation was achieved in all conditions for the internal structure, electronics, radiator and sensor components. The greatest variations occur for the fiberglass outercase which is highly influenced by variations in chamber positioning, IR lamp view and output and lunar surface simulator and cold wall temperature distribution and variation.

The flux evident on the LEAM radiator and up sensor was recorded by two radiometers. One radiometer recorded the incident flux on a second surface mirror surface (i.e. radiator) the other on parylene film vacuum deposited with aluminum (i.e. up sensor film). The incident thermal flux (watts/ft^2) profiles recorded by the film and second surface radiometers are shown in Figures 10.4 and 10.5 respectively. The temperature profiles recorded by the thermocouples of Figure 10.3 are presented in Figures 10.6 and 10.7.

Temperature profiles of the ALSEP flight data HK-84-1, -4 and -5 corresponding to the up microphone, central electronics and internal structure (referred to as survival on plot since this temperature is recorded during the survival mode) are shown in Figures 10.8, 10.9 and 10.10 respectively.

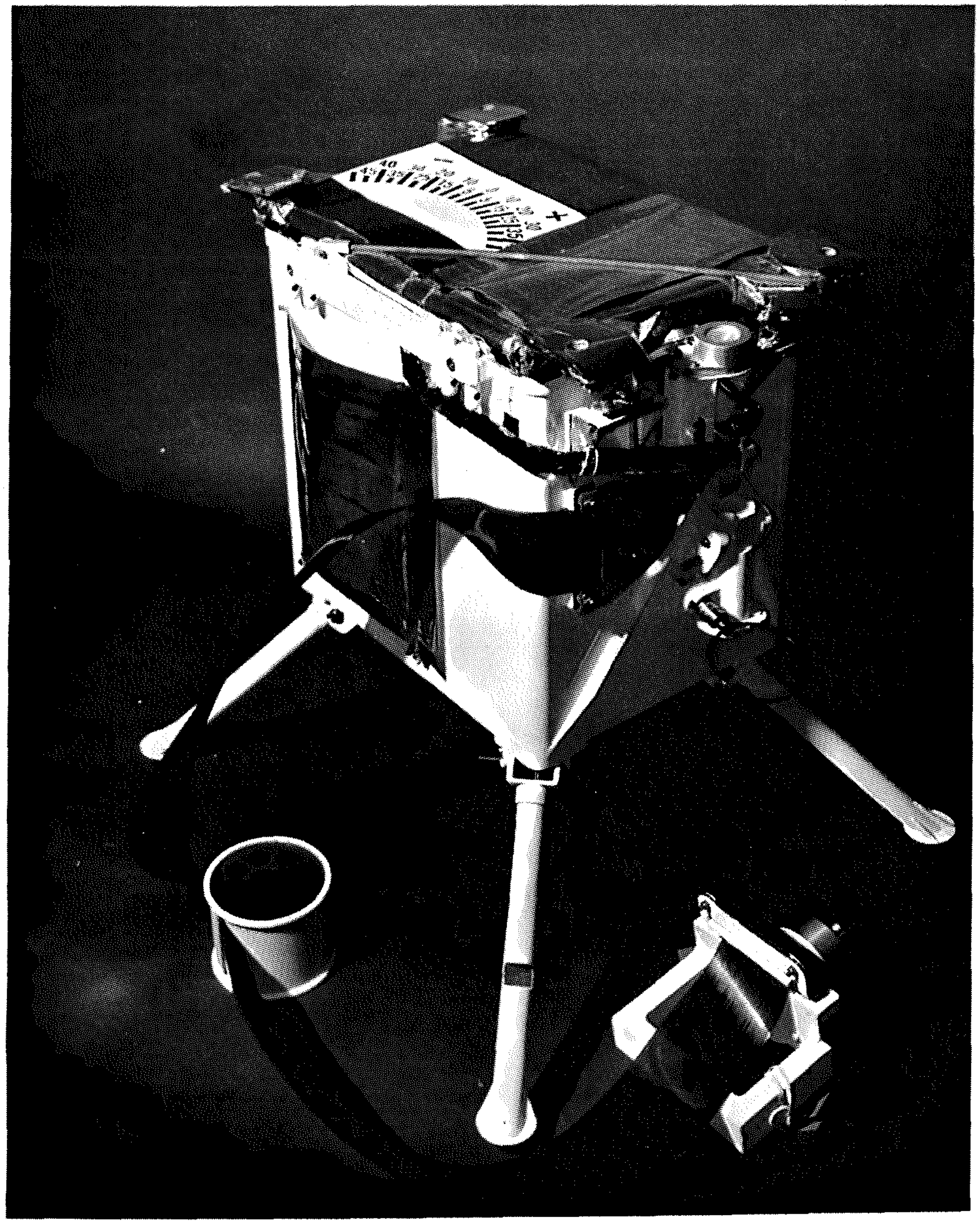

Figure 10.1 LEAM Qual Model Deployed - Dust Covers On

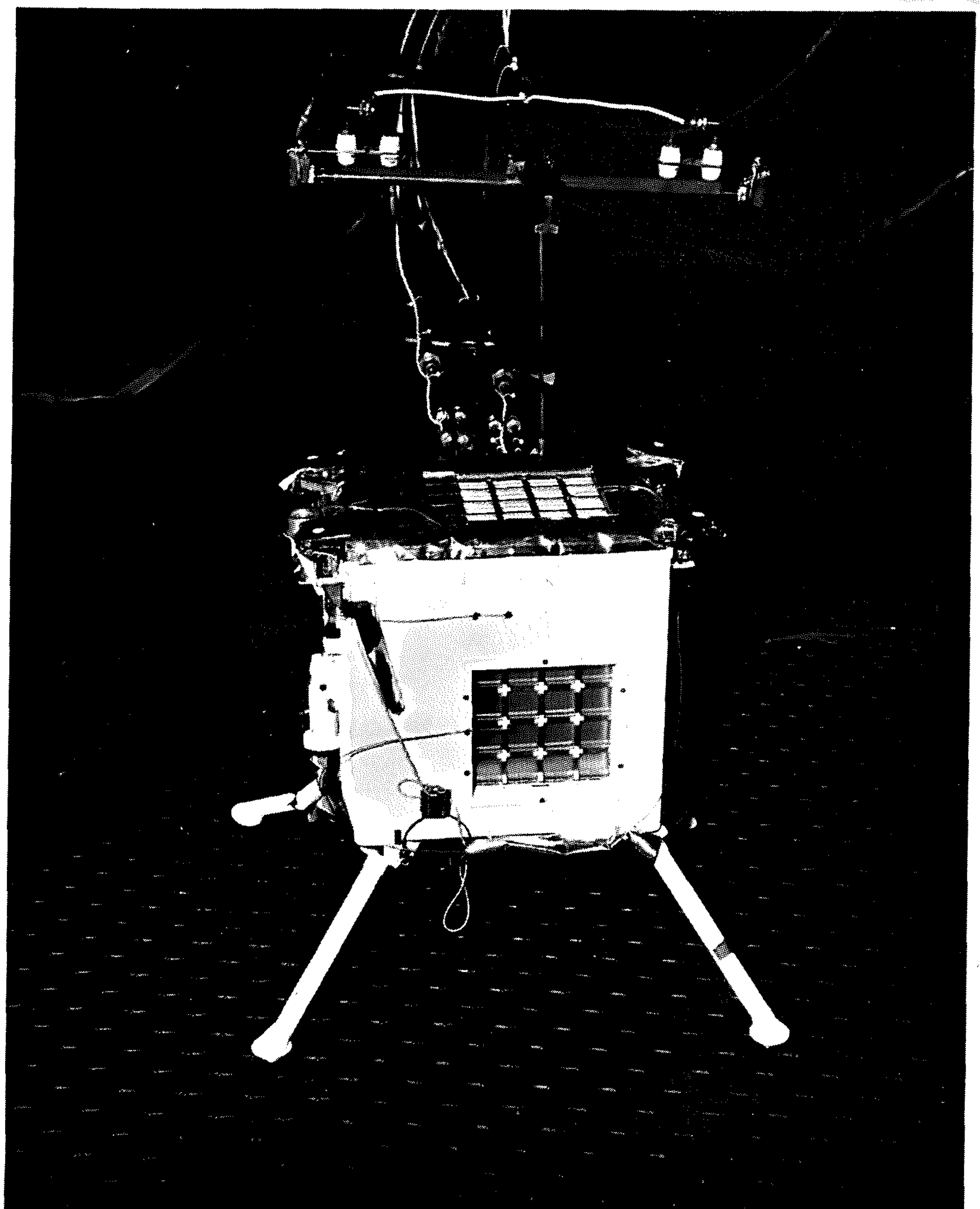

Figure 10.2 LEAM Qual Model Deployed in T/V Chamber
Dust Covers Off

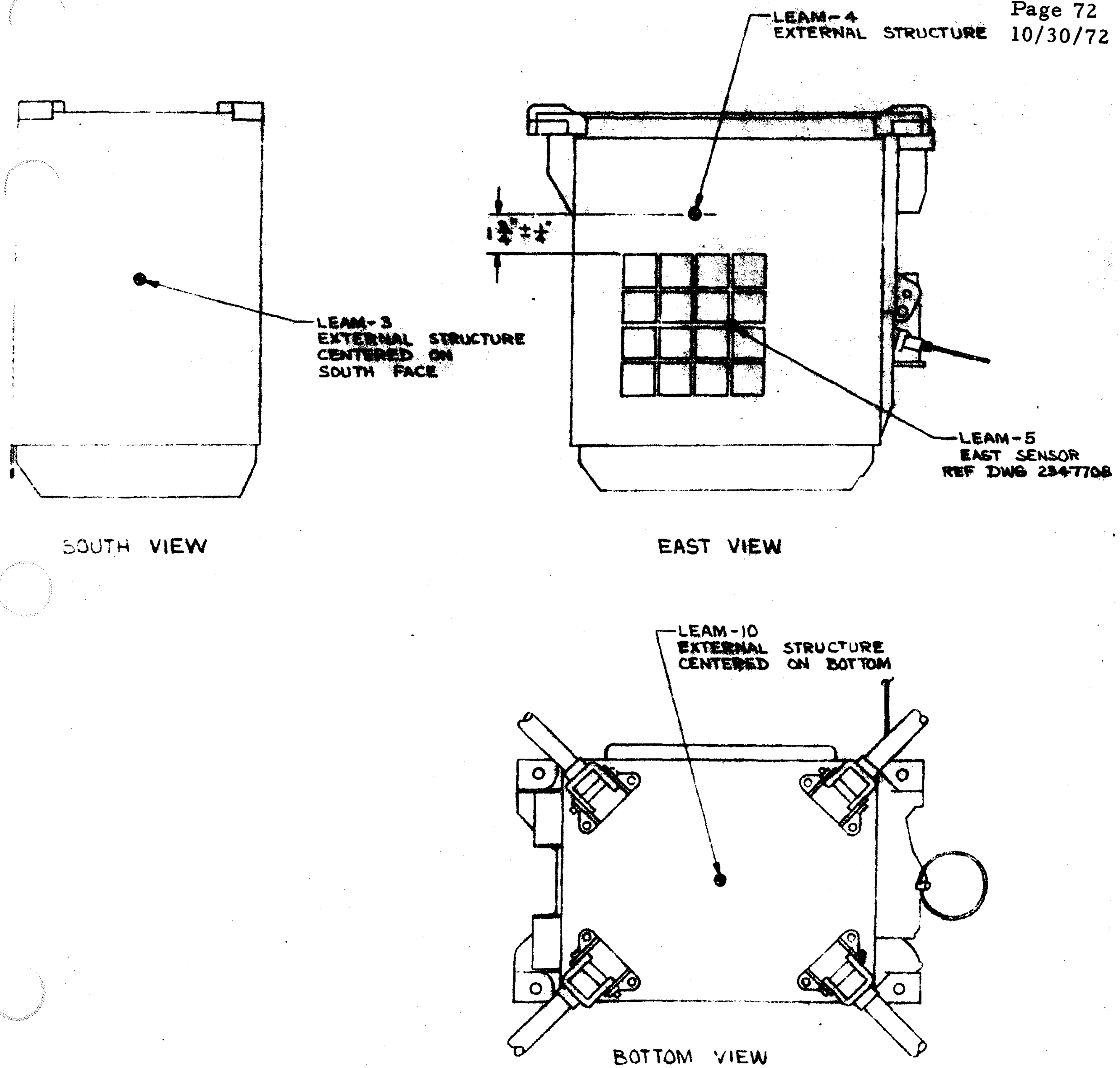

Figure 10.3 Qual Model T.C. Locations

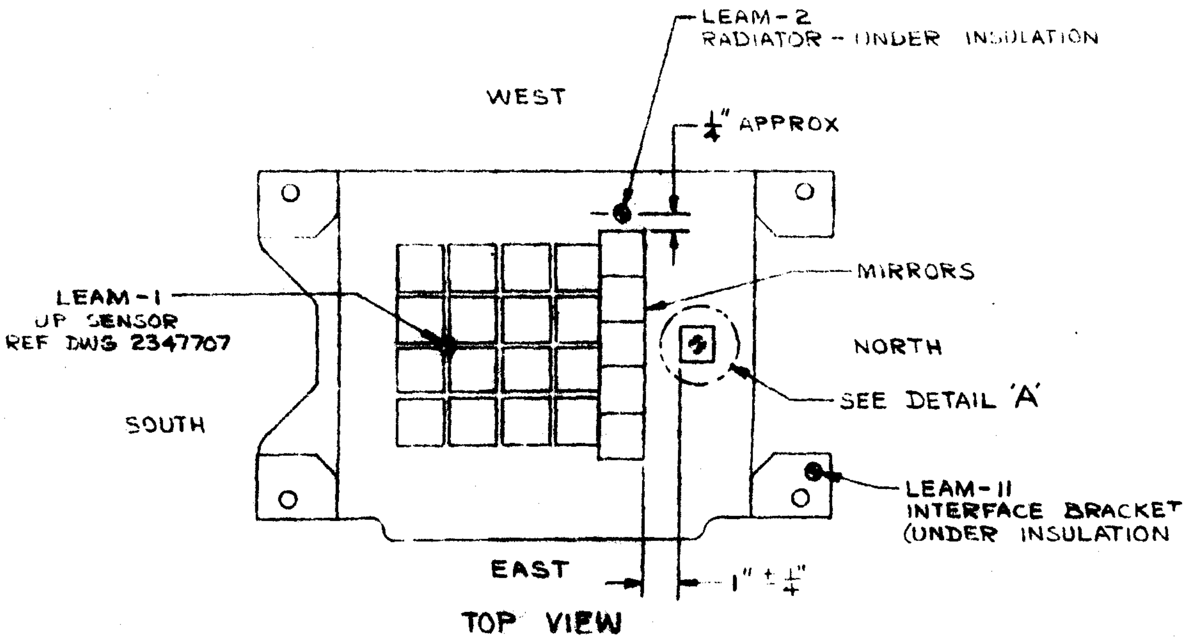

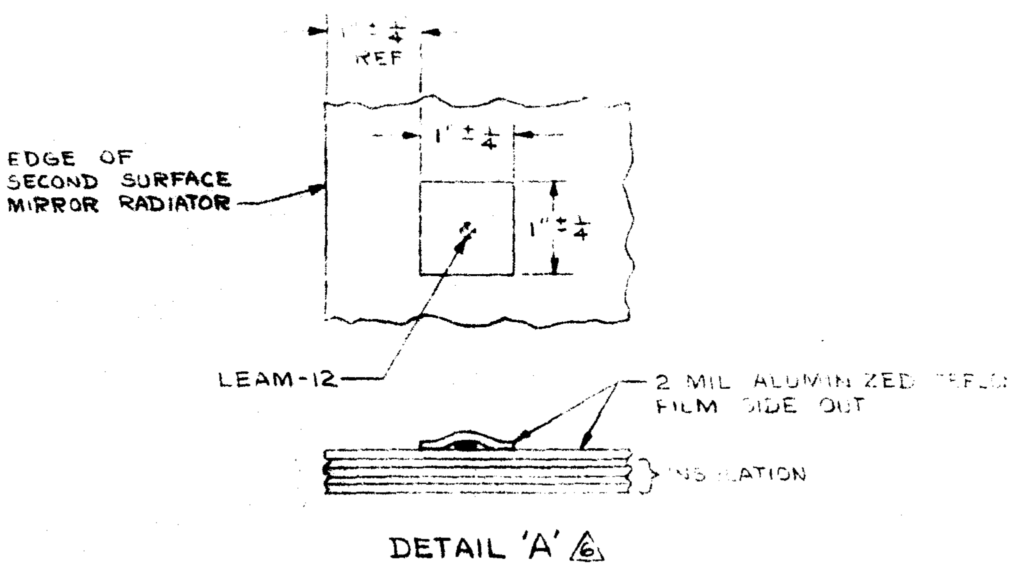

Figure 10.3 (cont) Qual Model T.C. Locations

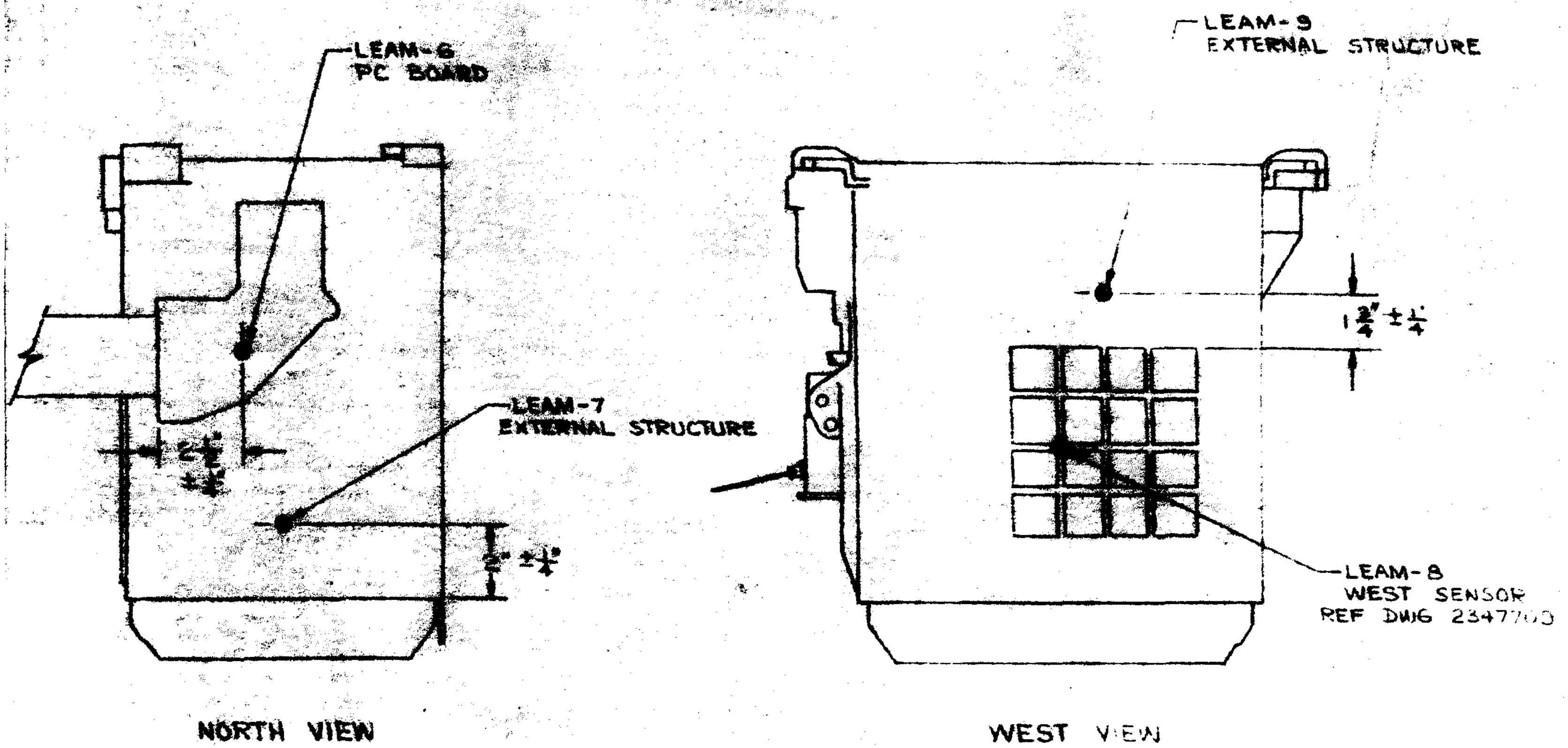

Figure 10.3 (cont) Qual Model T.C. Locations

	Lunar Noon	Design Limit	Lunar Night
Flux incident on S/S Mirrors (watts/ft^2)	546.0	430.3	-
Flux incident on Parylene Film (watts/ft^2)	78.0	48.0	-
Power (Watts)	3.17	3.17	6.56
Lunar Surface Simulator ($^\circ$F)	+250$\pm$10	+280$\pm$10	-300$\pm$10
Cold Wall ($^\circ$F)	-300$\pm$10	-300$\pm$ 10	-300$\pm$10
Chamber Pressure (torr)	2.57x10^{-7}	2.5x10^{-7}	2.5x10^{-7}

TABLE 10.1 Qual Test Conditions.

TABLE 10.2

LEAM QUALIFICATION TEST CORRELATION RESULTS

(Temperatures in °F)

Test			Lunar Noon**		Noon Design Limit**		Lunar Night***	
Identification	**DAS Channel**	**Node**	**Test**	**Analytical Model**	**Test**	**Analytical Model**	**Test**	**Analytical Model**
Central Electronics	HK	32	114.8	115.6	160.8	163.1	14.4	12.3
Microphone West	HK	230	98.5	107.5	136.6	141.2	-0.4	-13.0
Structure	HK	33	110.3	96.9	167.0	163.4	-0.4	-10.0
UP Sensor Outboard Grid	80	1	41.10	45.3	158.83	148.7	-68.02	-62.6
Radiator	81	24	101.59	100.5	159.81	160.9	-10.03	-10.8
External Structure (South)	82	61	90.63	129.8	113.07	154.1	-249.14	-247.5
External Structure (East)	83	64	115.04	129.0	144.48	144.2	-126.08	-292.8
East Sensor Outboard Grid	84	101	111.03	110.7	148.93	147.3	-55.61	-50.0
P.C. Board	85	—	134.19	—	164.15	—	-174.36	—
External Structure (North)	86	63	153.05	129.8	181.26	154.1	-205.35	-239.3
West Sensor Grid	87	209	109.37	113.7	143.79	141.0	-60.07	-87.6
External Structure (West)	88	62	96.66	129.0	115.75	152.1	-217.32	-295.9
External Structure (Bottom)	89	65	176.54	249.2	204.24	277.2	-239.45	-282.0
Interface Bracket	90	—	75.97	—	147.08	—	-114.83	—
Teflon Mask	91	93	-58.44	-70.1	61.73	64.1	-190.01	-192.4

* 2nd IR Reading

** 3.17 Watts Power Dissipation

*** 6.56 Watts Power Dissipation

Figure 10.4

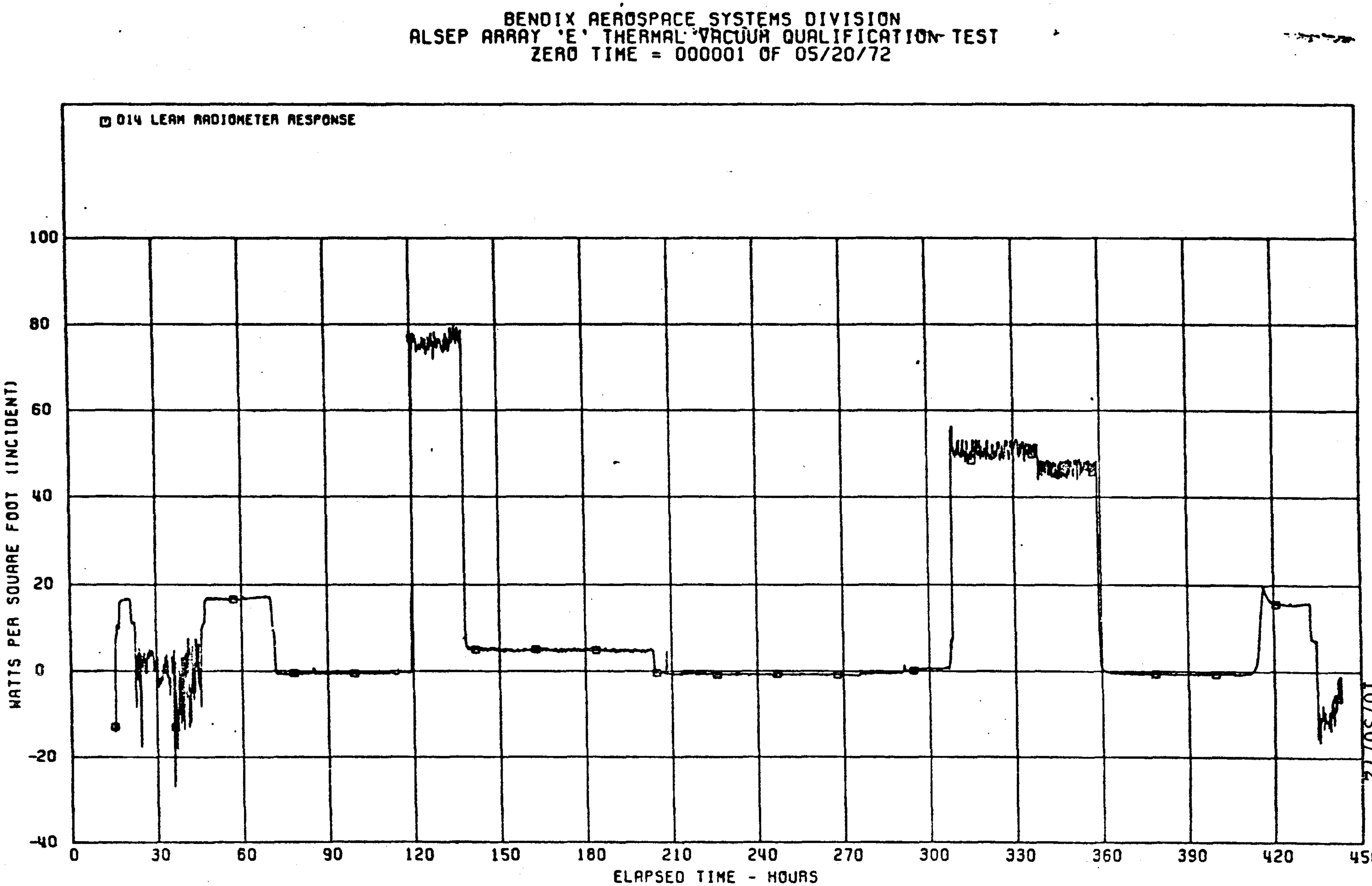

BENDIX AEROSPACE SYSTEMS DIVISION
ALSEP ARRAY 'E' THERMAL VACUUM QUALIFICATION TEST
ZERO TIME = 000001 OF 05/20/72
014 LEAM RADIOMETER RESPONSE
WATTS PER SQUARE FOOT (INCIDENT)
100
80
60
40
20
0
-20
-40
0
30
60
90
120
150
180
210
240
270
300
330
360
390
420
450
ELAPSED TIME - HOURS

Figure 10.5

BENDIX AEROSPACE SYSTEMS DIVISION
ALSEP ARRAY 'E' THERMAL VACUUM QUALIFICATION TEST
ZERO TIME = 000001 OF 05/20/72

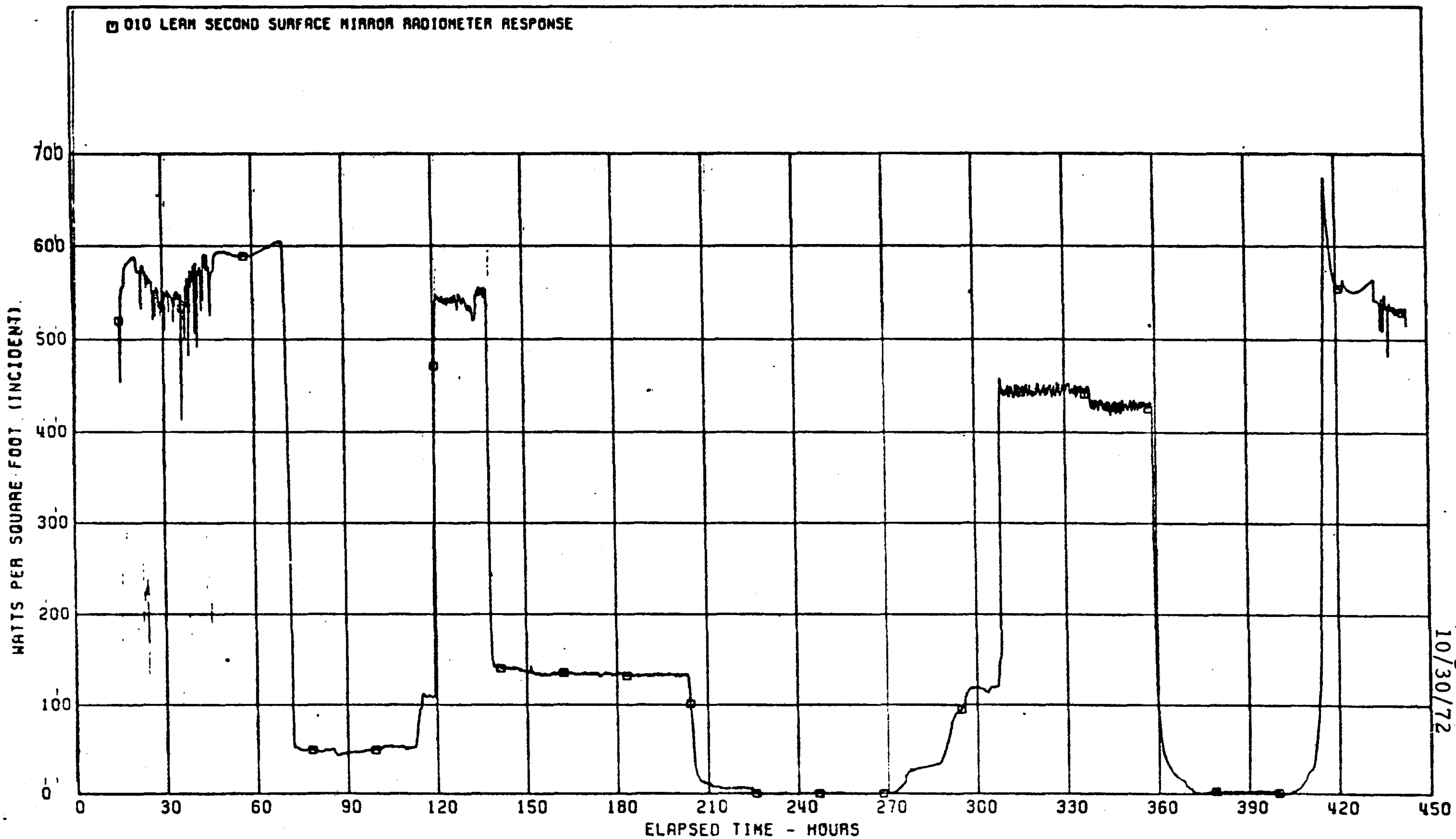

Figure 10.6

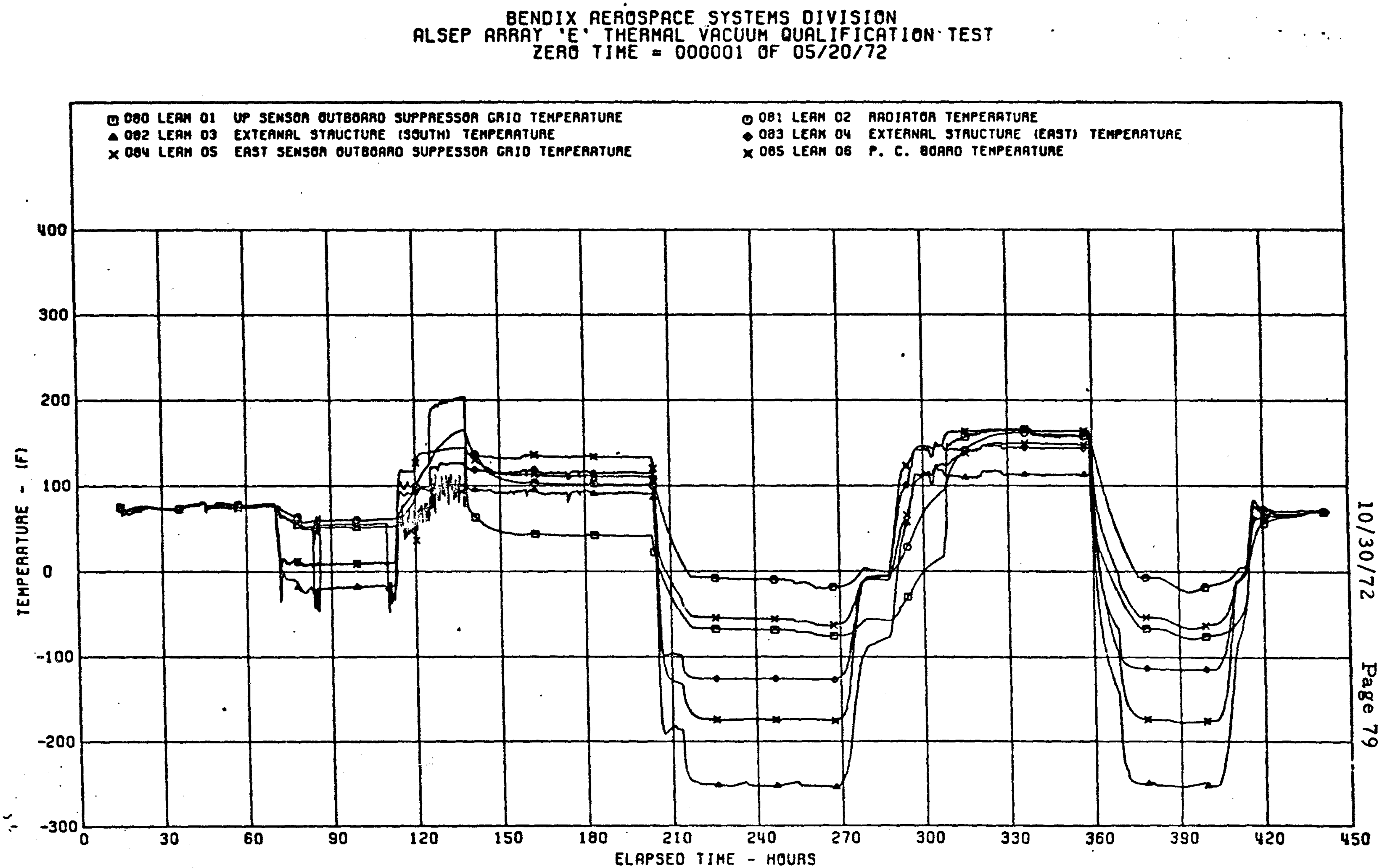

10/30/72

ATM 1118
Page 79

Figure 10.7

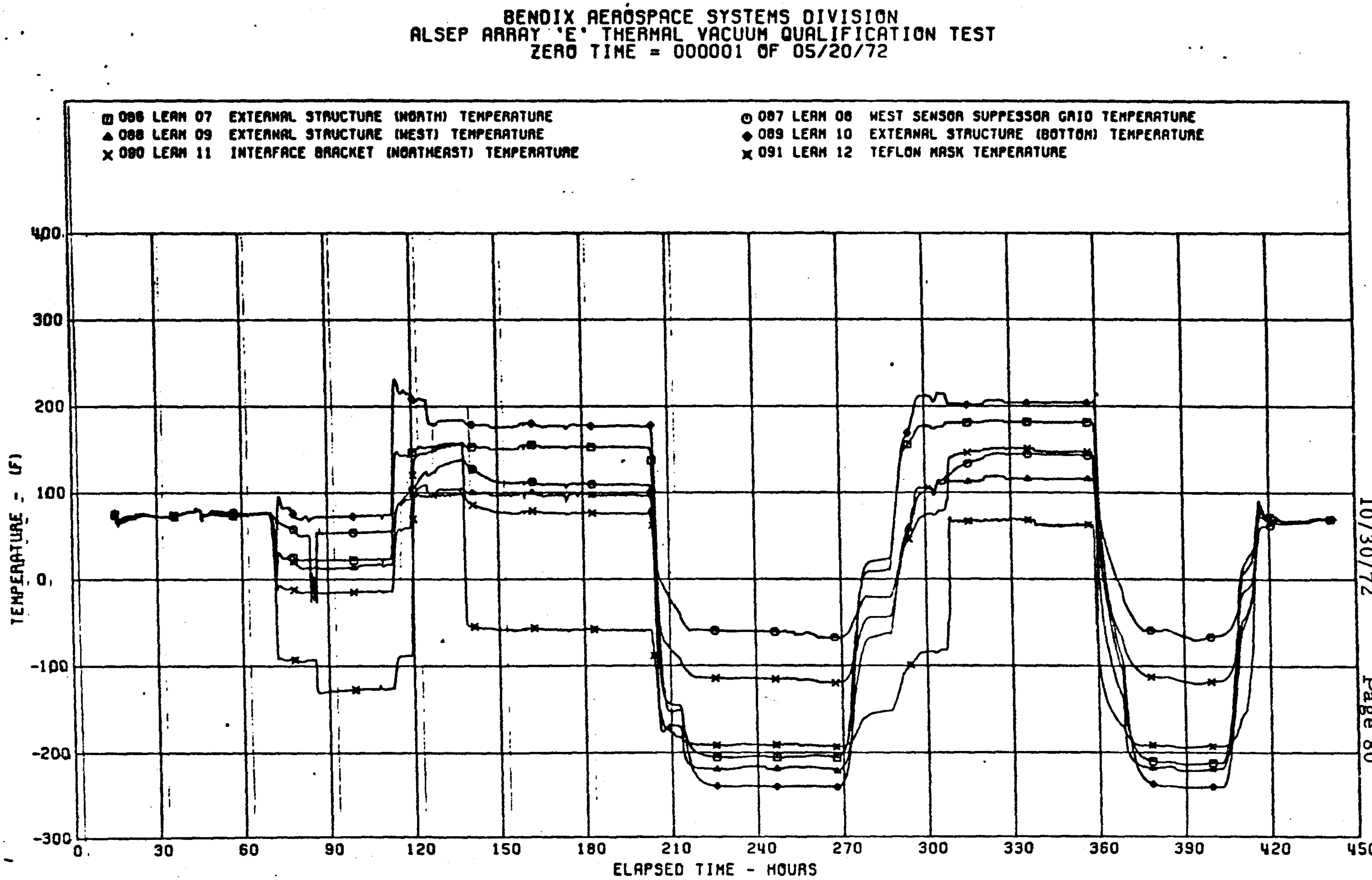

10/30/72

Figure 10.8

BENDIX AEROSPACE SYSTEMS DIVISION
ALSEP ARRAY E THERMAL VACUUM QUALIFICATION TEST
ZERO TIME : 0000 HOURS ON 05/20/72

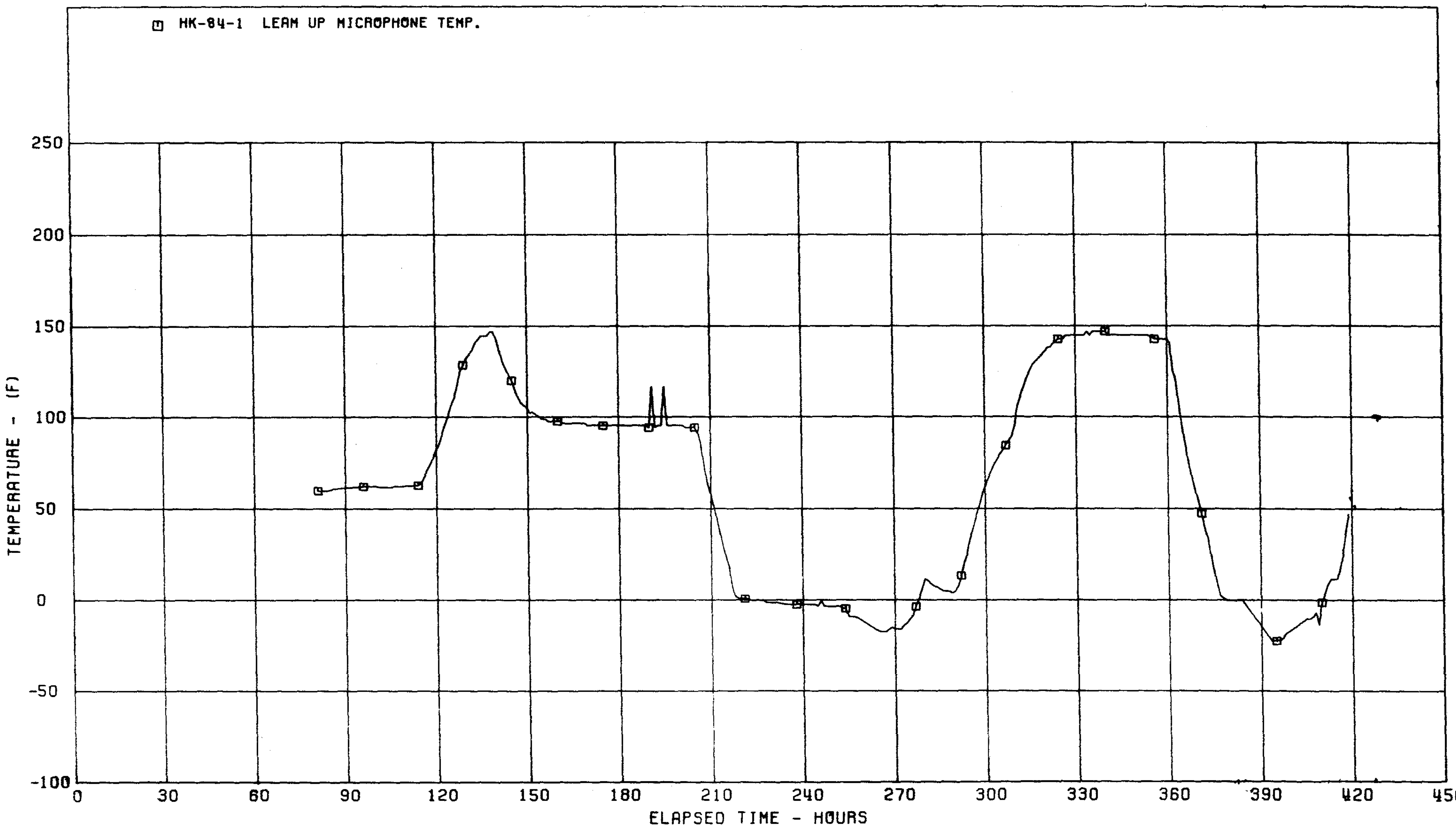

Figure 10.9

BENDIX AEROSPACE SYSTEMS DIVISION
ALSEP ARRAY E THERMAL VACUUM QUALIFICATION TEST
ZERO TIME : 0000 HOURS ON 05/20/72

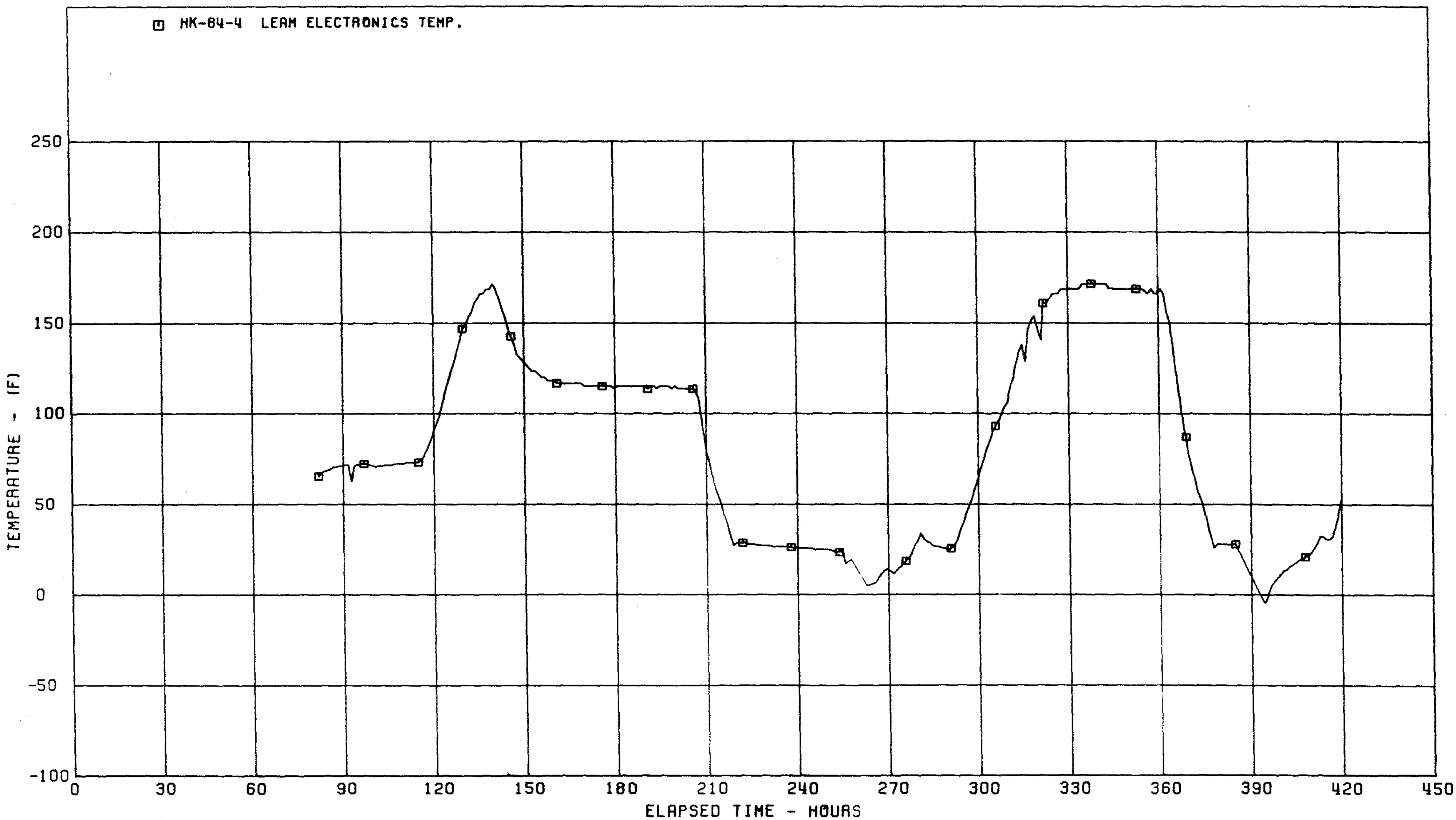

Figure 10.10

BENDIX AEROSPACE SYSTEMS DIVISION
ALSEP ARRAY E THERMAL VACUUM QUALIFICATION TEST
ZERO TIME : 0000 HOURS ON 05/20/72

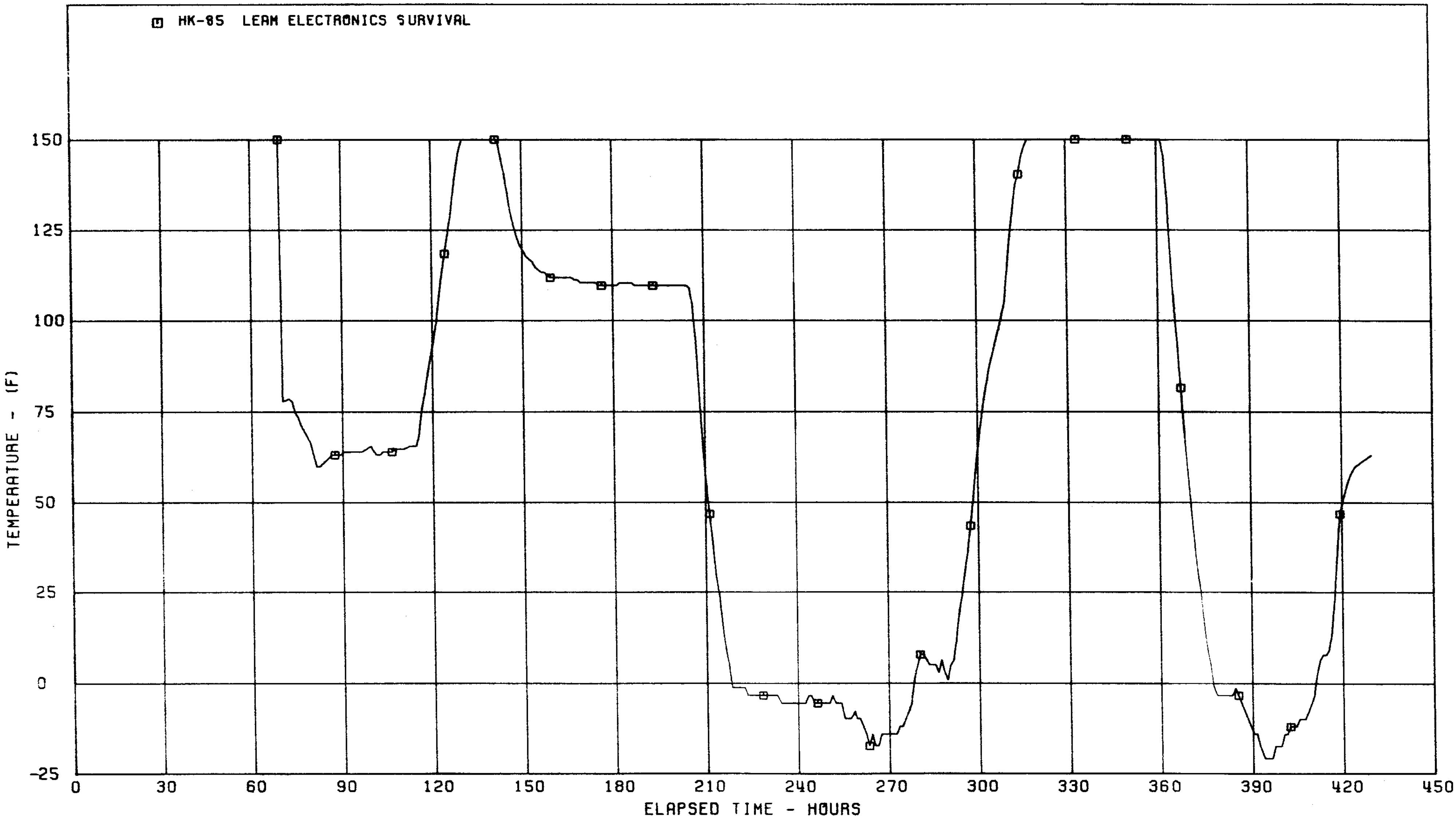

11.0 FLIGHT T/V ACCEPTANCE TEST

The flight T/V acceptance test was performed to verify the functional and thermal performance of the LEAM flight model at lunar noon and night conditions at the lunar equator.

With the Array E Flight Acceptance Thermal Vacuum Test results, it is possible to present a comparison of thermal test data for the qual and flight models of the LEAM which are of the same configuration. In particular, the Qual and Flight models were identical in all respects including radiator areas, masking area, coatings, power and multilayer insulation system. Summarized in Tables 11.1 and 11.2 are comparisons of lunar noon and night Qual and Flight test conditions, respectively. The only obvious difference is the level of solar flux simulation. The Qual test levels were used to bound anticipated lunar surface temperatures while the Flight test served to test the experiment at its normal operating temperatures.

The incident thermal flux histories on the second surface mirror and the aluminized parylene film radiometers are presented in Figures 11.1 and 11.2 respectively. Lunar noon condition was established from approximately 140 to 160 hours of elapsed time from the beginning of the test. During that period, the second surface radiometer output was 340.3 watts/ft^2 corresponding to an effective solar absorptance of 0.21. The aluminized parylene film radiometer output was 30 watts/ft^2 corresponding to an effective solar absorptance of 0.05.

Shown in Table 11.3 is a comparison of the three HK channels giving microphone, central electronics and structure temperatures for both tests. Note that Flight temperature levels lie between the bounds of the Qual test levels. Some variation (approximately 5°F) was observed for the microphone and structure temperatures for lunar night. This may be due to slightly different chamber configurations, or cold wall temperatures at the time data was reported. Note that a considerable design margin exists since the lower thermal design limit for the central electronics is -20°F and a low of +12.2°F was reached during the flight test.

During both lunar noon and night Flight tests, temperatures varied by only ±3°F over a 40 hour period indicating the stabilization criteria of 3°/hr had been met. Temperature profiles of the ALSEP data HK-84-1, -4 and -5 are presented in Figures 11.3, 11.4 and 11.5 respectively.

TABLE 11.1 Array E Qual/Flight/Analysis
Lunar Noon
Test Conditions Comparison

Condition	Qual		Flight	Analysis	
	1st IR	2nd IR		1st IR	2nd IR
Flux on S/S Mirrors (watts/ft^2)	546.0	130	340.3	546.0	130
Flux on Parylene Film (watts/ft^2)	78.0	4.68	30	78.0	4.68
Internal Power Dissipation(watts)	3.17		3.17	3.17	
Lunar Surface Simulator Temp ($^{\circ}$F)	+250 $\pm$ 10°F		+250$\pm$10°F	250°F	
Chamber Pressure (Torr)	2.57x10^{-7}		2.95x10^{-7}	-	

TABLE 11.2 Array E Qual/Flight/Analysis Lunar Night Test Conditions Comparison

Condition	Qual	Flight	Analysis
Lunar Surface Simulator Temperature (°F)	$-300 \pm 10^{\circ}F$	$-300 \pm 10^{\circ}F$	$-300^{\circ}F$
Cold Wall Temperature (°F)	$-300 \pm 10^{\circ}F$	$-300 \pm 10^{\circ}F$	$-300^{\circ}F$
Chamber Pressure (torr)	2.8×10^{-7}	2.9×10^{-7}	-
Power (watts)	6.56	6.56	6.56

FIGURE 11.1

BENDIX AEROSPACE SYSTEMS DIVISION
ALSEP ARRAY 'E' THERMAL VACUUM ACCEPTANCE TEST
ZERO TIME = 000001 OF 07/01/72

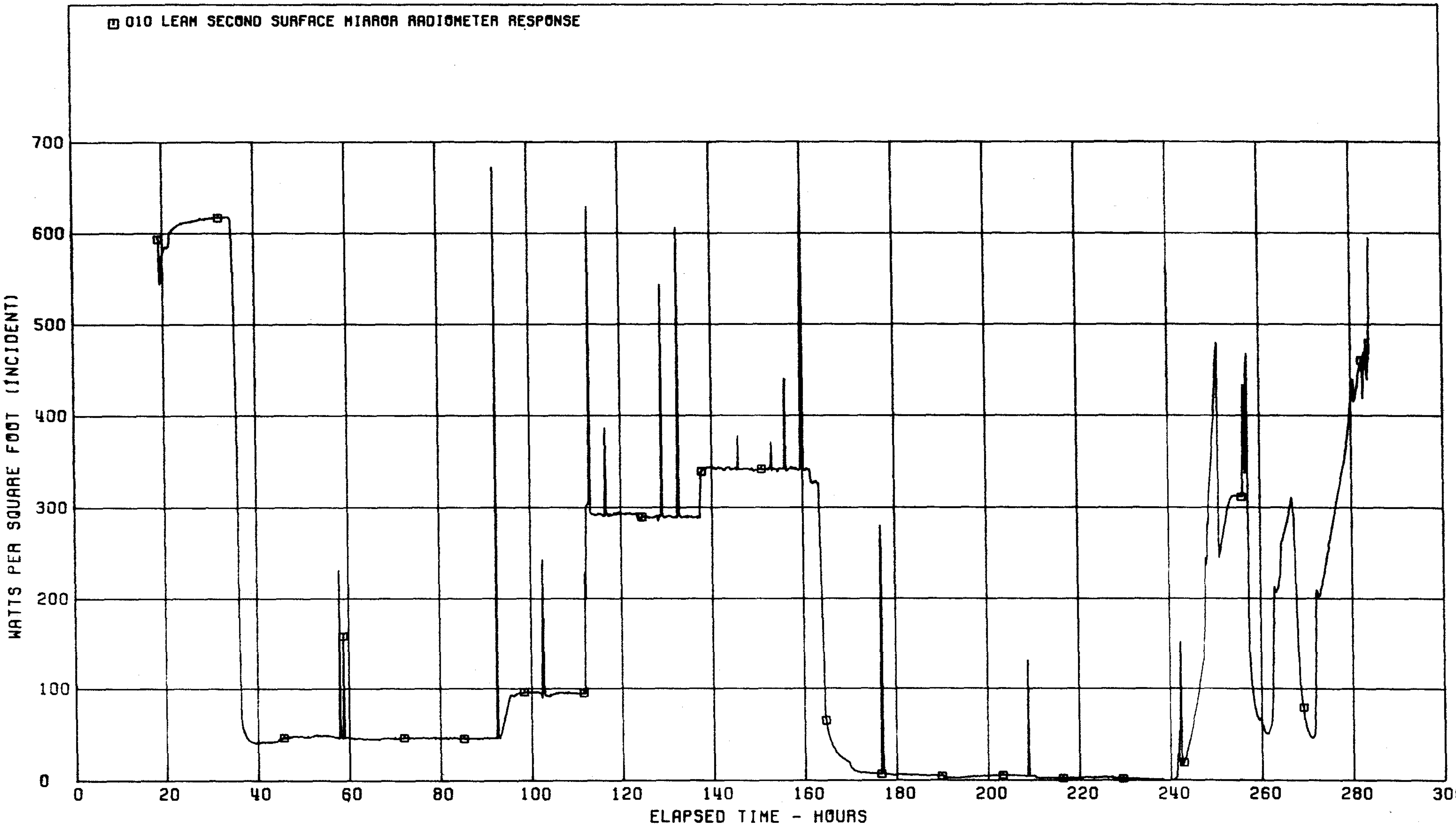

FIGURE 11.2

BENDIX AEROSPACE SYSTEMS DIVISION
ALSEP ARRAY 'E' THERMAL VACUUM ACCEPTANCE TEST
ZERO TIME = 000001 OF 07/01/72

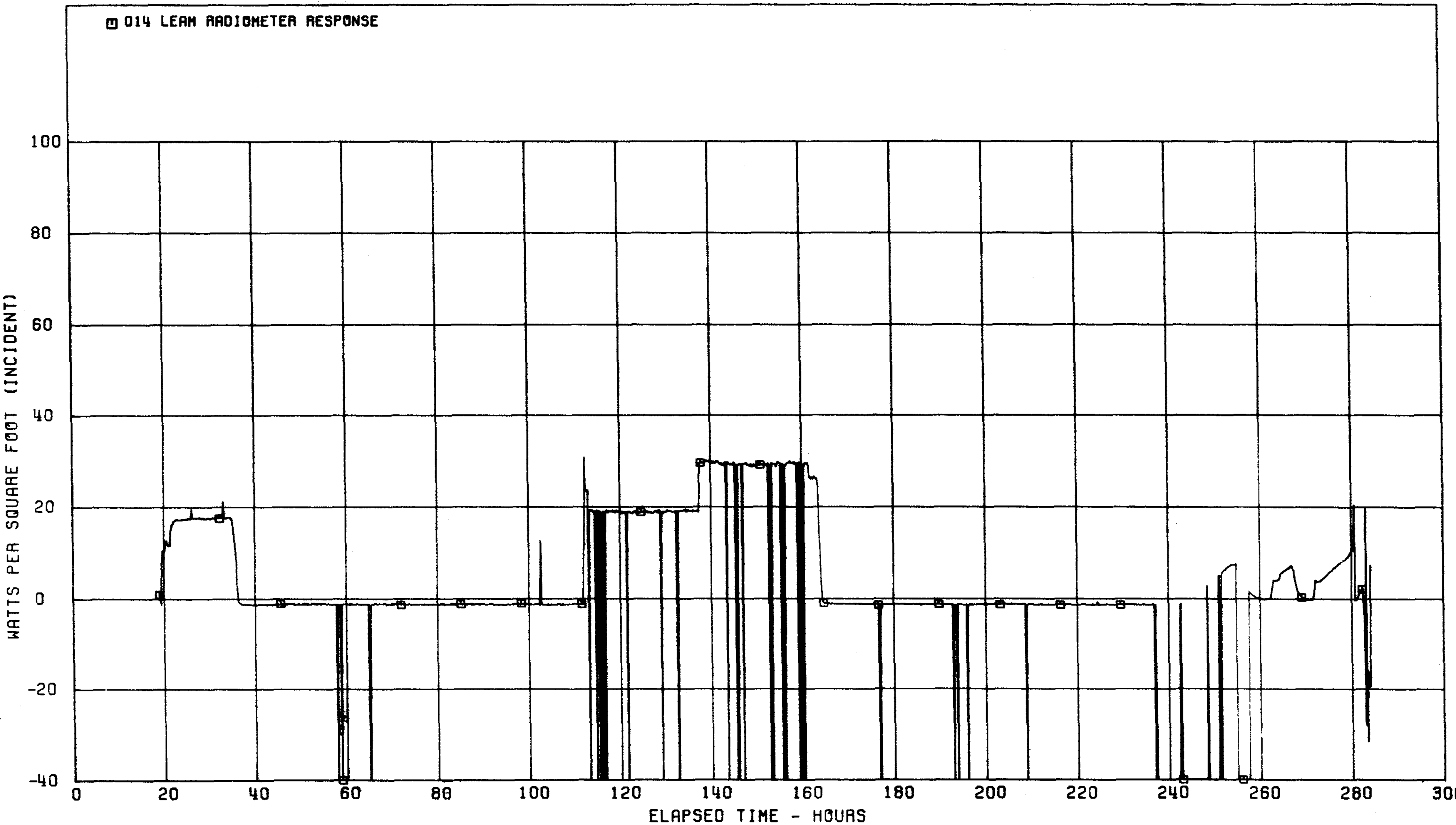

Identification	HK	Lunar Noon Qual	Lunar Noon Flight	Lunar Night Qual	Lunar Night Flight	Comments
Microphone-West	84-01	138/98.5°F	120.2°F	-0.4°F	-5.8°F	Noon variances due to differences in solar loads
Central Electronics	84-04	160.8/114.8°F	138°F	14.4°F	+12.2°F	"
Structure	85	167/110.3°F	138.2°F	-0.4°F	-5.8°F	"

TABLE 11.3 Comparison of LEAM Qual/Flight T/V Test Results

FIGURE 11.3

BENDIX AEROSPACE SYSTEMS DIVISION
ALSEP ARRAY E THERMAL VACUUM ACCEPTANCE TEST
ZERO TIME : 0000 HOURS ON 07/01/72

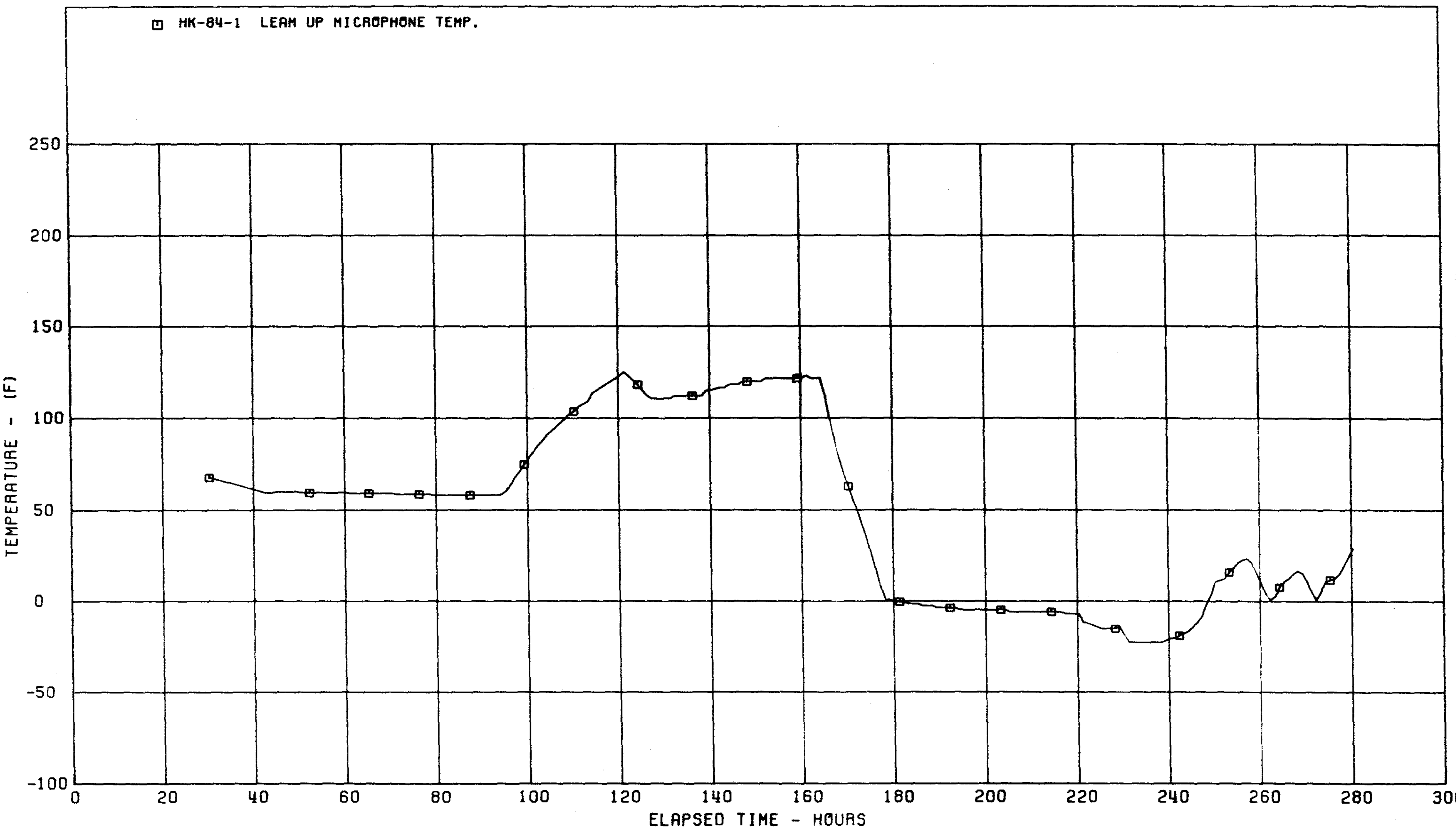

FIGURE 11.4

BENDIX AEROSPACE SYSTEMS DIVISION
ALSEP ARRAY E THERMAL VACUUM ACCEPTANCE TEST
ZERO TIME : 0000 HOURS ON 07/01/72

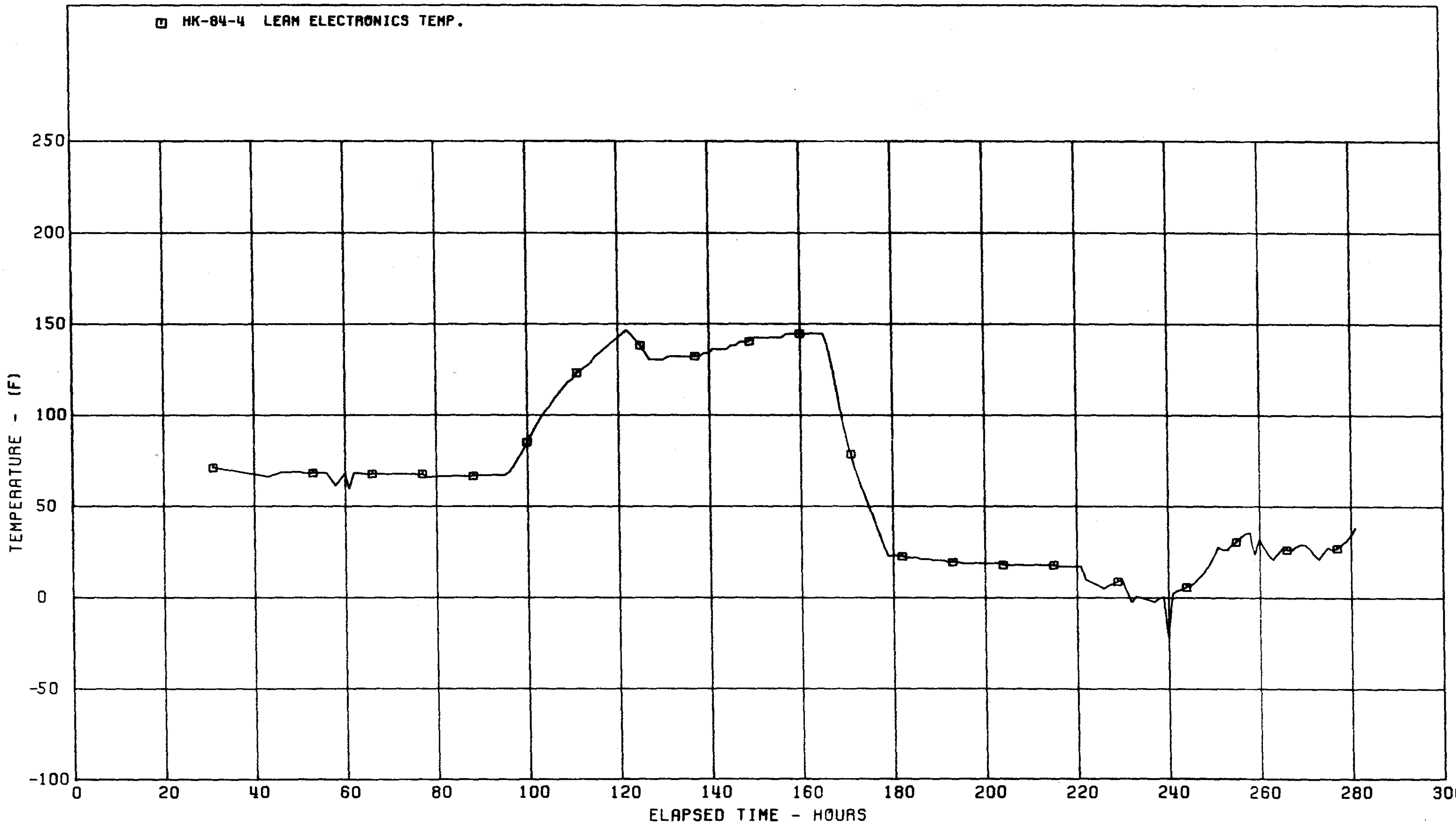

FIGURE 11.5

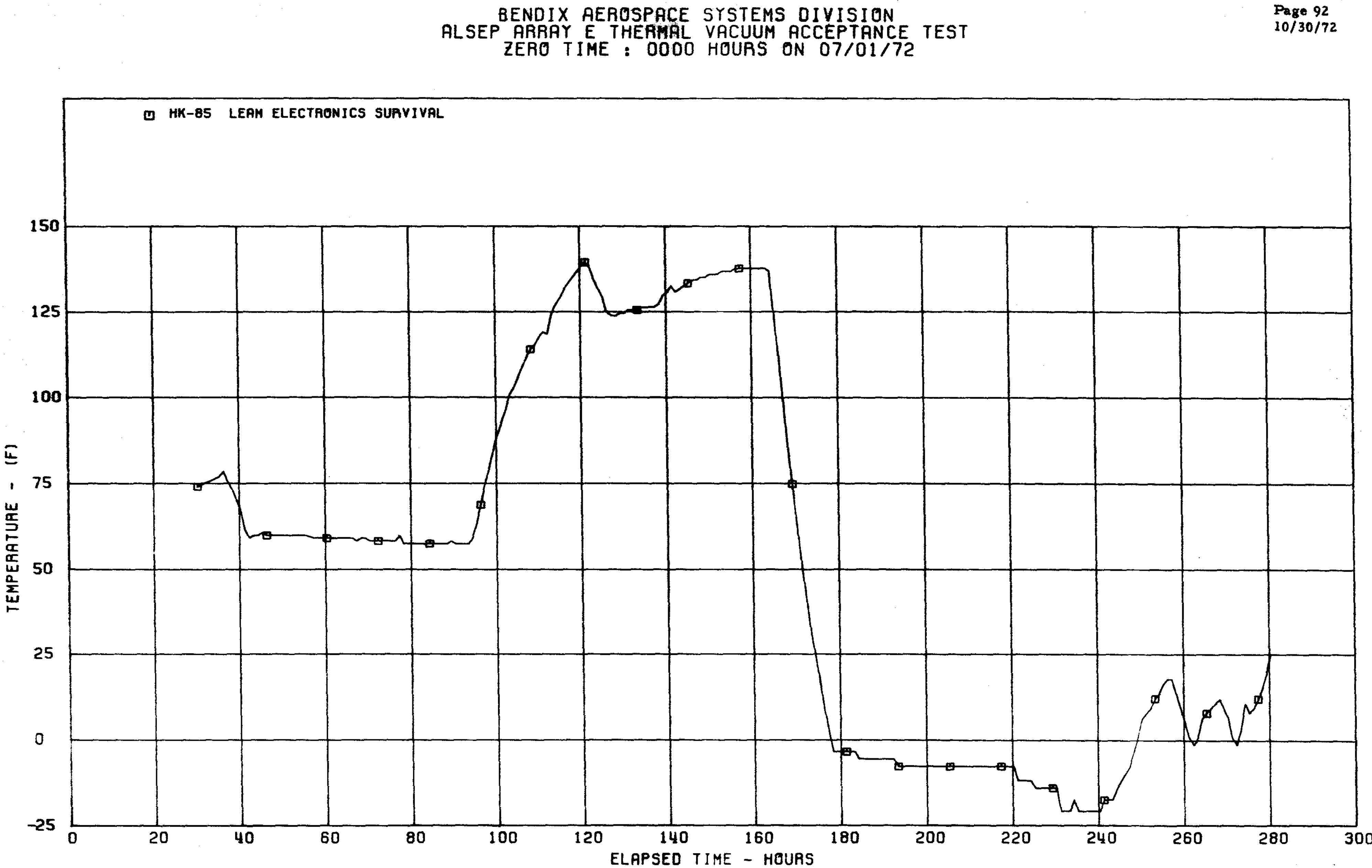
BENDIX AEROSPACE SYSTEMS DIVISION
ALSEP ARRAY E THERMAL VACUUM ACCEPTANCE TEST
ZERO TIME : 0000 HOURS ON 07/01/72
HK-85 LEAM ELECTRONICS SURVIVAL
TEMPERATURE - (F)
150
125
100
75
50
25
0
-25
0
20
40
60
80
100
120
140
160
180
200
220
240
260
280
300
ELAPSED TIME - HOURS

Figure 11.6 presents the central electronics temperature DVT, qual and flight T/V tests at lunar night conditions. The DVT T/V test was performed at various powers to determine the sensitivity of the experiment with power dissipation. The qual and flight T/V acceptance tests were performed at the design power level of 6.56 watts. This figure shows the effect of the reduction in radiator area between the DVT and qual/flight models from 15 to 5 square inches which brought the central electronics temperature well above the lower operating temperature limit.

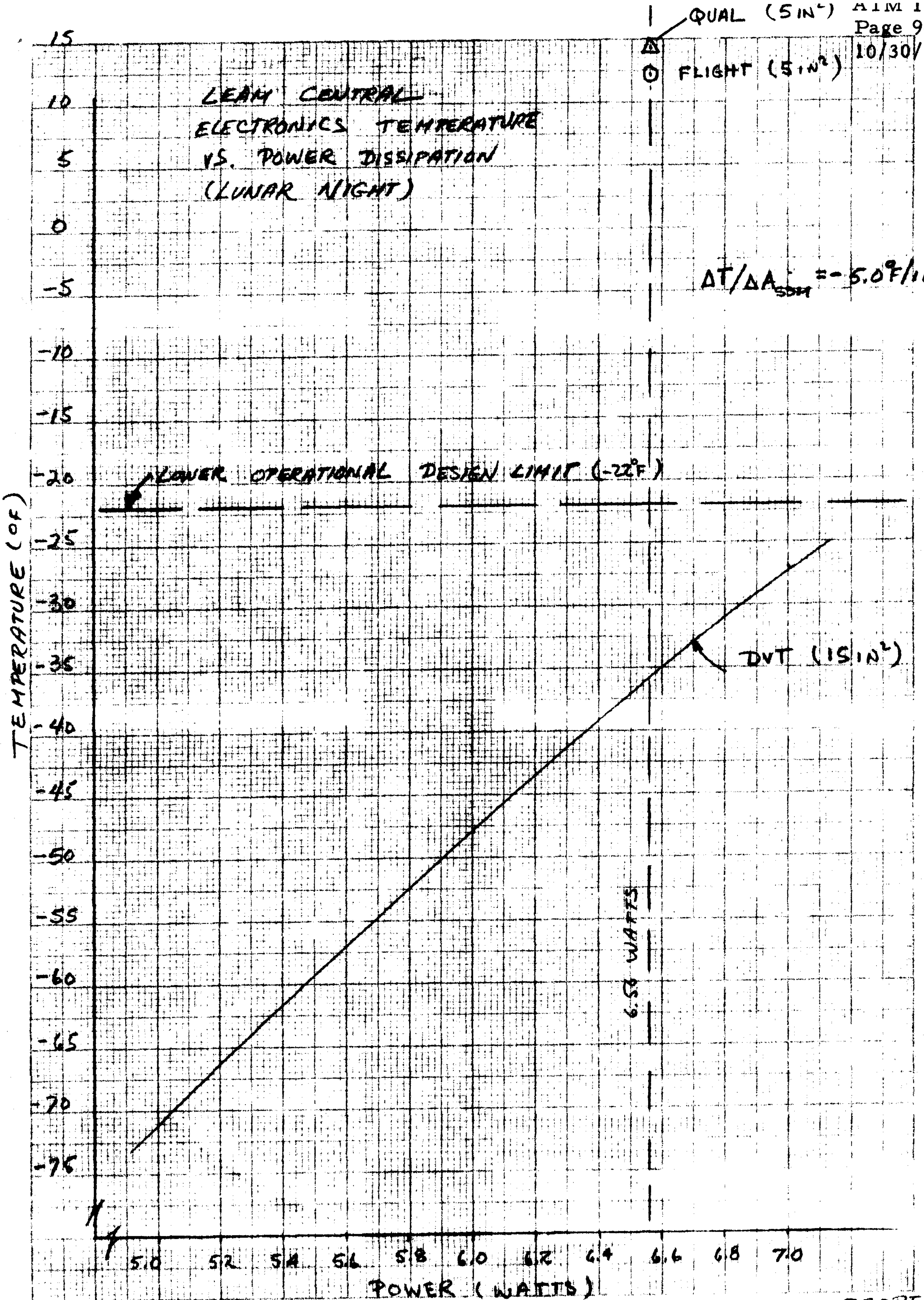

7 SEPT 1972
J. GRIFFIN

FIGURE 11.6

12.0 REFERENCES

1. BxA Handout 9712-1007, "Section 5, LEAM Thermal Design Summary", June 14-15, 1972

2. BxA Handout 9712-1007A, "Section 5, LEAM Thermal Design Summary, June 1972

3. BxA Memo LEAM 164, "LEAM Power Budget", 11/5/71

4. BxA Memo LEAM 172, "LEAM Power Dissipation", 12/15/71.

5. BxA Memo 9712-748, "LEAM Parametric Studies", 1/7/72.

6. BxA Memo 5032-19, "LEAM Array E Qual Thermal/Vac Correlation", 7/27/72.

7. BxA Memo 5032-36, "LEAM Qual/Flight Thermal Vacuum Test Results - Comparisons and Assessments", 7/27/72.

8. BxA Memo 5032-64, "LEAM Internal Temperature Profiles for Array E Data Book", 8/14/72.

9. Bell Laboratories Memo, "A Computer-Generated Panorama from The Apollo 17 LM Landing Site - Case 40058," 8/31/72.

10. BxA Memo 5032-94, "Lunar Terrain Effects on LEAM Thermal Performance", 9/8/72.

11. BxA Memo 5032-136, "Effective Slope of The Taurus Littrow Region as Observed from the Nominal Apollo 17 LM Landing Site", 10/11/72.

12. BxA Memo 70-210-375, "LEAM Film Development Parametric Study", 11/9/70.

13. ATM-995, "LEAM Film Development Test Report", 4/1/71.

14. ATM-1019, "LEAM DVT Thermal Test Report", 6/7/71.

15. ATM-1010, "LEAM Sensor Front Film Development Report", 6/11/71

16. ATM-1012, "LEAM DVT Mechanical Functional Test", 6/14/71.

17. BxA Memo 9712-549, "LEAM Qual T/V Testing", 9/1/71.

18. ITT Research Institute Report No. ITTRI-C9804-5, "Irradiation Study of Candidate (Vapor Deposited) Detector Materials", 6/19/72.

19. TRW Report No. 8526, 6-72-137, "Emittance and Absorptance of Bendix Aluminum Sample", 8/23/72.

20. ATM 1075, "LEAM Thermal Design Report," 10/25/71.